

AD-A038 775

NAVAL POSTGRADUATE SCHOOL MONTEREY CALIF

F/6 18/11

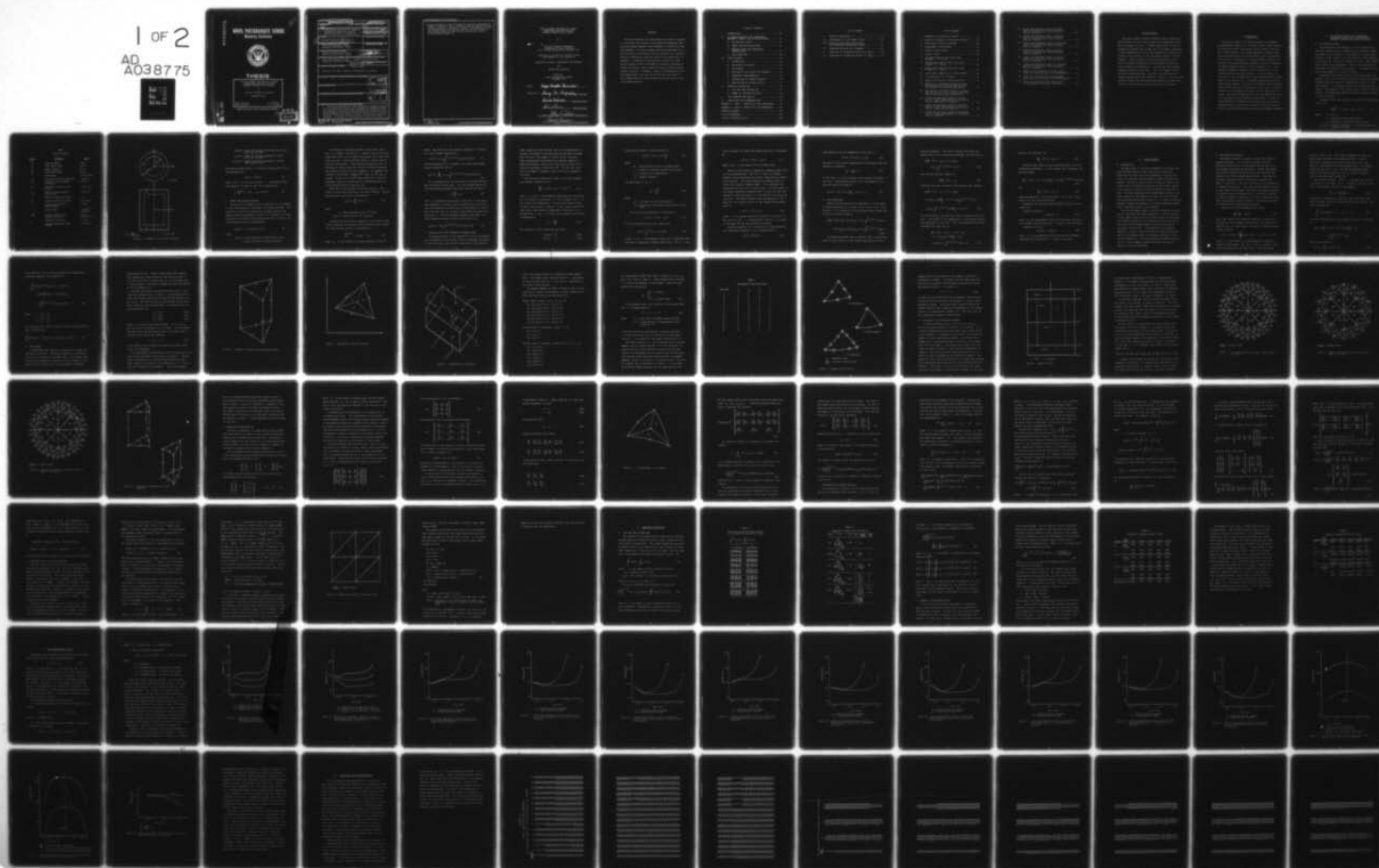
FINITE ELEMENT SOLUTION OF A THREE-DIMENSIONAL NONLINEAR REACTO--ETC(U)

DEC 76 E C BERMUDEZ

UNCLASSIFIED

NL

1 OF 2  
AD  
A038775







ADA 038775

1  
5

# NAVAL POSTGRADUATE SCHOOL

Monterey, California



## THESIS

FINITE ELEMENT SOLUTION OF A THREE-  
DIMENSIONAL NONLINEAR REACTOR  
DYNAMICS PROBLEM WITH FEEDBACK

by

Eulogio Conception Bermudes

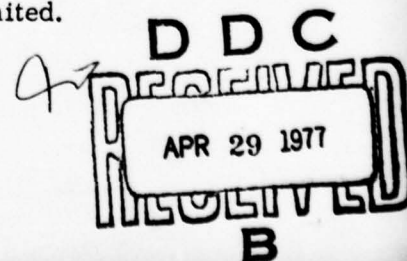
December 1976

Thesis Advisor:  
Thesis Advisor:

D. Salinas  
D. H. Nguyen

Approved for public release; distribution unlimited.

DDC FILE COPY



REPORT DOCUMENTATION PAGE		READ INSTRUCTIONS BEFORE COMPLETING FORM
1. REPORT NUMBER <u>2</u>	2. GOVT ACCESSION NO.	3. RECIPIENT'S CATALOG NUMBER <u>9</u>
4. TITLE (and Subtitle) Finite Element Solution of a Three-Dimensional Nonlinear Reactor Dynamics Problem with Feedback.		5. TYPE OF REPORT & PERIOD COVERED Master's Thesis, and Mechanical Engineer, Dec 1976
7. AUTHOR(s) <u>10</u> Eulogio Conception Bermudes		6. PERFORMING ORG. REPORT NUMBER
9. PERFORMING ORGANIZATION NAME AND ADDRESS Naval Postgraduate School Monterey, California 93940		8. CONTRACT OR GRANT NUMBER(s)
11. CONTROLLING OFFICE NAME AND ADDRESS Naval Postgraduate School Monterey, California 93940		10. PROGRAM ELEMENT, PROJECT, TASK AREA & WORK UNIT NUMBERS
14. MONITORING AGENCY NAME & ADDRESS (if different from Controlling Office) Naval Postgraduate School Monterey, California 93940		12. REPORT DATE <u>11</u> Dec 1976
		13. NUMBER OF PAGES 160
		18. SECURITY CLASS. (of this report) Unclassified
16. DISTRIBUTION STATEMENT (of this Report)  Approved for public release; distribution unlimited.		15. DECLASSIFICATION/DOWNGRADING SCHEDULE <u>12/160p.</u>
17. DISTRIBUTION STATEMENT (of the abstract entered in Block 20, if different from Report)		ACCESSION for NTIS White Section <input checked="" type="checkbox"/> DAS Buff Section <input type="checkbox"/> UNANNOUNCED <input type="checkbox"/> JUSTIFICATION BY DISTRIBUTION AVAILABILITY CODES Dist. Avail. and/or SPECIAL A
18. SUPPLEMENTARY NOTES		
19. KEY WORDS (Continue on reverse side if necessary and identify by block number)		
20. ABSTRACT (Continue on reverse side if necessary and identify by block number) This work examines the three-dimensional dynamic response of a nonlinear fast reactor with temperature-dependent feedback and delayed neutrons when subjected to uniform and local disturbances. The finite element method was employed to reduce the partial differential reactor equation to a system of ordinary differential equations which can be numerically integrated. A program for the numerical solution of large		

→ sparse systems of stiff differential equations developed by Franke and based on Gear's method solved the reduced neutron dynamics equation. Although a study of convergence by refining element mesh.sizes was not carried out, the crude finite element mesh.utilized yielded the correct trend of neutron dynamic behavior. ↗

FINITE ELEMENT SOLUTION OF A THREE-  
DIMENSIONAL NONLINEAR REACTOR  
DYNAMICS PROBLEM WITH FEEDBACK

by

Eulogio Conception Bermudes  
Lieutenant, United States Navy  
B.S., United States Naval Academy, 1970

Submitted in partial fulfillment of the  
requirements for the degrees of

MASTER OF SCIENCE IN MECHANICAL ENGINEERING

and

MECHANICAL ENGINEER

from the

NAVAL POSTGRADUATE SCHOOL  
December 1976

Author

Eulogio Conception Bermudes

Approved by:

Long H. Nguyen

Thesis Advisor

David Salinas

Thesis Advisor

Richard Francis

Second Reader

Allen E. Fuhs

Chairman, Department of Mechanical Engineering

Robert M. Johnson

Dean of Science and Engineering



## ABSTRACT

This work examines the three-dimensional dynamic response of a nonlinear fast reactor with temperature-dependent feedback and delayed neutrons when subjected to uniform and local disturbances. The finite element method was employed to reduce the partial differential reactor equation to a system of ordinary differential equations which can be numerically integrated. A program for the numerical solution of large sparse systems of stiff differential equations developed by Franke and based on Gear's method solved the reduced neutron dynamics equation. Although a study of convergence by refining element mesh sizes was not carried out, the crude finite element mesh utilized yielded the correct trend of neutron dynamic behavior.

## TABLE OF CONTENTS

I.	INTRODUCTION - - - - -	10
II.	THE NUCLEAR REACTOR WITH TEMPERATURE DEPENDENT FEEDBACK AND DELAYED NEUTRONS - - - -	11
	A. THE PHYSICAL SYSTEM - - - - -	11
	B. PROMPT AND DELAYED NEUTRONS - - - - -	14
	C. DOPPLER EFFECT AND TEMPERATURE FEEDBACK MODEL - - - - -	16
	D. FIELD EQUATIONS - - - - -	20
III.	FINITE ELEMENT - - - - -	23
	A. INTRODUCTION - - - - -	23
	B. THE METHOD OF GALERKIN - - - - -	24
	C. THE ELEMENT - - - - -	26
	D. DIVISION OF THE SYSTEM INTO ELEMENTS - - - -	35
	E. COORDINATE TRANSFORMATION - - - - -	42
	F. CONSTRUCTION OF ELEMENT MATRICES - - - - -	48
	G. CONSTRUCTION OF SYSTEM MATRICES - - - - -	54
IV.	NUMERICAL INTEGRATION - - - - -	60
	A. LINE AND AREA INTEGRATION - - - - -	60
	B. NUMBER OF INTEGRATION POINTS - - - - -	63
V.	TEST PROBLEMS AND RESULTS - - - - -	68
VI.	CONCLUSIONS AND RECOMMENDATIONS - - - - -	85
	APPENDIX A - MESH I CONVECTIVITY AND COORDINATES - -	87
	APPENDIX B - MESH II CONVECTIVITY AND COORDINATES - -	101
	COMPUTER PROGRAM - - - - -	121
	LIST OF REFERENCES - - - - -	159
	INITIAL DISTRIBUTION LIST - - - - -	160

## LIST OF TABLES

I.	Physical Coordinates - - - - -	12
II.	Coordinates of Local Nodal Points - - - - -	33
III.	Abscissae and Weight Coefficients of the Gaussian Quadrature Formula - - - - -	61
IV.	Numerical Formulas for Triangles - - - - -	62
V.	Selection of Integration Points for $[G_{ji}]$ - - -	65
VI.	Selection of Integration Points for $[GG_{ji}]$ - - -	67

## LIST OF FIGURES

1.	Schematic of cylindrical reactor	- - - - -	13
2.	Quadratic triangular prism parent element	- - - - -	28
3.	Definition of area coordinates	- - - - -	29
4.	Isoparametric coordinates	- - - - -	30
5.	Element classification	- - - - -	34
6.	Layers of mesh I	- - - - -	36
7.	Top nodal plane of the first layer of mesh I, $z = 110$ cm	- - - - -	38
8.	Middle nodal plane of the first layer of mesh I, $z = 95$ cm	- - - - -	39
9.	Bottom nodal plane of the first layer of mesh I, $z = 80$ cm	- - - - -	40
10.	Local nodal numbering of curved elements	- - - - -	41
11.	$\eta\xi$ coordinates in a triangle	- - - - -	46
12.	Sample grid used for illustrating OCS	- - - - -	57
13.	Neutron flux transient history at three test points with a uniform perturbation of 10 dollar of reactivity per second	- - - - -	70
14.	Neutron flux transient history at various test points for a local central perturba- tion of 100 dollar/sec of reactivity	- - - - -	71
15.	Linear and nonlinear fluxes at (0,0,0) due to a local perturbation of 100 dollar /sec of reactivity at (0,60,40)	- - - - -	72
16.	Linear and nonlinear fluxes at (60,0,0) due to a local perturbation of 100 dollar /sec of reactivity at (0,60,40)	- - - - -	73
17.	Linear and nonlinear fluxes at (-60,0,80) due to a local perturbation of 100 dollar /sec at (0,60,40)	- - - - -	74



18.	Linear and nonlinear fluxes at (0,0,0) due to a 50 dollar/sec local perturbation at (0,60,40) - - - - -	75
19.	Linear and nonlinear fluxes at (60,0,0) due to a 50 dollar/sec local perturbation at (0,60,40) - - - - -	76
20.	Linear and nonlinear fluxes at (-60,0,80) due to a 50 dollar/sec local perturbation at (0,60,40) - - - - -	77
21.	Linear and nonlinear fluxes at (0,0,0) due to a 10 dollar/sec local perturbation at (0,60,40) - - - - -	78
22.	Linear and nonlinear fluxes at (60,0,0) due to a 10 dollar/sec local perturbation at (0,60,40) - - - - -	79
23.	Linear and nonlinear fluxes at (-60,0,80) due to a 10 dollar/sec local perturbation at (0,60,40) - - - - -	80
24.	Radial flux distribution for the steady state and 100 dollar/sec local perturbation - - -	81
25.	Axial flux distribution for the steady state and 100 dollar/sec local perturbation - - -	82
26.	Early time history of the neutron flux at core center using mesh I and mesh II - - - - -	83

## ACKNOWLEDGEMENT

The author wishes to thank Professors Dong H. Nguyen and David Salinas for their moral support and professional guidance throughout this work. Sincere appreciation is also expressed to Professor Dick Franke for his priceless assistance in the implementation of the time integration package and to Professor Giles Cantin for his invaluable counsel on finite elements. Special thanks is given to Ed Donnellan, Kris Butler, and Manus Anderson at the NPS Computer Center for their patience and cooperation in running the long computer programs required by this work. Their willingness to help and their professionalism, I am sure, are recognized and greatly appreciated by NPS students. Finally, I wish to thank my wife, Carmen, who had served outstandingly as mother and father to our children during the course of this study.

## I. INTRODUCTION

The nuclear reactor with delayed neutrons and temperature-dependent feedback is a nonlinear system, whose response to uniform and local disturbances differs greatly from that of a linear reactor. The prompt temperature feedback model and one average group of delayed neutrons were incorporated in this work. Practically all neutron dynamics analysis today deals with two-dimensional geometry, implying a symmetry in neutron dynamics behavior during transient [1,2]. This symmetry assumption, however, could be unrealistic in the safety analysis of nuclear reactors. A unique feature of this work is the consideration of the three-dimensional dependence of the neutron flux. No symmetry assumptions were imposed on the problem. This work investigated neutron dynamics under uniform and local disturbances in the core. A uniform initial flux throughout the interior of the reactor was imposed. The finite element method (FEM) was employed to solve this nonlinear initial-boundary value problem. The FEM is quite effective in handling discontinuous forcing functions thereby making it particularly suited for examining the effects of localized perturbations and space-dependent feedbacks.

## II. THE NUCLEAR REACTOR WITH TEMPERATURE DEPENDENT FEEDBACK AND DELAYED NEUTRONS

### A. THE PHYSICAL SYSTEM

The system under consideration is a fast reactor of cylindrical geometry that is composed of two different regions. The reactor core or region I is cylindrical in shape and is fueled by U-235. Region II or the reflector region completely surrounds the core and is composed of U-238. Both regions were assumed to be homogeneous. Table I lists the physical properties and geometry for each region. A schematic of the fast reactor geometry is shown in figure 1.

Temperature and delayed neutron effects were taken into account. Also, a one-velocity or one-group model was assumed, thereby making the velocity independent of spatial or temporal effects. The delayed neutrons were considered only in region I since region II was assumed to be a non-multiplying medium. The temperature effects were also assumed to be only in the core region.

In general form, the one-velocity neutron diffusion equation is [3]

$$\frac{\partial N(\vec{r}, t)}{\partial t} = vD\nabla^2 N - \Sigma_a vN + S(\vec{r}, t) \quad (1)$$

where  $\vec{r} = (x, y, z)$

$D$  = neutron diffusion coefficient

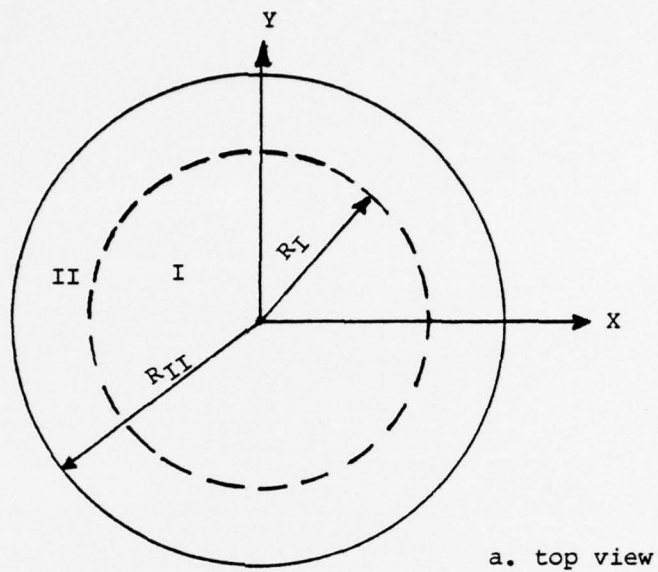
$\Sigma_a$  = macroscopic absorption cross-section

$N(\vec{r}, t)dV$  = number of neutrons in a volume element  $dV$  at a point  $\vec{r}$  at time  $t$

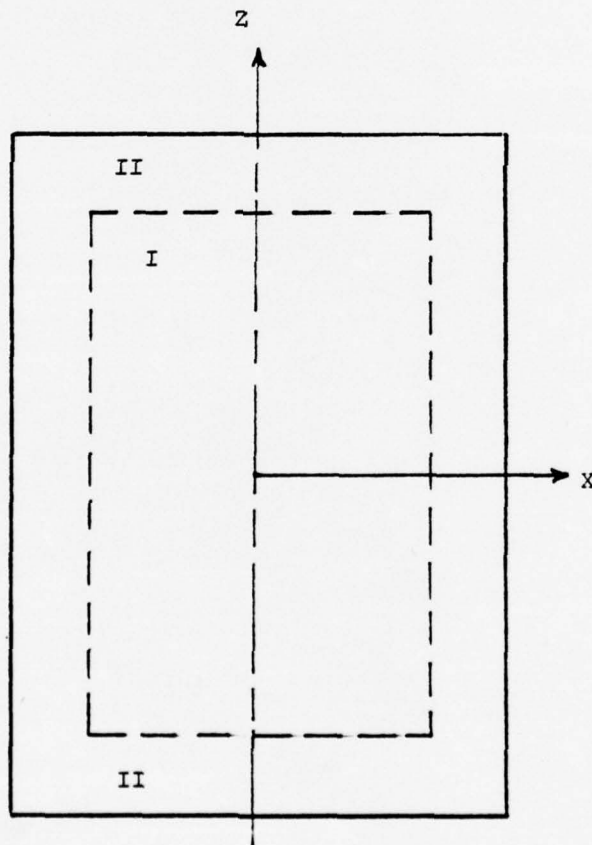


TABLE I  
Physical Constants

<u>SYMBOL</u>	<u>DEFINITION</u>	<u>VALUE</u>
$R_I$	radius of Region I	60 cm
$R_{II}$	total reactor radius	90 cm
$H_I$	height of Region I	160 cm
$H_{II}$	total reactor height	220 cm
$v$	neutron speed	$4.8 \times 10^7$ cm/sec
$D_I$	core neutron diffusion coefficient	0.913 cm
$D_{II}$	reflector neutron diffusion coefficient	1.200 cm
$\Sigma_{a_I}$	core neutron absorption cross section	$0.01401 \text{ cm}^{-1}$
$\Sigma_{a_{II}}$	reflector neutron absorption cross section	$0.0040 \text{ cm}^{-1}$
$\nu$	number of neutrons per fission	2.54
$\Sigma_f^*$	critical fission cross section	$0.005736 \text{ cm}^{-1}$
$\beta$	delayed neutron fraction; dollar reactivity	0.00642
$\epsilon$	fission energy	$7.652 \times 10^{-12}$ cal/fission
$\bar{h}(\frac{A}{V})$	modified convection heat transfer coefficient	0.0632 cal/(cm <sup>2</sup> sec °C)
$\alpha$	temperature coefficient	-0.004/°C
$\bar{\lambda}$	abundance-weighted mean decay constant	$0.4350 \text{ sec}^{-1}$



a. top view



b. front view

I - core  
II - reflector

Figure 1. Schematic of cylindrical reactor.

$vD\nabla^2 NdV$  = number of neutrons diffusing into  $dV$  per unit time at time  $t$

$\Sigma_a vN dV$  = number of neutrons absorbed in  $dV$  per unit time at time  $t$

$S(\bar{r},t)dV$  = number of neutrons produced in  $dV$  per unit time at time  $t$

The neutron number density is related to the neutron flux by the expression [4]

$$\phi(\bar{r},t) = vN(\bar{r},t) \quad (2)$$

where  $\phi(\bar{r},t)$  is the flux at time  $t$ . The neutron diffusion equation in terms of the flux is depicted by

$$\frac{1}{v} \frac{\partial \phi(\bar{r},t)}{\partial t} = D\nabla^2 \phi - \Sigma_a \phi + S(\bar{r},t) \quad (3)$$

#### B. PROMPT AND DELAYED NEUTRONS

The source or production term in equation (3) is composed of the contributions of the prompt and delayed neutrons. The majority of the fission neutrons are prompt neutrons that appear almost instantaneously (within  $10^{-7}$  second) on fission. Assuming a fast neutron non-leakage probability of unity, the prompt neutron source is described by

$$S_p(\bar{r},t) = (1-\beta)K_\infty(\bar{r},t) \phi(\bar{r},t) \quad (4)$$

where

$K_\infty(\bar{r},t)$  = infinite medium multiplication factor

$\beta$  = total fraction of delayed neutrons

The fraction of delayed neutrons is very small (note that  $\beta = 0.00642$  from Table I). However, they have a very significant effect on the reactivity because their mean lifetimes are long. Without delayed neutrons, reactor control would not be possible. These delayed neutrons are born in the decay by neutron emission of nuclei produced following the  $\beta$ -decay of certain fission fragments. For example, the  $\beta$ -decay of the fission fragment  $\text{Br}^{87}$  leads to  $\text{Kr}^{86}$  plus a neutron. Nuclei such as  $\text{Br}^{87}$  whose production in fission eventually leads to the emission of a delayed neutron are called delayed neutron precursors [4].

There are six main groups of delayed neutrons. Each group is classified according to its decay constant. The delayed neutron source term is portrayed by

$$S_d(\vec{r}, t) = \sum_{i=1}^6 C_i(\vec{r}, t) \lambda_i \quad (5)$$

where

$\lambda_i$  = decay constant of the  $i^{\text{th}}$  group

$C_i(\vec{r}, t)$  = density of the  $i^{\text{th}}$  precursor

Assuming that the fission fragments do not migrate appreciable distances and assuming a non-circulating fuel reactor [3], the precursor density is delineated by

$$\frac{\partial C_i(\vec{r}, t)}{\partial t} = \beta_i K_{\infty} \Sigma_a \phi - \lambda_i C_i \quad (6)$$

where  $\beta_i$  is the fraction of delayed neutrons of the  $i^{\text{th}}$



group. The solution to the precursor equation is in terms of a time integral expressed by

$$C_i(\bar{r}, t) = \beta_i \Sigma_a \int_0^t e^{-\lambda_i(t-t')} K_\infty(\bar{r}, t) \phi(\bar{r}, t) dt' \quad (7)$$

Inserting equation (7) in equation (5) yields the delayed neutron production term as

$$S_d(\bar{r}, t) = \sum_{i=1}^6 \beta_i \lambda_i \Sigma_a \int_0^t e^{-\lambda_i(t-t')} K_\infty(\bar{r}, t) \phi(\bar{r}, t) dt' \quad (8)$$

For convenience the six main groups of delayed neutrons were considered as one group. This was accomplished by using the abundance-weighted mean decay constant defined by

$$\bar{\lambda} = \frac{1}{\beta} \sum_{i=1}^6 \beta_i \lambda_i \quad (9)$$

This is a reasonable approximation since many of the important phenomena of nuclear reactor dynamics can be characterized satisfactorily by combining all the emitters or precursors into one, two, or, at most, three effective groups [3]. Replacing  $\lambda_i$  with the abundance-weighted mean decay constant showed the delayed neutron source term to be

$$S_d(\bar{r}, t) = \beta \bar{\lambda} \Sigma_a \int_0^t e^{-\bar{\lambda}(t-t')} K_\infty(\bar{r}, t) \phi(\bar{r}, t) dt' \quad (10)$$

#### C. DOPPLER EFFECT AND TEMPERATURE FEEDBACK MODEL

The Doppler effect in fast reactors is due to the temperature broadening of many closely spaced high-energy resonances in both the fission and parasitic-absorption cross-sections.

These resonances basically mean that as the temperature increases, the number of neutrons that are absorbed increases and, similarly, the number of fission events increases.

These nonproductive and productive processes compete in a complicated manner, and the net effect may be either an increase or decrease in reactivity [3]. For most fast reactors, the effect is negative, and it will be so assumed in this work.

The reactivity change with respect to the fuel temperature change is modeled by [2]

$$\frac{dK_{\infty}}{dT} = aT^{-3/2} + bT^{-1} + cT^{(m-1)} \quad (11)$$

where  $a$ ,  $b$ , and  $c$  are parameters determined from experimental or neutronic calculations,  $m$  is an integer, and  $T$  is the current fuel temperature. For most fast reactor cores (ceramic-fueled cores),  $TdK_{\infty}/dT$  is very close to being constant over a wide range of temperatures. Therefore, it is assumed that  $a$  and  $c$  are zero and the Doppler coefficient is expressed by

$$b = T \frac{dK_{\infty}}{dT} \quad (12)$$

The following initial conditions were used:

$$K_{\infty}(\bar{r}, 0^+) = K_{\infty}^0 \quad (12a)$$

$$T(\bar{r}, 0^+) = T_0 \quad (12b)$$

The reactivity model is then expressed by

$$K_{\infty}(\bar{r}, t) = K_{\infty}^{\circ} + b \ln \left( \frac{T}{T_0} \right) \quad (13)$$

where

- $K_{\infty}^{\circ}$  = multiplication factor at steady-state
- $\nu$  = number of neutrons produced per fission
- $T_0$  = original fuel temperatures
- $b$  = Doppler constant

The definition of  $K_{\infty}^{\circ}$  is

$$K_{\infty}^{\circ} = \frac{\nu \Sigma_f^*}{\Sigma_a} \quad (14)$$

where

- $\Sigma_f^*$  = critical fission cross-section
- $\Sigma_a^c$  = macroscopic absorption cross-section of the core

The rise in fuel temperature is depicted by

$$\theta(\bar{r}, t) = T(\bar{r}, t) - T_0(\bar{r}) \quad (15)$$

This is also described by the integral [5]

$$\theta(\bar{r}, t) = \int_0^t f(t-t') \psi(\bar{r}, t) dt' \quad (16)$$

where  $f(t-t')$  is the feedback kernel and is dependent upon the type of temperature feedback model used.  $\psi(\bar{r}, t)$  is the

rise in neutron flux above the steady state and is expressed by

$$\psi(\bar{r}, t) = \phi(\bar{r}, t) - \phi_0(r) \quad (17)$$

where  $\phi_0(r)$  is the neutron flux at steady state.

There are three types of temperature feedback models that can be considered here. The first is known as "Newton's feedback" which determines the reactor temperature by Newton's law of cooling. The second temperature feedback model is called the adiabatic feedback model. This represents the temperature for the loss of coolant case. The third model is the prompt temperature feedback model in which the fuel temperature follows the behavior of the neutron flux without delay [5,6]. The prompt feedback model was employed in this analysis. The feedback kernel for this temperature feedback model is

$$f(t-t') = \frac{K}{\gamma} \delta(t-t') \quad (18)$$

where  $K$  is an energy production operator with units of  $^{\circ}\text{C}$  per unit flux and  $\gamma$ , a dimensionless quantity, is related to the mean time for heat transfer to coolant.

Inserting equation (18) in equation (16) and performing the integration produced a rise in temperature of

$$\theta(\bar{r}, t) = \frac{K}{\gamma} \psi(\bar{r}, t) \quad (19)$$



From equation (19) the temperature of the fuel is

$$T(\bar{r}, t) = \frac{K}{\gamma} \psi(\bar{r}, t) + T_0(\bar{r}) \quad (20)$$

The ratio of the current temperature to the steady-state temperature is therefore

$$\frac{T}{T_0} = \frac{K}{\gamma T_0} \psi + 1 \quad (21)$$

In this work  $T_0$  was considered to be constant throughout the core. Incorporating equation (21) into equation (13) gave the reactivity model of

$$K_\infty(\bar{r}, t) = K_\infty^0 + b \ln \left[ \frac{K}{\gamma T_0} \psi(\bar{r}, t) + 1 \right] \quad (22)$$

#### D. FIELD EQUATIONS

Before establishing the field equations it is desirable to express equation (3) in terms of the rise in flux. Using equation (17) in equation (3) and grouping terms yielded the following diffusion equation:

$$\begin{aligned} \frac{1}{v} \frac{\partial \psi}{\partial t} = & [D \nabla^2 \psi - \Sigma_a \psi + (1-\beta) K_\infty \Sigma_a \psi + \beta \bar{\lambda} \Sigma_a \int_0^t e^{-\bar{\lambda}(t-t')} K_\infty \psi dt'] \\ & + [D \nabla^2 \phi_0 - \Sigma_a \phi_0 + (1-\beta) K_\infty \Sigma_a \phi_0 + \beta \bar{\lambda} \Sigma_a \int_0^t e^{-\bar{\lambda}(t-t')} K_\infty \phi_0 dt'] \end{aligned} \quad (23)$$

The second bracketed term in equation (23) is identically equal to zero since it is the steady state portion of the

diffusion equation. The rise in neutron flux above its steady state value is therefore expressed, for the core, by

$$\begin{aligned} \frac{1}{v} \frac{\partial \psi}{\partial t} = & D \nabla^2 \psi - \Sigma_a \psi + (1-\beta) K_{\infty} \Sigma_a \psi \\ & + \beta \bar{\lambda} \Sigma_a \int_0^t e^{-\bar{\lambda}(t-t')} K_{\infty} \psi dt' \end{aligned} \quad (24)$$

and, for the reflector region, by

$$\frac{1}{v} \frac{\partial \psi}{\partial t} = D \nabla^2 \psi - \Sigma_a \psi \quad (25)$$

Inserting the reactivity model into equation (24) yielded

$$\begin{aligned} \frac{1}{v} \frac{\partial \psi}{\partial t} = & D \nabla^2 \psi - \Sigma_a \psi + (1-\beta) \Sigma_a K_{\infty}^0 \psi \\ & + (1-\beta) b \Sigma_a \left\{ \ln \left[ \frac{K \psi}{\gamma T_0} + 1 \right] \right\} \psi + \beta \bar{\lambda} K_{\infty}^0 \int_0^t e^{-\bar{\lambda}(t-t')} \psi dt' \\ & + \beta \bar{\lambda} \Sigma_a b \left\{ \int_0^t e^{-\bar{\lambda}(t-t')} \left[ \ln \left( \frac{K \psi}{\gamma T_0} + 1 \right) \right] \psi dt' \right\} \end{aligned} \quad (26)$$

For the reflector, the last four terms of equation (26) are zero. The effects of the temperature on the delayed neutrons were neglected in this work. The field equations can now be expressed, for the core, as

$$\begin{aligned} \frac{\partial \psi}{\partial t} - v D \nabla^2 \psi + [v \Sigma_a - v(1-\beta) v \Sigma_f] \psi \\ + [-(1-\beta) v \Sigma_a b] \left[ \ln \left( \frac{K \psi}{\gamma T_0} + 1 \right) \right] \psi \\ + [-\beta \bar{\lambda} v \Sigma_f v] \left[ \int_0^t e^{-\bar{\lambda}(t-t')} \psi dt' \right] = 0 \end{aligned} \quad (27)$$

and, for the reflector, as

$$\frac{\partial \psi}{\partial t} - v D \nabla^2 \psi + v \Sigma_a \psi = 0 \quad (28)$$

The non-linear terms of the core field equation will be linearized accordingly. In more compact form, equations (27) and (28) became

$$\frac{\partial \psi}{\partial t} - c_1 \nabla^2 \psi + c_2 \psi + c_4 \left[ \ln \left( \frac{K \psi}{\gamma T_0} + 1 \right) \right] \psi + c_5 \left[ \int_0^t e^{-\bar{\lambda}(t-t')} \psi dt' \right] = 0 \quad (29)$$

and

$$\frac{\partial \psi}{\partial t} - c_1 \nabla^2 \psi + c_2 \psi = 0 \quad (30)$$

where the meanings of the coefficients  $c_1$ ,  $c_2$ , etc., are obvious for the core and reflector.

Equations (29) and (30) were subjected to the following conditions:

boundary condition:

$$\psi_R(\bar{r}_B, t) = 0 \quad (31)$$

where  $\bar{r}_B$  are coordinates of points on the outer surface of the reflector and the subscript  $R$  refers to the reflector  
continuity of flux:

$$\psi_R(\bar{r}, t) = \psi_c(\bar{r}_I, t) \quad (32)$$

where  $\bar{r}_I$  are coordinates of points on the core-reflector interface and the subscript  $c$  refers to the core.

### III. FINITE ELEMENT

#### A. INTRODUCTION

The application of the finite elements of nonlinear continua has been mostly in the field of solid mechanics. Prior work [1] using the finite elements of nonlinear continua on a nonlinear reactor dynamics problem has been successful. The FEM in this work was utilized to reduce a nonlinear partial differential equation of the nuclear reactor to a system of nonlinear ordinary differential equations in time. The time integration was accomplished by using a computer program for the numerical solution of stiff differential equations developed by Franke [7]. In order to minimize computer storage requirements, an optimum compacting scheme (OCS), described by Ref. 8, was adopted.

The finite element models of operator equations are generally classified into three categories: a) the variational finite element models such as the Ritz method, b) the weighted residuals method such as the method of Galerkin, and c) the direct finite element models which are not based on functional minimization. From experience in structural mechanics, the most effective method for generating acceptable finite element models of nonlinear equations is the Galerkin method [1]. This work adopted the method of Galerkin in a finite element approximation over the spatial domain of the field equations.



## B. THE METHOD OF GALERKIN

The Galerkin method is a special case of the method of weighted residuals. It involves a rational choice of weighting function that is consistent with the type of finite element approximation considered. Indeed, the weighting functions chosen are the basis or shape functions employed in the finite element approximation. There are two favorable characteristics of the Galerkin method which makes it attractive. The first attribute is its amenability to integration by parts. This supplied the freedom of using a lower order finite element than might be otherwise possible. The second favorable characteristic of the Galerkin method is that the symmetric operators in the field equations transform into symmetric matrix operators. Both these attributes are attractive for computational purposes.

Consider the initial-boundary-value problem

$$\frac{\partial \psi}{\partial t} = \mathcal{L}\psi - f(\bar{r}, t) \quad (33)$$

where  $\mathcal{L}$  contains the nonlinear operators. According to the spatial finite element discretization, the solution of equation (33) is in the form of an union of an  $\bar{N}$ -term approximation given by

$$\psi(\bar{r}, t) \approx \tilde{\psi}(\bar{r}, t) = \bigcup_{j=1}^{\bar{N}} \psi_j(t) G_j(\bar{r}) , \quad j=1, 2, \dots, \bar{N} \quad (34)$$

where  $\bar{N}$  is the number of system degrees of freedom (i.e., number of coordinates), and  $G_j(\bar{r})$  are the system or global basis functions which span the space of the approximate

solution  $\tilde{\psi}(\bar{r}, t)$  [1]. The Einstein summation is used. The global basic functions are "pyramid functions", each of which has a prescribed functional description over a sub-domain of the system and is zero elsewhere [9]. The unknown coordinate functions  $\psi_j(t)$  are the time-dependent magnitudes of the approximated flux  $\tilde{\psi}(\bar{r}, t)$  and/or its derivatives at discrete nodal points [10].

The residual function,  $R(\bar{r}, t)$ , is defined such that it is identical to zero when  $\tilde{\psi}(\bar{r}, t)$  is equal to the exact solution. The residual function is expressed by

$$R(\bar{r}, t) = \frac{\partial \tilde{\psi}}{\partial t} - \mathcal{L} \tilde{\psi} - f \quad (35)$$

The Galerkin orthogonality condition (using the basis functions as weight functions), when applied to the residual function, requires that

$$\int_{Vol} G_I R(\bar{r}, t) dVol = 0, \quad I=1, 2, \dots, \bar{N} \quad (36)$$

From the field equations, the residual function for the core is

$$\begin{aligned} R(\bar{r}, t) = & \frac{\partial \tilde{\psi}}{\partial t} - c1 \nabla^2 \tilde{\psi} + c2 \tilde{\psi} + c4 \left[ \ln \left( \frac{K \tilde{\psi}}{\gamma T_0} + 1 \right) \right] \tilde{\psi} \\ & + c5 \left[ \int_0^t e^{-\bar{\lambda}(t-t')} \tilde{\psi} dt' \right] \end{aligned} \quad (37)$$

and for the reflector

$$R(\bar{r}, t) = \frac{\partial \tilde{\psi}}{\partial t} - c1 \nabla^2 \tilde{\psi} + c2 \tilde{\psi} \quad (38)$$

Using equation (34) and applying Galerkin's orthogonality condition produced a core equation of

$$\begin{aligned} \int_{Vol} G_I \{ G_J \dot{\psi}_J(t) - \nabla^2 G_J(c1 \cdot \psi)_J + G_J(c2 \cdot \psi)_J \\ + [\ln(\frac{K}{\gamma T_0} G_K \psi_K + 1)] G_J(c4 \cdot \psi)_J \\ + [\int_0^t e^{-\bar{\lambda}(t-t')} (c5 \cdot \psi)_J dt'] G_J \} = 0 \end{aligned} \quad (39)$$

where  $I = 1, 2, \dots, \bar{N}$   
 $J = 1, 2, \dots, \bar{N}$   
 $K = 1, 2, \dots, \bar{N}$

The reflector has a similar equation without the nonlinearity and is expressed by

$$\int_{Vol} G_I \{ G_J \dot{\psi}_J(t) - \nabla^2 G_J(c1 \cdot \psi)_J + G_J(c2 \cdot \psi)_J \} dVol = 0 \quad (40)$$

### C. THE ELEMENT

A three-dimensional quadratic isoparametric element was employed in this work. The parent element is a triangular prism or solid wedge with straight sides. The element shape functions are expressed in terms of area coordinates in the plane of the triangle and by an isoparametric coordinate

along the prism axis. Figure 2 shows the parent element. This element was chosen because of the ease with which it fits the cylindrical structure when it is transformed into a curved element. This type of element has been used before as filler elements [11].

The area coordinates are defined by area ratios. Consider the triangle shown in figure 3. An arbitrary point P within the triangle defines three subareas designated by  $A_1$ ,  $A_2$ , and  $A_3$ . The ratio of each of the subareas to the total area is known as an area coordinate. In equation form, the area coordinates are

$$L_1 = A_1/A \quad (41a)$$

$$L_2 = A_2/A \quad (41b)$$

$$L_3 = A_3/A \quad (41c)$$

where  $A$  is total area of the triangle.  $L_1$ ,  $L_2$ , and  $L_3$  are the natural coordinates for a triangle. The requirement that the sum of the subareas be equal to the total area is obviously satisfied by the identity

$$L_1 + L_2 + L_3 = 1 \quad (42)$$

In the plane of the triangle, only two of the area coordinates are independent.

The isoparametric coordinates are best visualized by considering the rectangular prism shown in figure 4. Isoparametric coordinates are normalized coordinates such that their values on the faces of the rectangle are  $\pm 1$ . The  $\xi\eta\zeta$  axes are in general not orthogonal. They are orthogonal

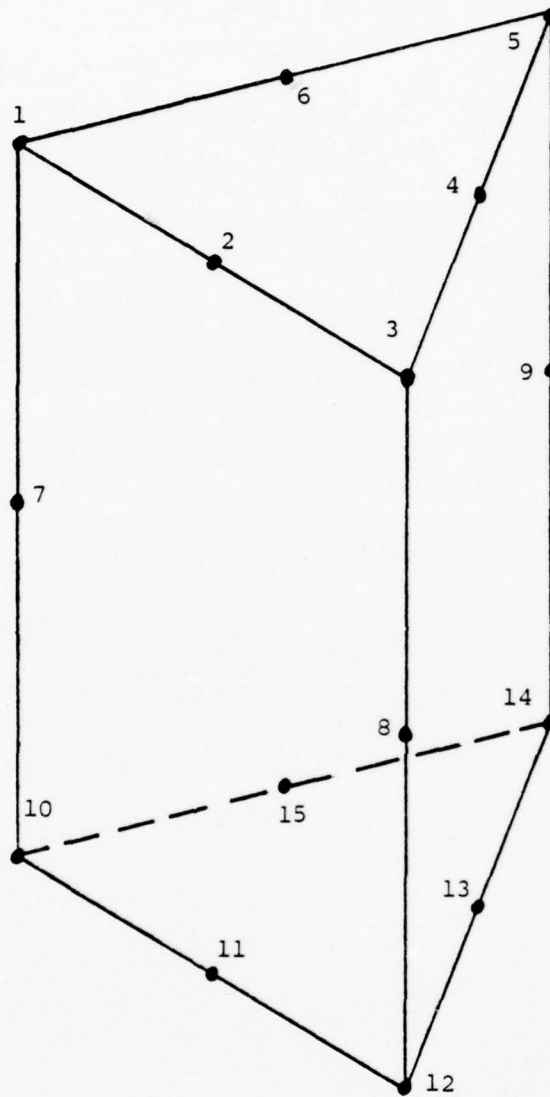


Figure 2. Quadratic triangular prism parent element



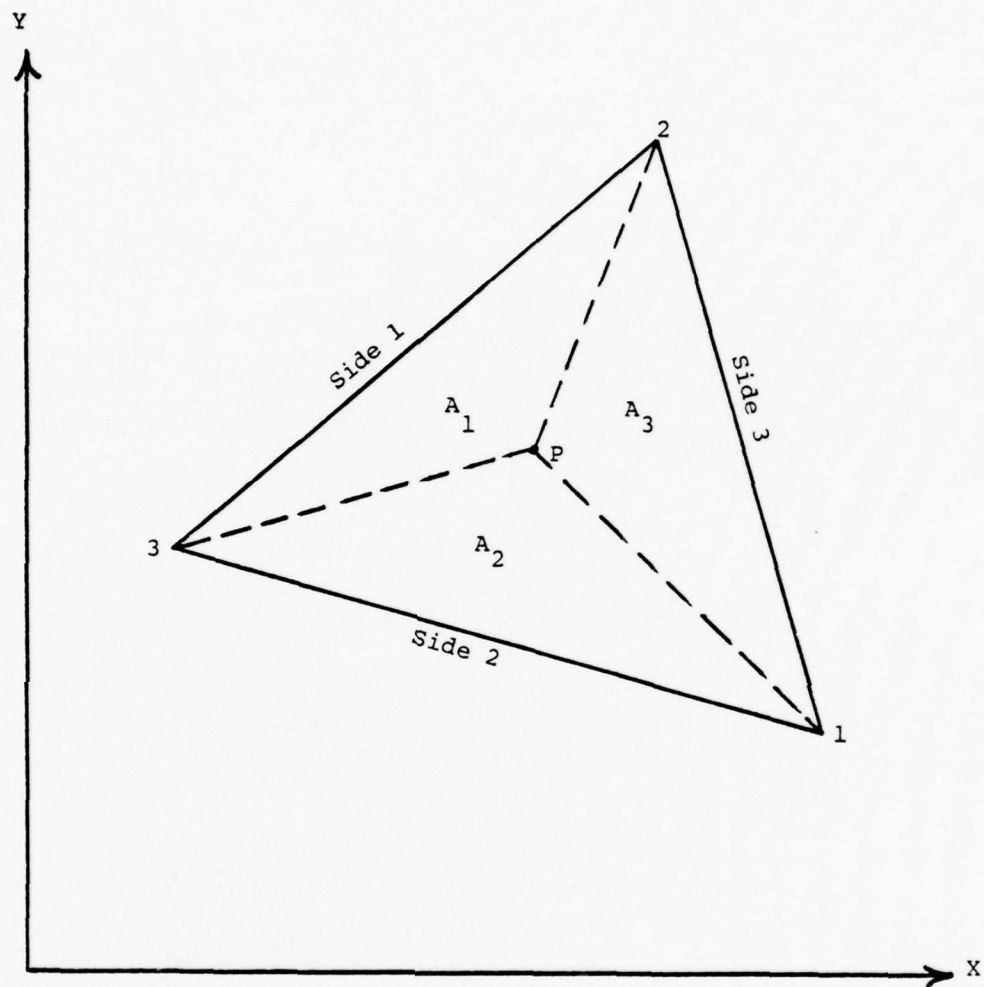


Figure 3. Definition of area coordinates

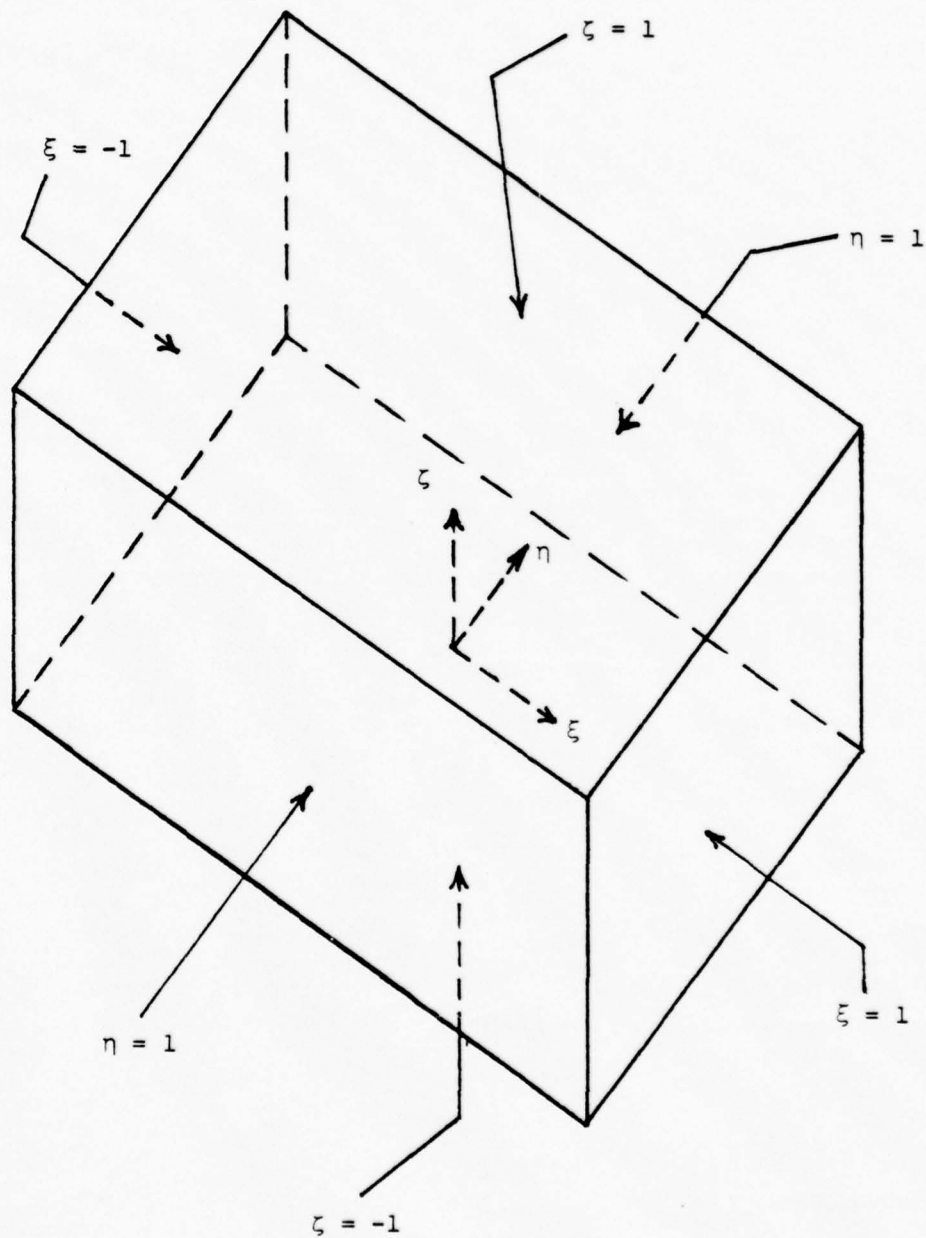


Figure 4. Isoparametric coordinates

only in the special case of a rectangular prism element [12]. The element basis functions use the  $\zeta$  coordinate in the prism axis and the  $L_1$ ,  $L_2$ , and  $L_3$  coordinates in the plane of the triangle.

The parent element, as shown in figure 2, has 15 local nodal points around its periphery. As such, there are 15 basis functions which are given below [11]:

Corner nodes: (nodes 1, 3, 5, 10, 12, 14)

$$N_1 = \frac{1}{2} L_1 (2L_1 - 1)(1 + \zeta) - \frac{1}{2} L_1 (1 - \zeta^2)$$

$$N_3 = \frac{1}{2} L_2 (2L_2 - 1)(1 + \zeta) - \frac{1}{2} L_2 (1 - \zeta^2)$$

$$N_5 = \frac{1}{2} L_3 (2L_3 - 1)(1 + \zeta) - \frac{1}{2} L_3 (1 - \zeta^2)$$

$$N_{10} = \frac{1}{2} L_1 (2L_1 - 1)(1 - \zeta) - \frac{1}{2} L_1 (1 - \zeta^2)$$

$$N_{12} = \frac{1}{2} L_2 (2L_2 - 1)(1 - \zeta) - \frac{1}{2} L_2 (1 - \zeta^2)$$

$$N_{14} = \frac{1}{2} L_3 (2L_3 - 1)(1 - \zeta) - \frac{1}{2} L_3 (1 - \zeta^2)$$

Midside nodes of rectangles: (nodes 7, 8, 9)

$$N_7 = L_1 (1 - \zeta^2)$$

$$N_8 = L_2 (1 - \zeta^2)$$

$$N_9 = L_3 (1 - \zeta^2)$$

Midside nodes of triangles: (nodes 2, 4, 6, 11, 13, 15)

$$N_2 = 2L_1 L_2 (1 + \zeta)$$

$$N_4 = 2L_2 L_3 (1 + \zeta)$$

$$N_6 = 2L_3 L_1 (1 + \zeta)$$

$$N_{11} = 2L_1 L_2 (1 - \zeta)$$

$$N_{13} = 2L_2 L_3 (1 - \zeta)$$

$$N_{15} = 2L_3 L_1 (1 - \zeta)$$



The coordinates of each local node, in terms of  $L_1$ ,  $L_2$ ,  $L_3$ , and  $\zeta$  are listed in table II. These element basis functions  $\langle N \rangle$  define the geometry of the element. Note that they satisfy the relationship

$$N_i = \begin{cases} 1, & \text{at node } i \\ 0, & \text{at other nodes} \end{cases} \quad (43)$$

On the element level, the variation of the unknown function  $\psi$  is approximated by

$$\tilde{\psi}^e = \langle N' \rangle \{ \psi \}^e \quad (44)$$

where  $\langle N' \rangle$  = row vector of element shape functions  
 $\{ \psi \}^e$  = column vector of time-dependent nodal values of  $\tilde{\psi}^e$

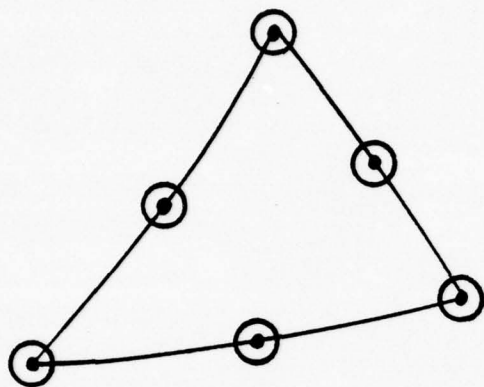
To satisfy continuity requirements, the shape functions  $\langle N' \rangle$  have to be such that the continuity of the unknown function  $\psi$  is preserved in the parent coordinates [11].

The shape functions  $\langle N \rangle$  which characterize the element geometry and the shape functions  $\langle N' \rangle$  which describe the unknown function do not necessarily have to be the same. There is no requirement that the nodal values be associated with the same nodes which were used to define the element geometry, though in practice it is often the case. Consider for example, the illustrations in figure 5. If the nodes defining the element geometry and the nodes defining the

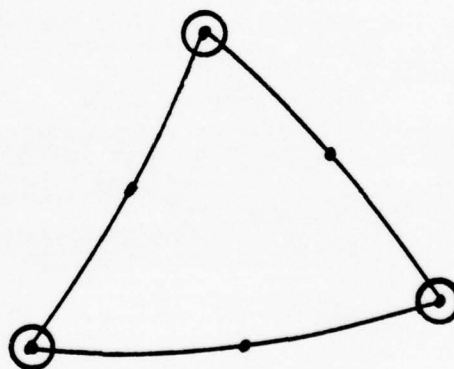
TABLE II

Coordinates of Local Nodal Points

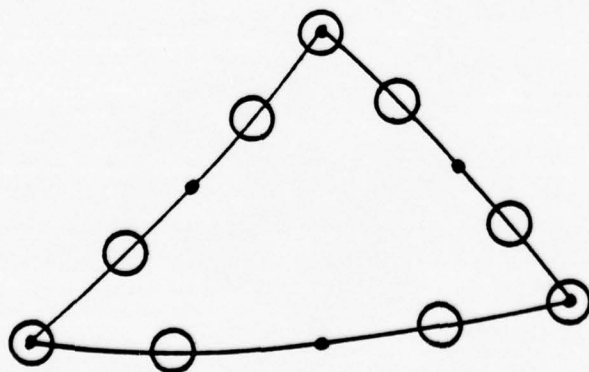
Local Node	$L_1$	$L_2$	$L_3$	5
1	1	0	0	1
2	$\frac{1}{2}$	$\frac{1}{2}$	0	1
3	0	1	0	1
4	0	$\frac{1}{2}$	$\frac{1}{2}$	1
5	0	0	1	1
6	$\frac{1}{2}$	0	$\frac{1}{2}$	1
7	1	0	0	0
8	0	1	0	0
9	0	0	1	0
10	1	0	0	-1
11	$\frac{1}{2}$	$\frac{1}{2}$	0	-1
12	0	1	0	-1
13	0	$\frac{1}{2}$	$\frac{1}{2}$	-1
14	0	0	1	-1
15	$\frac{1}{2}$	0	$\frac{1}{2}$	-1



(a) Isoparametric



(b) Super-parametric



(c) Sub-parametric

- - geometry nodes
- - variable function nodes

Figure 5. Element classification

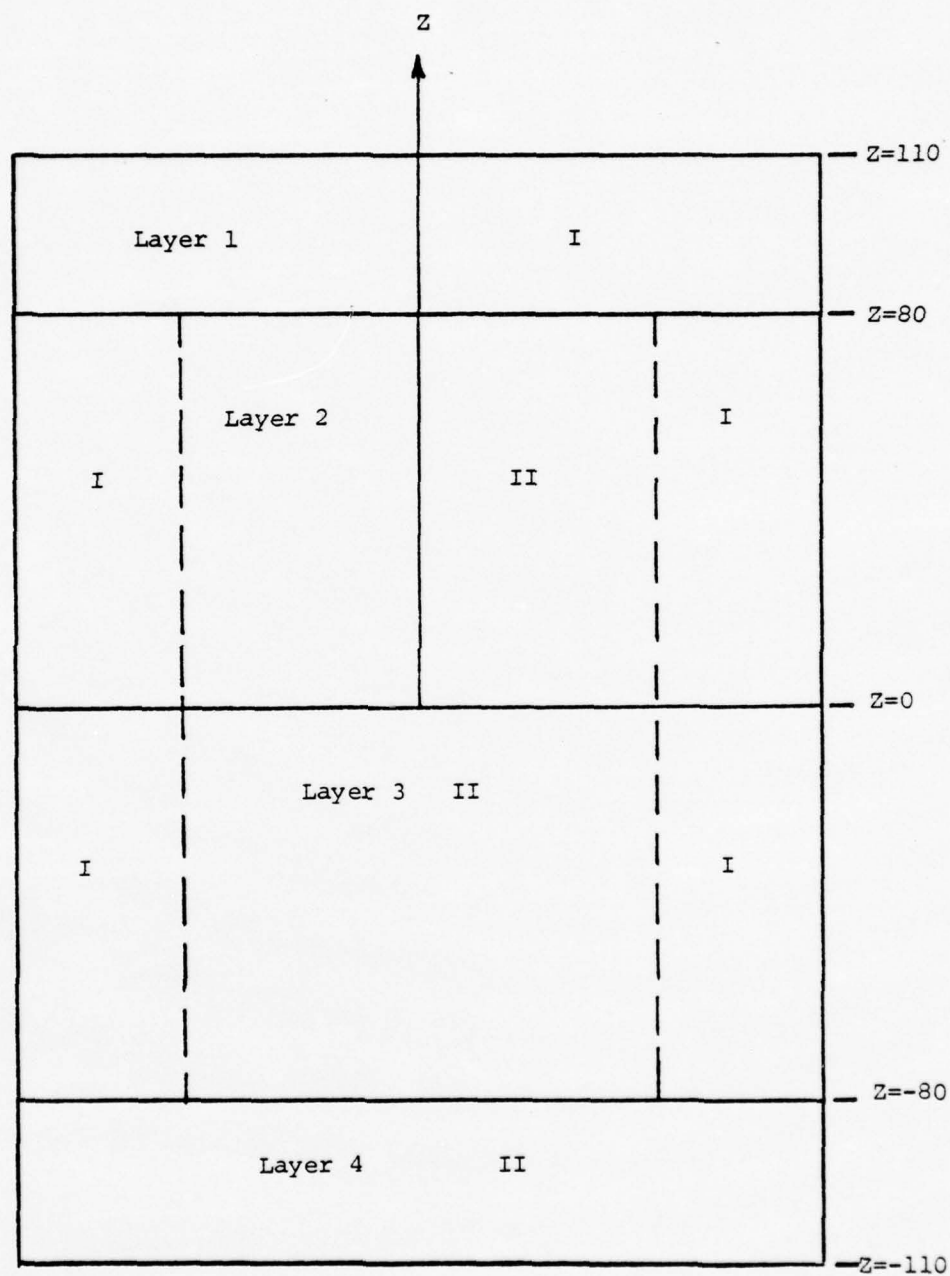
unknown function are identical, the element is known as an isoparametric element. This means that the shape functions describing the geometry and the shape functions describing the unknown function  $\psi$  are equal, or

$$\langle N' \rangle = \langle N \rangle \quad (45)$$

If there are more nodes defining the geometry than nodes defining the variable function, the element is called a superparametric element. Using more nodal points to define the unknown function than to describe the geometry of the element results in a subparametric element [11]. This work utilized the isoparametric element classification.

#### D. DIVISION OF THE SYSTEM INTO ELEMENTS

In three-dimensional space, the division of the system into discrete elements is difficult to visualize. It is virtually impossible to show every nodal point of the system in one schematic. To present a clear view of the discretized domain, a "layer" approach was adopted. The first finite element grid or mesh employed here consisted of 128 elements. Under this grid (mesh I), the reactor was divided into four layers as shown in figure 6. Each layer was composed of 32 elements. The first and fourth layers were each 30 cm in height and each contained entirely reflector elements. The second and third layers were each 80 cm in height and together they encompassed the entire core plus the remaining reflector elements. Each layer, in turn, was partitioned into three horizontal (xy) planes. The top plane included all the global



I - core      II - reflector

Figure 6. Layers of mesh I



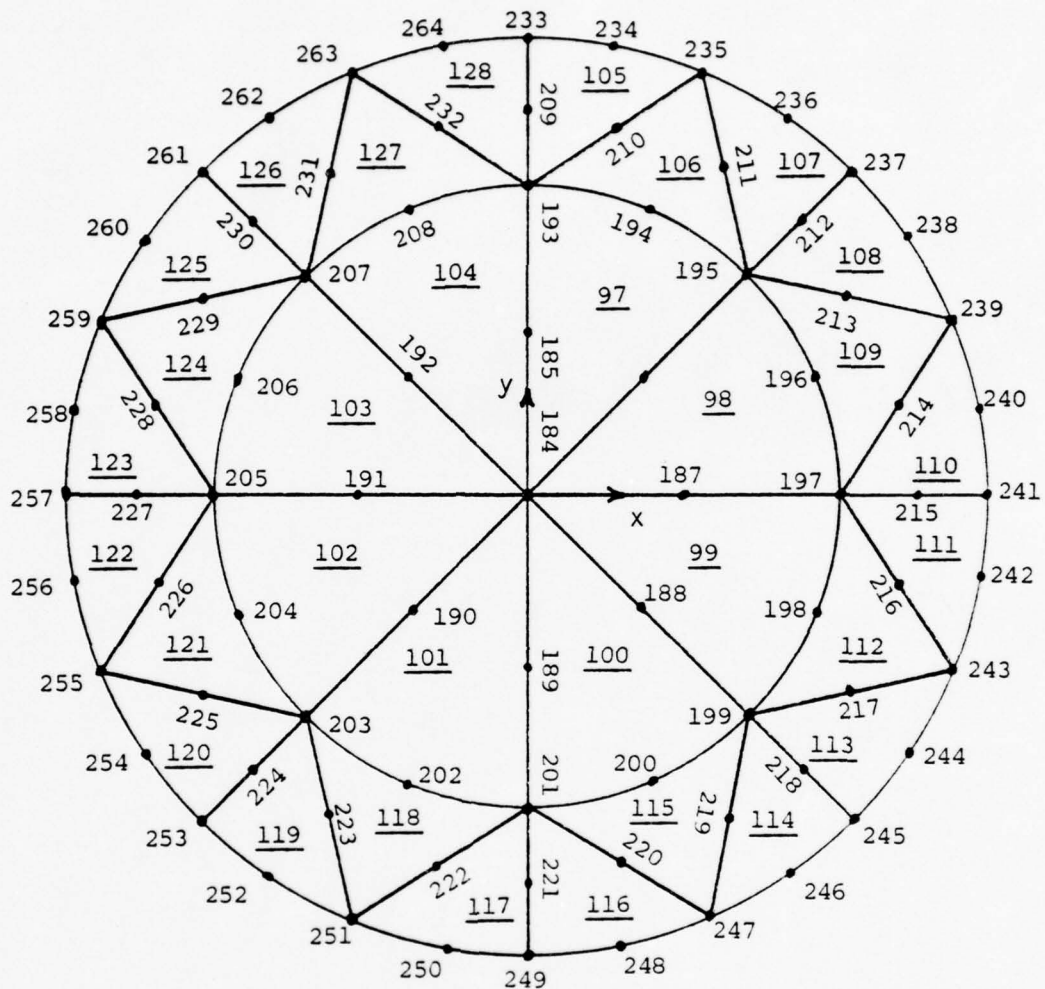
or system nodes corresponding to local or element nodes 1 through 6. The middle plane contained all the system nodes corresponding to the local nodes 7, 8, and 9. System nodes corresponding to element nodal points 10 through 15 comprised the bottom plane. To fix ideas, the three nodal planes of the first layer of mesh I are shown in figures 7, 8, and 9.

In this work there was only one curved side which was in the plane of the triangle, as shown in figure 10. The first, seventh, and tenth element nodes were each arbitrarily assigned to have as an opposite side the curved side of the triangle. The remaining local nodes in each of the respective planes of the element were then numbered consecutively in the counter-clockwise direction.

At this point it is appropriate to define connectivity. The connectivity of an element is a row vector array that relates the local nodes to system nodal points. The connectivity lists the system nodal points that are "connected" to form the element domain in the sequence of local nodal numbering. Thus, the connectivity matrix for mesh I is a matrix of size  $128 \times 15$ . To illustrate, the connectivity of element number 106 is

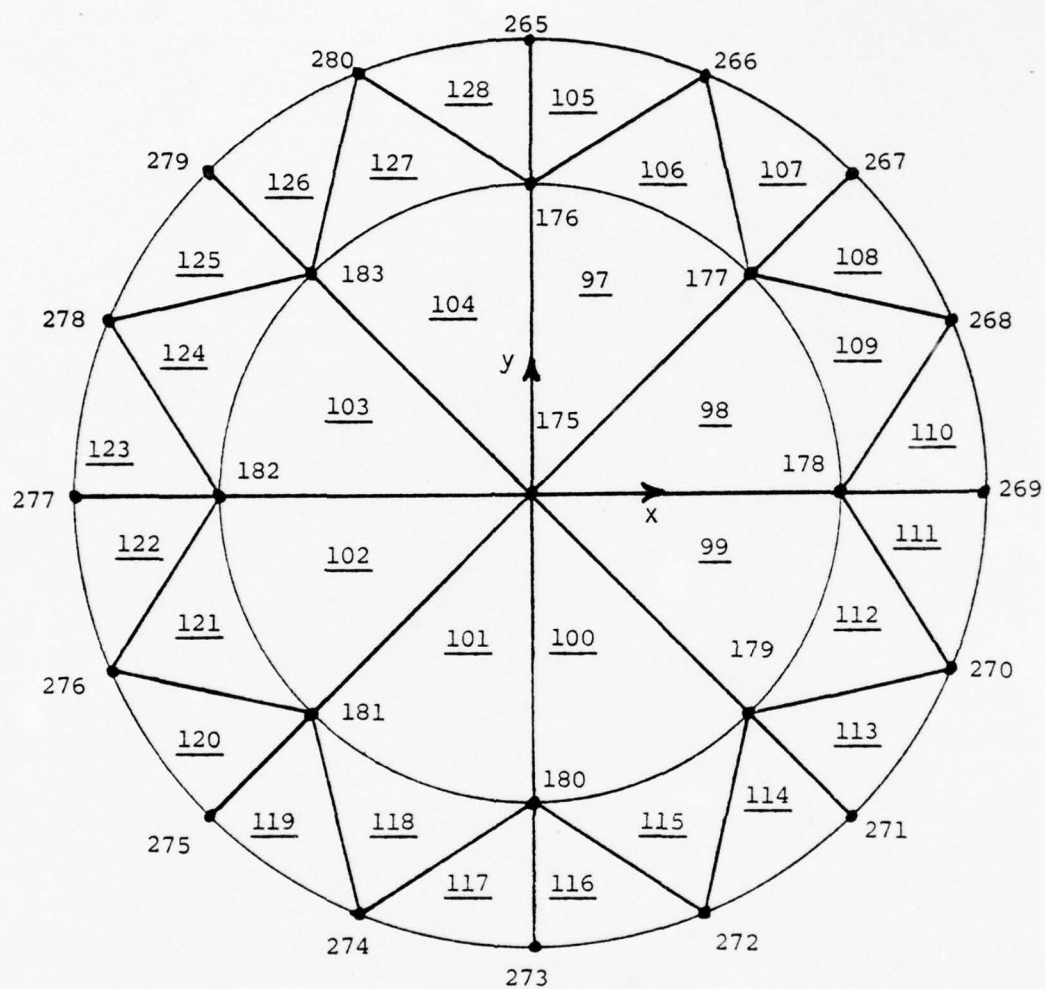
<235, 210, 193, 194, 195, 211, 266, 176, 177, 283, 152, 10, 11, 12, 53>

A second finite element mesh (mesh II) consisting of 192 elements was developed. It contained the same number of elements per layer as mesh I. However, mesh II has six layers. The second and third layers of mesh I were each divided in



Number - element number

Figure 7. Top nodal plane of the first layer of mesh I,  
z = 110 cm



Number - element number

Figure 8. Middle nodal plane of the first layer of mesh I,  $z = 95$  cm



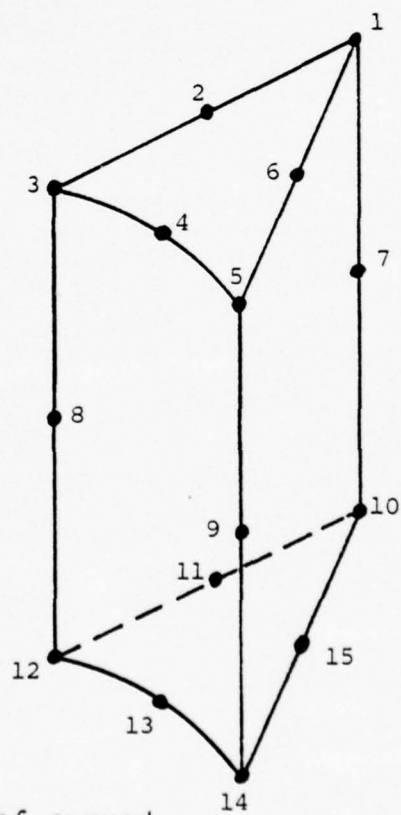
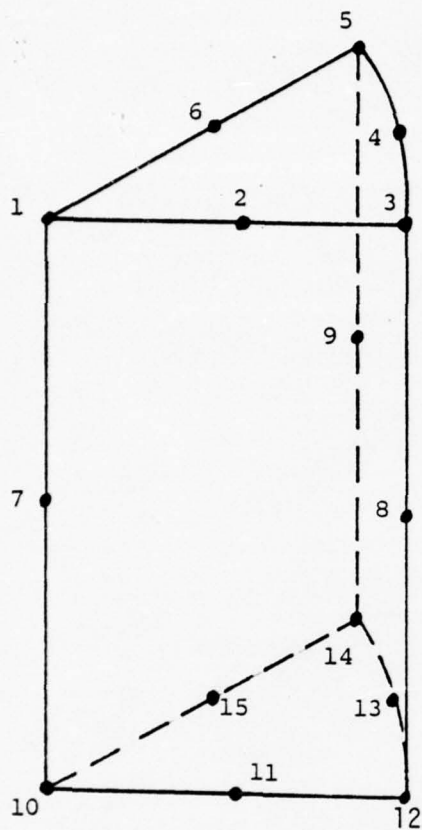


Figure 10. Local nodal numbering of curved elements



half, thus forming the two additional layers of mesh II. The connectivity matrix and the coordinates of each global node for mesh I are given in Appendix A. Appendix B lists the connectivity matrix and nodal coordinates of mesh II. The reader can construct the different layers and elements without much difficulty by using the nodal coordinates and the connectivity matrix. A mesh generator was not utilized in this work.

#### E. COORDINATE TRANSFORMATION

The use of a quadratic or higher order element permits the transformation or mapping of the straight-sided parent element into an element with curved sides. Distorted or curved elements provide a better fit to curved domains than linear elements, and thus a smaller number of elements is required to represent the structure adequately.

The transformation from cartesian coordinates to curvilinear coordinates can be accomplished by employing a one-to-one correspondence defined by [11]

$$\begin{pmatrix} x \\ y \\ z \end{pmatrix} = f \begin{pmatrix} \xi \\ \eta \\ \zeta \end{pmatrix} \quad \text{or} \quad f \begin{pmatrix} L_1 \\ L_2 \\ L_3 \\ \xi \end{pmatrix} \quad (46)$$

The element shape functions are utilized to achieve this transformation via the relation

$$\begin{pmatrix} x \\ y \\ z \end{pmatrix} = \begin{pmatrix} \sum_i N_i x_i \\ \sum_i N_i y_i \\ \sum_i N_i z_i \end{pmatrix}, \quad i=1,2,\dots,n^e \quad (47)$$

where  $n^e$  is the number of element nodes, and the element shape functions  $N_i$  are in terms of local coordinates. Each set of local coordinates corresponds to only one set of cartesian coordinates.

In performing the transformation, the compatibility requirement must be met. The transformation into the new, curved elements should leave no gaps between adjacent elements. If two adjacent elements are generated from parents in which the element shape functions satisfy continuity requirements, then the curved elements will be contiguous [11]. For the isoparametric element, uniqueness of coordinates ensures compatibility. Continuity is assured when adjacent elements are given the same sets of coordinates at common nodes.

Since the element shape functions are in terms of local coordinates, an element of volume,  $dx dy dz$ , must be transformed into an element of volume expressed in local coordinates. This is achieved through the use of the Jacobian matrix defined below. Using the chain rule, the relationship between  $\xi, \eta, \zeta$  and a corresponding set of cartesian coordinates  $x, y, z$  is

$$\begin{Bmatrix} \frac{\partial N_i}{\partial \xi} \\ \frac{\partial N_i}{\partial \eta} \\ \frac{\partial N_i}{\partial \zeta} \end{Bmatrix} = \begin{bmatrix} \frac{\partial x}{\partial \xi} & \frac{\partial y}{\partial \xi} & \frac{\partial z}{\partial \xi} \\ \frac{\partial x}{\partial \eta} & \frac{\partial y}{\partial \eta} & \frac{\partial z}{\partial \eta} \\ \frac{\partial x}{\partial \zeta} & \frac{\partial y}{\partial \zeta} & \frac{\partial z}{\partial \zeta} \end{bmatrix} \begin{Bmatrix} \frac{\partial N_i}{\partial x} \\ \frac{\partial N_i}{\partial y} \\ \frac{\partial N_i}{\partial z} \end{Bmatrix} \quad (48)$$

The Jacobian matrix  $[J]$  is defined as

$$[J] = \begin{bmatrix} \frac{\partial x}{\partial \xi} & \frac{\partial y}{\partial \xi} & \frac{\partial z}{\partial \xi} \\ \frac{\partial x}{\partial \eta} & \frac{\partial y}{\partial \eta} & \frac{\partial z}{\partial \eta} \\ \frac{\partial x}{\partial \zeta} & \frac{\partial y}{\partial \zeta} & \frac{\partial z}{\partial \zeta} \end{bmatrix} \quad (49)$$

From equation (47), the Jacobian matrix becomes

$$[J] = \begin{bmatrix} \sum_i \frac{\partial N_i}{\partial \xi} x_i & \sum_i \frac{\partial N_i}{\partial \xi} y_i & \sum_i \frac{\partial N_i}{\partial \xi} z_i \\ \sum_i \frac{\partial N_i}{\partial \eta} x_i & \sum_i \frac{\partial N_i}{\partial \eta} y_i & \sum_i \frac{\partial N_i}{\partial \eta} z_i \\ \sum_i \frac{\partial N_i}{\partial \zeta} x_i & \sum_i \frac{\partial N_i}{\partial \zeta} y_i & \sum_i \frac{\partial N_i}{\partial \zeta} z_i \end{bmatrix} \quad (50)$$

The determinant of the Jacobian is used to transform the volume of element in cartesian coordinates to local coordinates. For a volume of element [11],

$$dx dy dz = \det [J] d\xi d\eta d\zeta \quad (51)$$

Note that the determinant of the Jacobian is a variable for elements of curved geometry. Only in the case of straight-sided elements is the determinant of the Jacobian a constant.

In the plane of the triangle, the area coordinates ( $L_1, L_2, L_3$ ) number one more than the cartesian coordinates ( $x, y$ ). Thus,  $L_3$  is defined as a dependent variable. This establishes the origin of the  $\xi\eta$  coordinate system at corner point 3, as

illustrated in figure 11. Recall that the  $\xi\eta$  axes need not be orthogonal. As such

$$\xi = L_1 \quad (52a)$$

$$\eta = L_2 \quad (52b)$$

Using equation (42),

$$L_3 = 1 - \xi - \eta \quad (52c)$$

Applying the chain rule yields

$$\frac{\partial N_i}{\partial \xi} = \frac{\partial N_i}{\partial L_1} \frac{\partial L_1}{\partial \xi} + \frac{\partial N_i}{\partial L_2} \frac{\partial L_2}{\partial \xi} + \frac{\partial N_i}{\partial L_3} \frac{\partial L_3}{\partial \xi} \quad (53a)$$

$$\frac{\partial N_i}{\partial \eta} = \frac{\partial N_i}{\partial L_1} \frac{\partial L_1}{\partial \eta} + \frac{\partial N_i}{\partial L_2} \frac{\partial L_2}{\partial \eta} + \frac{\partial N_i}{\partial L_3} \frac{\partial L_3}{\partial \eta} \quad (53b)$$

Using equations (52a), (52b), and (52c) in equations (53a) and (53b) gives

$$\frac{\partial N_i}{\partial \xi} = \frac{\partial N_i}{\partial L_1} - \frac{\partial N_i}{\partial L_3} \quad (54a)$$

$$\frac{\partial N_i}{\partial \eta} = \frac{\partial N_i}{\partial L_2} - \frac{\partial N_i}{\partial L_3} \quad (54b)$$

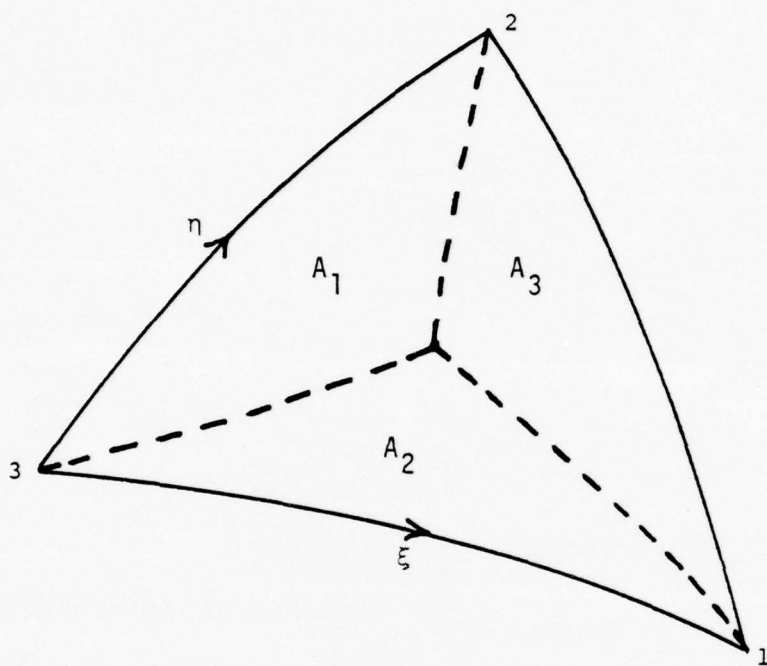


Figure 11.  $\eta\xi$  coordinates in a triangle



Now the Jacobian matrix can be evaluated using the shape functions  $N_i = N_i(L_1, L_2, L_3, \zeta)$ . Inserting equations (54a) and (54b) in equation (50) produces

$$[J(L_1, L_2, L_3, \zeta)] = \begin{bmatrix} \sum_i \left( \frac{\partial N_i}{\partial L_1} - \frac{\partial N_i}{\partial L_3} \right) x_i & \sum_i \left( \frac{\partial N_i}{\partial L_1} - \frac{\partial N_i}{\partial L_3} \right) y_i & \sum_i \left( \frac{\partial N_i}{\partial L_1} - \frac{\partial N_i}{\partial L_3} \right) z_i \\ \sum_i \left( \frac{\partial N_i}{\partial L_2} - \frac{\partial N_i}{\partial L_3} \right) x_i & \sum_i \left( \frac{\partial N_i}{\partial L_2} - \frac{\partial N_i}{\partial L_3} \right) y_i & \sum_i \left( \frac{\partial N_i}{\partial L_2} - \frac{\partial N_i}{\partial L_3} \right) z_i \\ \sum_i \left( \frac{\partial N_i}{\partial \zeta} \right) x_i & \sum_i \left( \frac{\partial N_i}{\partial \zeta} \right) y_i & \sum_i \left( \frac{\partial N_i}{\partial \zeta} \right) z_i \end{bmatrix} \quad (55)$$

To summarize, suppose it is required to transform the integral

$$I = \int_{Vol} F'(L_1, L_2, L_3, \zeta) \, dx dy dz \quad (56)$$

to an integral entirely in terms of local coordinates. The determinant of equation (55) is then utilized to give

$$I = \int_{-1}^1 \int_0^1 \int_0^{1-L_1} F'(L_1, L_2, L_3, \zeta) \det[J(L_1, L_2, L_3, \zeta)] dL_1 dL_2 d\zeta \quad (57)$$

Equation (56) is now in a form suitable for numerical integration.

The development of coordinate transformation to this point has been under the general assumption that all the sides of the element are curved. In this work, the only

curved side is in the plane of the triangle. The sides of the element along the prism axis are straight. As such, a modified Jacobian matrix can be employed, thereby reducing the number of calculations to be performed. This modified Jacobian is the 2x2 matrix defined by

$$[J^*] = \begin{bmatrix} \sum_i \left( \frac{\partial N_i}{\partial L_1} - \frac{\partial N_i}{\partial L_3} \right) x_i & \sum_i \left( \frac{\partial N_i}{\partial L_1} - \frac{\partial N_i}{\partial L_3} \right) y_i \\ \sum_i \left( \frac{\partial N_i}{\partial L_2} - \frac{\partial N_i}{\partial L_3} \right) x_i & \sum_i \left( \frac{\partial N_i}{\partial L_1} - \frac{\partial N_i}{\partial L_3} \right) y_i \end{bmatrix} \quad (58)$$

Along the prism axis or  $\zeta$  direction, it can be shown that

$$dz = \frac{h}{2} d\zeta \quad (59)$$

where  $h$  = height of the element. The volume relationship is then given by

$$dxdydz = \frac{h}{2} \det[J^*] dL_1 dL_2 d\zeta \quad (60)$$

The integral of equation (56) then assumes the form of

$$I = \frac{h}{2} \int_{-1}^1 \int_0^1 \int_0^{1-L_1} F(L_1, L_2, L_3, \zeta) \det[J^*(L_1, L_2, L_3, \zeta)] dL_1 dL_2 d\zeta \quad (61)$$

Equation (61) is the basis of numerical integration applied in this work.

#### F. CONSTRUCTION OF ELEMENT MATRICES

The system matrix operators can be constructed through the use of the global basis functions  $G_j$  or through the

application of the element shape functions. Although the global basis functions were used to demonstrate the method of Galerkin, the construction of the system matrices in this work was achieved through element considerations. The solution of the unknown variable  $\psi$  within the element domain was approximated by

$$\tilde{\psi}^e = \sum_{i=1} N_i \psi_i^e(t), \quad i=1,2,\dots,n^e \quad (62)$$

where  $n^e$  is the number of element nodal points,  $N_i$  are the element shape functions, and  $\psi_i^e(t)$  are the time-dependent nodal magnitudes of  $\tilde{\psi}^e$ . The element contribution to the system matrix operators is defined by Galerkin's orthogonality condition expressed by

$$\int_{Vol} N_j R^e dVol = 0, \quad j=1,2,\dots,n^e \quad (63)$$

where  $R^e$  is defined by replacing  $\tilde{\psi}$  with  $\tilde{\psi}^e$  in equations (37) and (38), and the integration is over the element volume. Using equation (62), the element contribution is portrayed for the core by

$$\begin{aligned} & \left[ \int_{Vol} N_j N_i dVol \right] \{ \dot{\psi}_i^e(t) \} - \left[ \int_{Vol} N_j \nabla^2 N_i dVol \right] \{ (c1 \cdot \psi^e)_i \} + \left[ \int_{Vol} N_j N_i dVol \right] \{ (c2 \cdot \psi^e)_i \} \\ & + \left[ \int_{Vol} N_j N_i \ln(1 + \frac{K}{\gamma T_o} \sum_k N_k \psi_k^e(t)) dVol \right] \{ (c4 \cdot \psi^e)_i \} \\ & + \left[ \int_{Vol} N_j N_i dVol \right] \left\{ \int_0^t e^{-\bar{\lambda}(t-t')} (c5 \cdot \psi(t'))_i dt' \right\} = 0 \end{aligned} \quad (64)$$

where  $i, j, k = 1, 2, \dots, 15$ , and  $c_1, c_2$ , etc., are constants at node  $i$ . The bracketed expressions represent square matrices of size  $15 \times 15$ , and the braced expressions represent column vectors of size  $15 \times 1$ . For the reflector, the last two terms of equation (64) are zero. Before any operation can be performed on equation (64), the nonlinear terms (last two terms) must be "linearized" and the term with the  $\nabla^2$  operator must be integrated by parts.

The nonlinear feedback term,  $\lambda n[1 + \frac{K}{\gamma T_0} \sum_{k=1}^{15} N_k \psi_k^e(t)]$ , was linearized by using predicted values of the unknown function at time  $t$ . These predicted values come from the time integration scheme by Franke [7]. Basically, the integration scheme utilizes a predictor-corrector method which predicts values of the unknown function at the next time by using the derivatives of the function. Adopting the predicted values  $\psi_k^P$  enabled integration over space. The term in equation (64) involving the nonlinear feedback can be written as

$$\left[ \int_{Vol} N_j N_i \lambda n \left( 1 + \frac{K}{\gamma T_0} (N_1 \psi_1^P + N_2 \psi_2^P + \dots + N_{15} \psi_{15}^P) \right) dVol \right] \{ (c_4 \cdot \psi)_i \}$$

The last term of equation (64) describes the delayed neutron contribution. In general,

$$\begin{aligned} e^{-\bar{\lambda} t_n} \int_0^n e^{\bar{\lambda} t'} \psi_i^e(t') dt' &= e^{-\bar{\lambda} (t_n - t_{n-1})} \left[ e^{-\bar{\lambda} t_{n-1}} \int_0^{t_{n-1}} e^{\bar{\lambda} t'} \psi_i^e(t') dt' \right] \\ &+ e^{-\bar{\lambda} t_n} \int_{t_{n-1}}^n e^{\bar{\lambda} t'} \psi_i^e(t') dt' \end{aligned} \quad (65)$$

where  $n$  is number of time steps,  $t_n$  is the current time,

and  $t_{n-1}$  is the previous time. To approximate the integrals in equation (65), the predicted values  $\psi_i^P$  were employed in a simple trapezoidal rule. The trapezoidal rule was believed to be sufficient since very small time steps were utilized in this work. For example, at time  $t_2$ ,

$$(SUM_i) = (\text{previous } SUM_i) e^{-\bar{\lambda}H} + \frac{H}{2} (e^{\bar{\lambda}H} \psi_i^e(t_1) + \psi_i^P)$$

where

$$H = \text{current time step} = t_2 - t_1$$

$$(SUM_i) = e^{-\bar{\lambda}t_2} \int_0^{t_2} e^{\bar{\lambda}t'} \psi_i^e(t') dt'$$

$$(\text{previous } SUM_i) = e^{-\bar{\lambda}t_1} \int_0^{t_1} e^{\bar{\lambda}t'} \psi_i^e(t') dt'$$

The previous sum is formed by accumulating the trapezoidal integration of each time step. In general then, for time  $t_n$

$$(SUM_i) = (\text{previous } SUM_i) e^{-\bar{\lambda}H} + \frac{H}{2} (e^{\bar{\lambda}H} \psi_i^e(t_{n-1}) + \psi_i^P) \quad (66)$$

The delayed neutron term in equation (64) can be expressed as

$$\left[ \int_{Vol} N_j N_i dVol \right] \{ (c5 \cdot SUM)_i \}$$



In order to bring equation (64) to final form, the  $\nabla^2$  operator was integrated by parts. Since the flux at the surface of the reactor is zero, integration by parts yields

$$\int_{Vol} N_j \nabla^2 N_i dx dy dz = - \int_{Vol} \left( \frac{\partial N_i}{\partial x} \frac{\partial N_j}{\partial x} + \frac{\partial N_i}{\partial y} \frac{\partial N_j}{\partial y} + \frac{\partial N_i}{\partial z} \frac{\partial N_j}{\partial z} \right) dx dy dz \quad (67)$$

In vector notation, equation (67) is expressed as

$$\int_{Vol} N_j \nabla^2 N_i dx dy dz = - \int_{Vol} \left\langle \frac{\partial N_i}{\partial x}, \frac{\partial N_i}{\partial y}, \frac{\partial N_i}{\partial z} \right\rangle \begin{Bmatrix} \frac{\partial N_j}{\partial x} \\ \frac{\partial N_j}{\partial y} \\ \frac{\partial N_j}{\partial z} \end{Bmatrix} dx dy dz \quad (68)$$

Using the chain rule produces

$$\begin{Bmatrix} \frac{\partial N_i}{\partial x} \\ \frac{\partial N_i}{\partial y} \\ \frac{\partial N_i}{\partial z} \end{Bmatrix} = \begin{bmatrix} \frac{\partial L_1}{\partial x} & \frac{\partial L_2}{\partial x} & 0 \\ \frac{\partial L_1}{\partial y} & \frac{\partial L_2}{\partial y} & 0 \\ 0 & 0 & \frac{\partial \zeta}{\partial z} \end{bmatrix} \begin{Bmatrix} \left( \frac{\partial N_i}{\partial L_1} - \frac{\partial N_i}{\partial L_3} \right) \\ \left( \frac{\partial N_i}{\partial L_2} - \frac{\partial N_i}{\partial L_3} \right) \\ \left( \frac{\partial N_i}{\partial \zeta} \right) \end{Bmatrix} \quad (69)$$

Letting the 3x3 matrix above be  $[B']$ , the  $\nabla^2$  term becomes

$$\int_{Vol} N_j \nabla^2 N_i dx dy dz = - \int_{Vol} \left\langle \left( \frac{\partial N_i}{\partial L_1} - \frac{\partial N_i}{\partial L_3} \right), \left( \frac{\partial N_i}{\partial L_2} - \frac{\partial N_i}{\partial L_3} \right), \frac{\partial N_i}{\partial \zeta} \right\rangle [B']^T [B'] \begin{Bmatrix} \left( \frac{\partial N_j}{\partial L_1} - \frac{\partial N_j}{\partial L_3} \right) \\ \left( \frac{\partial N_j}{\partial L_2} - \frac{\partial N_j}{\partial L_3} \right) \\ \frac{\partial N_j}{\partial \zeta} \end{Bmatrix} dx dy dz \quad (70)$$

where  $[B']^T$  is the transpose of  $[B']$ . By applying the chain rule in equation (47) and using equation (59), it can be shown that for this work

$$[B'] = \begin{bmatrix} \frac{1}{(\frac{\partial N_1}{\partial L_1} x_1 + \dots + \frac{\partial N_{15}}{\partial L_1} x_{15})}, \frac{1}{(\frac{\partial N_1}{\partial L_2} x_1 + \dots + \frac{\partial N_{15}}{\partial L_2} x_{15})}, 0 \\ \frac{1}{(\frac{\partial N_1}{\partial L_1} y_1 + \dots + \frac{\partial N_{15}}{\partial L_1} y_{15})}, \frac{1}{(\frac{\partial N_1}{\partial L_2} y_1 + \dots + \frac{\partial N_{15}}{\partial L_2} y_{15})}, 0 \\ 0, 0, \frac{2}{h} \end{bmatrix} \quad (71)$$

$[B']^T$  can be derived from equation (71).

Note from equation (64) that there are three basic element matrices which are defined as follows after applying equation (60):

$$[G_{ji}] = \frac{h}{2} \int_{-1}^1 \int_0^1 \int_0^{1-L_1} N_j N_i \det[J^*] dL_1 dL_2 d\zeta \quad (72)$$

$$[GG_{ji}] = \frac{h}{2} \int_{-1}^1 \int_0^1 \int_0^{1-L_1} \left( \frac{\partial N_i}{\partial L_1} - \frac{\partial N_i}{\partial L_3}, \left( \frac{\partial N_i}{\partial L_2} - \frac{\partial N_i}{\partial L_3} \right), \left( \frac{\partial N_i}{\partial \zeta} \right) \right) [B']^T$$

$$[B'] \left\{ \begin{array}{c} \left( \frac{\partial N_j}{\partial L_1} - \frac{\partial N_j}{\partial L_3} \right) \\ \left( \frac{\partial N_j}{\partial L_2} - \frac{\partial N_j}{\partial L_3} \right) \\ \frac{\partial N_j}{\partial \zeta} \end{array} \right\} \det[J^*] dL_1 dL_2 d\zeta \quad (73)$$

$$[GGG_{ji}] = \frac{h}{2} \int_{-1}^1 \int_0^1 \int_0^{1-L_1} N_j N_i \ln \left( 1 + \frac{K}{\gamma T_0} (N_1 \psi_1^p + \dots + N_{15} \psi_{15}^p) \right) \det[J^*] dL_1 dL_2 d\zeta$$

(74)

Element matrices  $[G_{ji}]$  and  $[GG_{ji}]$  are independent of time. However,  $[GGG_{ji}]$  is time dependent due to the utilization of the predicted values  $\psi_i^P$  which changes with time. In terms of these three basic element matrices, equation (64) is

$$\begin{aligned}
 & [G_{ji}]\{\dot{\psi}_i^e\} + [GG_{ji}]\{c1 \cdot \psi_i^e\} + [G_{ji}]\{(c2 \cdot \psi_i^e)\} \\
 & + [GGG_{ji}]\{(c4 \cdot \psi_i^e)\} + [G_{ji}]\{(c5 \cdot \text{SUM})_i\} = 0 \quad (75)
 \end{aligned}$$

The last two terms of equation (75) are zero for the reflector.

#### G. CONSTRUCTION OF THE SYSTEM MATRICES

The 15x15 coefficient element matrices were calculated according to equations (72), (73), and (74); and the results were collected element by element into the corresponding system coefficient matrices. The system coefficient matrix  $[BIGG]$  is developed from  $[G_{ji}]$ ,  $[BIGGG]$  from  $[GG_{ji}]$ , and  $[BIGH]$  from  $[GGG_{ji}]$ .  $[BIGG]$  and  $[BIGGG]$  are independent of time and can be constructed once and for all from geometry considerations.  $[BIGH]$  is dependent on both geometry and time due to the time dependence of the predicted flux utilized in the feedback term. Thus,  $[BIGH]$  is recalculated at each time increment.

Non-zero contributions to a global nodal point I come only from adjacent elements sharing that same nodal point I. Thus, the system matrices are sparse and banded. The process of assembling contributions from element matrices

requires the identification of a local nodal point ( $i=1,2,\dots,15$ ) with a global nodal point ( $I=1,2,\dots,\text{NUMNP}$ , where NUMNP is the total number of system nodes). This correspondence between element and global nodes is accomplished via the connectivity matrix.

The formal treatment of the field equations in terms of the system coefficient matrices is described by the equation

$$[\text{BIGG}] \{\dot{\psi}_I\} + [\text{BIGGG}] \{(c1 \cdot \psi)_I\} + [\text{BIGG}] \{(c2 \cdot \psi)_I\} \\ + [\text{BIGH}] \{(c4 \cdot \psi)_I\} + [\text{BIGG}] \{(c5 \cdot \text{SUM})_I\} = 0 \quad (76)$$

where the system matrices are NUMNP x NUMNP and the column vectors are of length NUMNP x 1. However, the direct application of equation (76) requires a large amount of computer storage. To take advantage of the sparsity of the system matrices, an optimum compacting scheme described by Ref. 8 was employed.

The concept behind OCS is simply to store only the non-zero terms of a coefficient matrix. OCS requires two integer arrays, say JB and NAME, and a vector of non-zero coefficients of the square system matrix. For purposes of illustration, the square system matrix is called B, and the vector of non-zero coefficients of B is called BB. The  $i^{\text{th}}$  integer entry in the NUMNP x 1 JB vector is the number  $q_i$ . This number is defined by

$$q_i = 1 + \sum_{j=1}^{i=1} p_j, \quad i=1,2,\dots,\text{NUMNP} \quad (77)$$

where  $p_j$  is the number of terms in the  $i^{\text{th}}$  equation. In

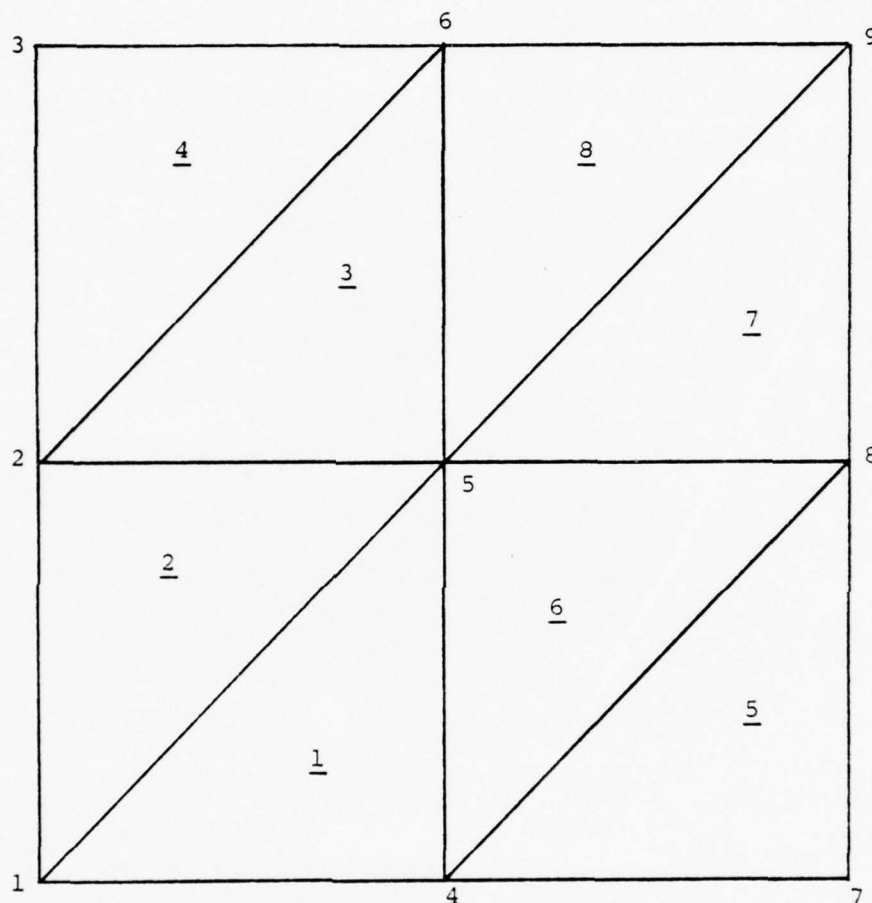
other words,  $p_j$  is the number of nodes that the  $i^{\text{th}}$  node "sees". JB is therefore a pointer vector of length NUMNP+1 whose  $i^{\text{th}}$  term locates the initial position in the BB vector of the contributing coefficients to the  $i^{\text{th}}$  equation. The NAME vector of length Mx1, where  $M = \sum_{i=1}^{\text{NUMNP}} p_i$ , consists of NUMNP successive vector blocks of variable length  $p_i$ ,  $i=1,2,\dots,\text{NUMNP}$ . The  $p_i$  integer numbers in the  $i^{\text{th}}$  block of NAME list the  $p_i$  contributors to the  $i^{\text{th}}$  equation. The Mx1 BB vector contains the real non-zero coefficients of the NUMNPxNUMNP B matrix, arranged in the same contiguous block arrangement as the NAME vector. The  $j^{\text{th}}$  term in the  $i^{\text{th}}$  block or  $\text{BB}(\text{JB}(I) + J - 1)$  is  $B(I,K)$ , where  $K = \text{NAME}(\text{JB}(I) + J - 1)$ . To illustrate, consider the grid shown in figure 12. The two array vectors and the coefficient vector matrix of non-zero terms are:

$$\begin{aligned} \text{JB} &= \langle 1, 5, 10, 13, 18, 25, 30, 33, 38, 42 \rangle \\ \text{NAME} &= \langle 1, 2, 4, 5 | 2, 3, 1, 6, 5 | \text{---} | 9, 8, 6, 5 \rangle \\ \text{BB} &= \langle B_{11}, B_{12}, B_{14}, B_{15} | B_{22}, B_{23}, B_{21}, B_{26}, B_{25} | \text{---} | B_{99}, B_{98}, B_{96}, B_{95} \rangle \end{aligned}$$

In this illustration, NUMNP = 9 and M = 41 [8].

In this work, a judicious method of numbering the system nodal points was adopted to further reduce computer storage requirements. Since the surface boundary nodes of the reactor represent zero neutron fluxes, the contributions of these nodes to interior or non-zero nodes can be discarded. Thus, only the interior nodal points need to be considered. These non-zero nodes were numbered first in the finite element mesh





Number - element number

Figure 12. Sample grid used for illustrating OCS

used so that in the OCS, the number of non-zero nodes (NNZ) replaces NUMNP.

The vectors of non-zero coefficients will be designated BIGG, BIGGG and BIGH since the square coefficient matrices described in equation (76) were not utilized. To illustrate the application of OCS in the system, the following sample program is given:

```

DO 450 I=1, NNZ
  JBB = JB(I)
  JE = JB(I+1)-1
  DY(I) = 0.0
  DO 500 J=JBB, JE
    LL = NAME(J)
    DY(I) = DY(I) + BIGG(J)* $\dot{\psi}$ (LL) + BIGGG(J)*c1(LL)*
 $\psi$ (LL) + BIGG(J)*c2(LL)* $\psi$ (LL) + BIGH(J)*c4(LL)*
 $\psi$ (LL) + BIGG(J)*c5(LL)*SUM(LL)
  500 CONTINUE
450 CONTINUE

```

(78)

where

LL = nodal point "seen" by node I

JE-JBB = total number of nodal points that node I "sees"

DY(I) = summation of all contributions to node I and  
should sum to zero as stated by the field equation

The assumption of a homogeneous reflector was relaxed in the application of equation (78). Interface nodes were assigned properties of the core. Therefore, if LL is a reflector

node not on the core reflector interface, the last two terms of equation (78) are nonexistent.

#### IV. NUMERICAL INTEGRATION

##### A. LINE AND AREA INTEGRATION

The solution of the element matrix equations was achieved through numerical integration since an exact closed form solution cannot be established. The volume integration was accomplished by using a line integration in the  $\zeta$ -direction and an area integration in the plane of the triangle. The line integral is described by the Gaussian quadrature formula [12]

$$\int_{-1}^1 f(\zeta) d\zeta \approx \sum_{k=1}^n H_k f(a_k) \quad (79)$$

where  $n$  is the number of Gauss integration points

$H_k$  = weighting coefficients

$f(a_k)$  = the function  $f(\zeta)$  evaluated at Gauss point  $a_k$

Table III lists  $a_k$ ,  $H_k$  and  $n$  [11].

The area integration was achieved by the equation

$$\int_0^1 \int_0^{1-L_1} f(L_1, L_2, L_3) dL_1 dL_2 \approx \sum_{m=1}^{\bar{m}} w_m f(L_1^m, L_2^m, L_3^m) \quad (80)$$

where  $\bar{m}$  is the number of area integration points and  $w_m$  are the weights. The numerical integration points for the area integration are given in Table IV which was extracted

TABLE III

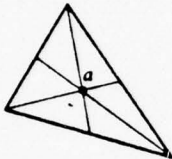
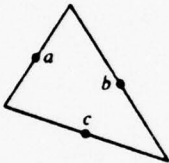
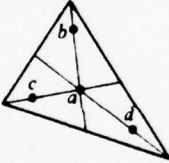
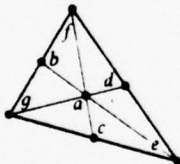
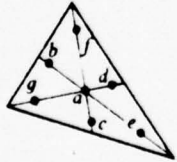
Abscissae and Weight Coefficients  
of the Gaussian Quadrature Formula

$$\int_{-1}^1 f(\zeta) d\zeta = \sum_{k=1}^n H_k f(a_k)$$

$\pm a$			$H$		
$n = 2$					
0.57735	02691	89626	1.00000	00000	00000
$n = 3$					
0.77459	66692	41483	0.55555	55555	55556
0.00000	00000	00000	0.88888	88888	88889
$n = 4$					
0.86113	63115	94053	0.34785	48451	37454
0.33998	10435	84856	0.65214	51548	62546
$n = 5$					
0.90617	98459	38664	0.23692	68850	56189
0.53846	93101	05683	0.47862	86704	99366
0.00000	00000	00000	0.56888	88888	88889
$n = 6$					
0.93246	95142	03152	0.17132	44923	79170
0.66120	93864	66265	0.36076	15730	48139
0.23861	91860	83197	0.46791	39345	72691
$n = 7$					
0.94910	79123	42759	0.12948	49661	68870
0.74153	11855	99394	0.27970	53914	89277
0.40584	51513	77397	0.38183	00505	05119
0.00000	00000	00000	0.41795	91836	73469
$n = 8$					
0.96028	98564	97536	0.10122	85362	90376
0.79666	64774	13627	0.22238	10344	53374
0.52553	24099	16329	0.31370	66458	77887
0.18343	46424	95650	0.36268	37833	78362
$n = 9$					
0.96816	02395	07626	0.08127	43883	61574
0.83603	11073	26636	0.18064	81606	64857
0.61337	14327	00590	0.26061	06964	02935
0.32425	34234	03809	0.31234	70770	40003
0.00000	00000	00000	0.33023	93550	01260
$n = 10$					
0.97390	65285	17172	0.06667	13443	08688
0.86506	33666	88985	0.14945	13491	50581
0.67940	95682	99024	0.21908	63625	15982
0.43339	53941	29247	0.26926	67193	09996
0.14887	43389	81631	0.29552	42247	14753



TABLE IV  
Numerical Formulas for Triangles

Order	Fig.	Error	Points	Triangular Co-ordinates	Weights $2W_i$
Linear		$R = O(h^2)$	$a$	$\frac{1}{3}, \frac{1}{3}, \frac{1}{3}$	1
Quadratic		$R = O(h^3)$	$a, b, c$	$\begin{matrix} \frac{1}{2}, \frac{1}{2}, 0 \\ 0, \frac{1}{2}, \frac{1}{2} \\ \frac{1}{2}, 0, \frac{1}{2} \end{matrix}$	$\frac{1}{3}, \frac{1}{3}, \frac{1}{3}$
Cubic		$R = O(h^4)$	$a, b, c, d$	$\begin{matrix} \frac{1}{3}, \frac{1}{3}, \frac{1}{3} \\ \frac{1}{2}, \frac{1}{2}, 0 \\ \frac{1}{2}, 0, \frac{1}{2} \\ \frac{1}{2}, 0, \frac{1}{2} \end{matrix}$	$-\frac{17}{24}, \frac{1}{24}, \frac{1}{24}, \frac{1}{24}$
Cubic		$R = O(h^4)$	$a, b, c, d, e, f, g$	$\begin{matrix} \frac{1}{3}, \frac{1}{3}, \frac{1}{3} \\ \frac{1}{2}, \frac{1}{2}, 0 \\ 0, \frac{1}{2}, \frac{1}{2} \\ \frac{1}{2}, 0, \frac{1}{2} \\ 1, 0, 0 \\ 0, 1, 0 \\ 0, 0, 1 \end{matrix}$	$\frac{17}{240}, \frac{1}{240}, \frac{1}{240}, \frac{1}{240}, \frac{1}{240}, \frac{1}{240}, \frac{1}{240}$
Quintic		$R = O(h^6)$	$a, b, c, d, e, f, g, h$	$\begin{matrix} \frac{1}{3}, \frac{1}{3}, \frac{1}{3} \\ x_1, \beta_1, \beta_1 \\ \beta_1, x_1, \beta_1 \\ \beta_1, \beta_1, x_1 \\ x_2, \beta_2, \beta_2 \\ \beta_2, x_2, \beta_2 \\ \beta_2, \beta_2, x_2 \end{matrix}$	$0.225, 0.13239415, 0.12593918$

with  
 $x_1 = 0.05971587$   
 $\beta_1 = 0.47014206$   
 $x_2 = 0.79742699$   
 $\beta_2 = 0.10128651$

from Ref. 11. The volume integration of the function  $f(L_1, L_2, L_3, \zeta)$  using numerical integration is therefore

$$\int_{-1}^1 \int_0^1 \int_0^{1-L_1} f(L_1, L_2, L_3, \zeta) dL_1 dL_2 d\zeta \approx \sum_{k=1}^{\bar{n}} w_k \sum_{m=1}^{\bar{m}} w_m f(L_1^m, L_2^m, L_3^m, \zeta^k) \quad (81)$$

where  $w_k = H_k$ . In the manner of equation (81), the element matrices become

$$[G_{ji}] = \frac{h}{2} \sum_{k=1}^{\bar{n}} w_k \sum_{m=1}^{\bar{m}} w_m N_j(L_1^m, L_2^m, L_3^m, \zeta^k) N_i \det[J^*] \quad (82)$$

$$[GG_{ji}] = \frac{h}{2} \sum_{k=1}^{\bar{n}} w_k \sum_{m=1}^{\bar{m}} w_m F(L_1^m, L_2^m, L_3^m, \zeta^k) \det[J^*] \quad (83)$$

$$[GGG_{ji}] = \frac{h}{2} \sum_{k=1}^{\bar{n}} w_k \sum_{m=1}^{\bar{m}} w_m T(L_1^m, L_2^m, L_3^m, \zeta^k) \det[J^*] \quad (84)$$

where  $F$  and  $T$  are easily derived from equations (73) and (74), respectively. Note that  $N_i$  and  $\det[J^*]$  are also evaluated at each integration point. They are not shown as such merely for the sake of convenience in writing the equations.

#### B. NUMBER OF INTEGRATION POINTS

It is difficult to estimate the number of integration points required for good accuracy due to the complexity of the functions involved. The basic rule that the best number of integration points is found by trial and experience was adopted. For the  $[G_{ji}]$  element matrix, the numbers involved

can be approximated. This was done by letting the determinant of the Jacobian equal to twice the area of the curved triangle (checking  $\det[J^*]$  at each integration point showed that this assumption was not too unreasonable). With  $\det[J^*]$  outside the integration process,  $[G_{ji}]$  can be solved in closed form by integrating out  $\zeta$  from -1 to +1 and then applying the closed form equation [12]

$$\int_{\text{Area}} L_1^{m_1} L_2^{m_2} L_3^{m_3} d(\text{Area}) = 2A \frac{m_1! m_2! m_3!}{(m_1 + m_2 + m_3 + 2)!} \quad (85)$$

where  $m_1, m_2, m_3$  are positive integer exponents and  $A$  is the area of the triangle.

Five test points within the 15x15 element matrix were selected, as listed in Table V. The values obtained from the application of equation (85) are also given in Table V. Three sets of area integration points, each with a different number of  $\zeta$  Gauss points, were used. These three sets of area integration points, given in Table IV, are:

1. cubic order (4 points)
2. cubic order (7 points)
3. quintic order (7 points)

Using each of the three integration points above with different  $\zeta$  Gauss points in equation (82) produced the results obtained in Table V. From these results, the quintic order area integration points were selected for the element matrix  $[G_{ji}]$  with three  $\zeta$  Gauss points in the prism axes. This set of integration points was also used for  $[GGG_{ji}]$ .

TABLE V.  
Selection of Integration Points for  $[G_{ji}]$

$\zeta$ points	Area points	G(1,1)	G(2,2)	G(1,9)	G(6,9)	G(9,9)
13	cubic (4 pts)	1415	5278	-2756	5072	8536
5	"	1817	5278	-3170	5072	10240
7	"	1817	5278	-3170	5072	10240
3	cubic (7 pts)	3248	8247	-3114	4960	10243
5	"	3249	8247	-3114	4960	10240
7	"	3249	8247	-3114	4960	10240
3	quintic (7 pts)	2464	6600	-3144	5020	10240
5	"	2464	6600	-3144	5020	10240
7	"	2464	6600	-3144	5020	10240
Approximated values		2500	6700	-3142	5026	10053

The numbers for the  $[GG_{ji}]$  element matrix could not be approximated. The best that could be done was to obtain an idea of the order of magnitude of this element matrix. Towards this end, a linear triangular element was assumed. Using linear approximation, the order of magnitude was found to be about  $10^3$ . Using the three different area integration points mentioned above with varying  $\zeta$  Gauss points in equation (83) yielded the results given in Table VI. Further checks on the  $[GG_{ji}]$  element matrix showed that the cubic order with four area integration points yielded the desired order of magnitude. Thus, the fourth order cubic with five  $\zeta$  Gauss points was employed for the  $[GG_{ji}]$  element matrix. A note should be mentioned here in regards to the vast difference in results obtained for  $[GG_{ji}]$  using different area integration points. Most likely, it was due to the  $[B']$  and  $[B']^T$  matrices which required the inversion of  $\frac{\partial x}{\partial L_1}$ ,  $\frac{\partial x}{\partial L_2}$ , etc. Or perhaps it was caused by the nature of the hybrid element used in this work. In any case, further investigation is warranted in this area.



TABLE VI

Selection of Integration Points for  $[GG_{ji}]$ 

$\zeta$ points	Area points	GG(1,9)	GG(3,3)	GG(14,9)	GG(8,8)	GG(15,15)
3	cubic (4 pts)	18.4	170.1	-165	165.9	106.1
5	"	22.0	177.6	-186	195.9	106.1
7	"	22.0	177.6	-186	195.9	106.1
3	cubic (7 pts)	$-1.03 \times 10^4$	$2.11 \times 10^7$	$1.05 \times 10^7$	$8.42 \times 10^7$	2056
5	"	$-1.03 \times 10^4$	$2.11 \times 10^7$	$1.05 \times 10^7$	$8.42 \times 10^7$	2056
7	"	$-1.03 \times 10^4$	$2.11 \times 10^7$	$1.05 \times 10^7$	$8.41 \times 10^7$	2056
3	quintic (7 pts)	-52.6	$1.27 \times 10^4$	$-6.64 \times 10^4$	$6.84 \times 10^4$	$1.51 \times 10^5$
5	"	-52.6	$1.27 \times 10^4$	$-6.64 \times 10^4$	$6.84 \times 10^4$	$1.51 \times 10^5$
7	"	-52.6	$1.27 \times 10^4$	$-6.64 \times 10^4$	$6.84 \times 10^4$	$1.51 \times 10^5$

## V. TEST PROBLEMS AND RESULTS

The reactor was subjected to uniform and local perturbations in the form of a ramp input described by

$$\Sigma_f = \Sigma_f^* + \alpha t \quad (86)$$

where  $\alpha$  is the change in  $\Sigma_f$  per unit time and  $\Sigma_f^*$  is the critical fission cross-section.  $\Sigma_f^*$  must first be obtained before the perturbations can be applied. This was accomplished by trial and error until a stationary solution was reached. For mesh I,  $\Sigma_f^*$  was found to be 0.0057360 per cm. No attempt was made to find  $\Sigma_f^*$  for mesh II due to time limitations. As such, the test problems outlined below were applied to mesh I. Future work is planned to apply the test problems on mesh II.

The following perturbations were applied:

a) Uniform perturbation of 10 dollar of reactivity per second:

$$\Sigma_f(\vec{r}, t) = \Sigma_f^* + \alpha t, \quad \text{in the core}$$

where  $\alpha = 0.005893/\text{cm-sec}$

b) Local perturbation at the core center of 100 dollar of reactivity per second:

$$\Sigma_f(\vec{r}, t) = \Sigma_f^* + \alpha t \delta(\vec{r}_0), \quad \text{in the core}$$

where  $\bar{r}_0$  is (0,0,0) and  $\alpha = 0.015407/\text{cm-sec}$

c) Local, off-center perturbation:

$$\Sigma_f(\bar{r}, t) = \Sigma_f^* + \alpha_i t \delta(\bar{r}_i) , \quad i = 1, 2, 3, \text{ in the core}$$

where

$$\bar{r}_1 = (0, 60, 40)$$

$$\alpha_1 = 0.015407/\text{cm-sec} = 100 \text{ dollar per second}$$

$$\alpha_2 = 0.008123/\text{cm-sec} = 50 \text{ dollar per second}$$

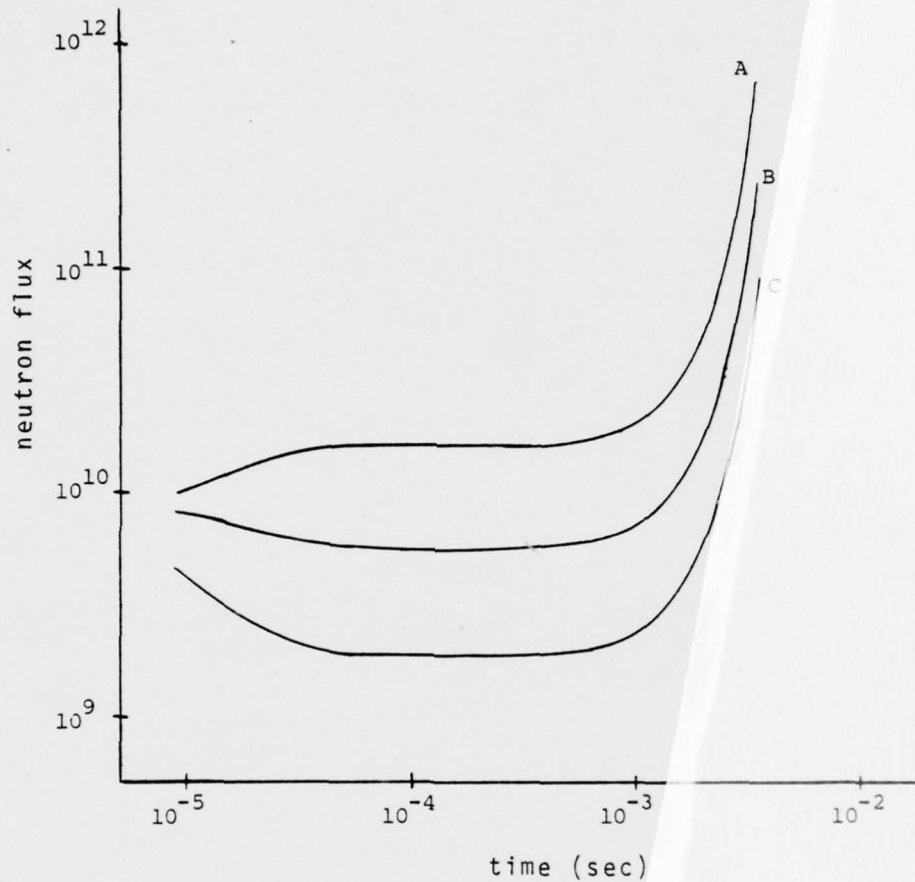
$$\alpha_3 = 0.005894/\text{cm-sec} = 10 \text{ dollar per second}$$

Three test points, (0,0,0), (60,0,0), and (-60,0,80), were selected to trace the neutron time history. For cases a) and b), the neutron flux was plotted at each test point during transience. This is shown in figures 13 and 14. Case c) involved three ramp inputs and were conducted for both the linear and nonlinear reactor equations. The linear and nonlinear responses were compared at each test point for each ramp input and are illustrated in figures 15 through 23. The radial and axial flux distributions at time  $t = 0.0123$  second were plotted for the steady state and the 100 dollar perturbation case. These are embodied in figures 24 and 25. Finally, a neutron flux early time history between mesh I and mesh II was plotted to check the effect of using a finer element mesh. The result is portrayed in figure 26.

Figures 13 and 14 revealed a clear space dependence of the neutron flux during transience as expected. Figures 15 through 23 demonstrated the effects of temperature feedback

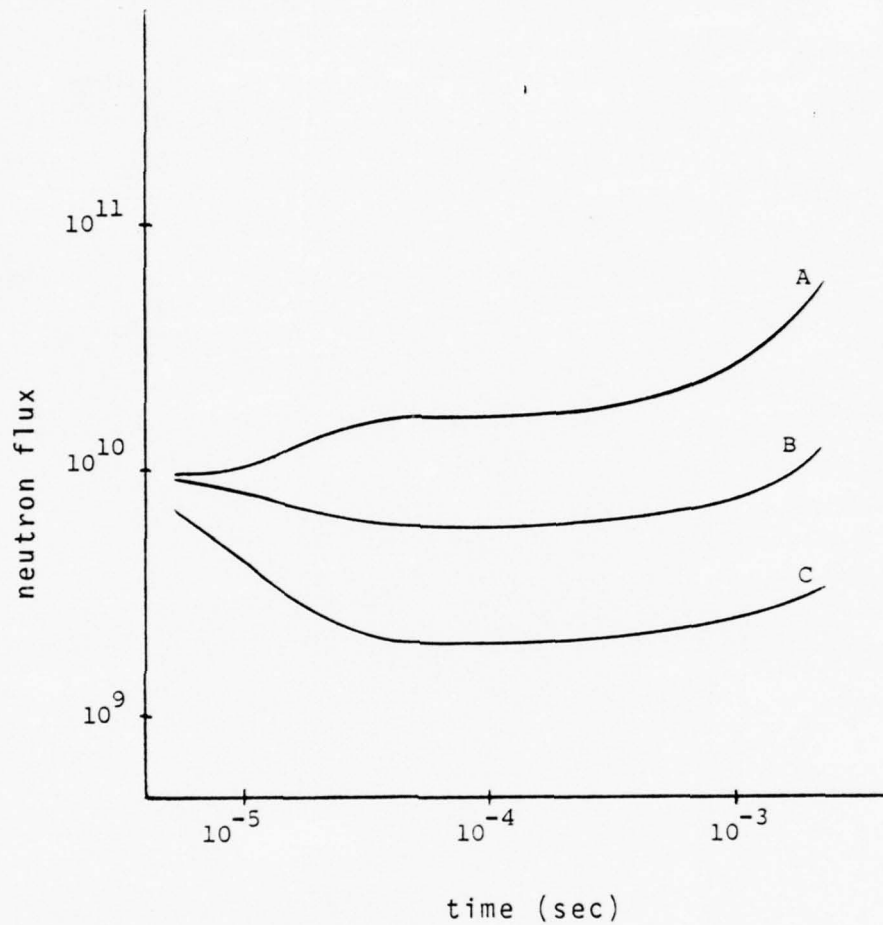
only the interior nodal points need to be considered. These non-zero nodes were numbered first in the finite element mesh

56



A - neutron flux at test point (0,0,0)  
B - neutron flux at test point (60,0,0)  
C - neutron flux at test point (-60,0,80)

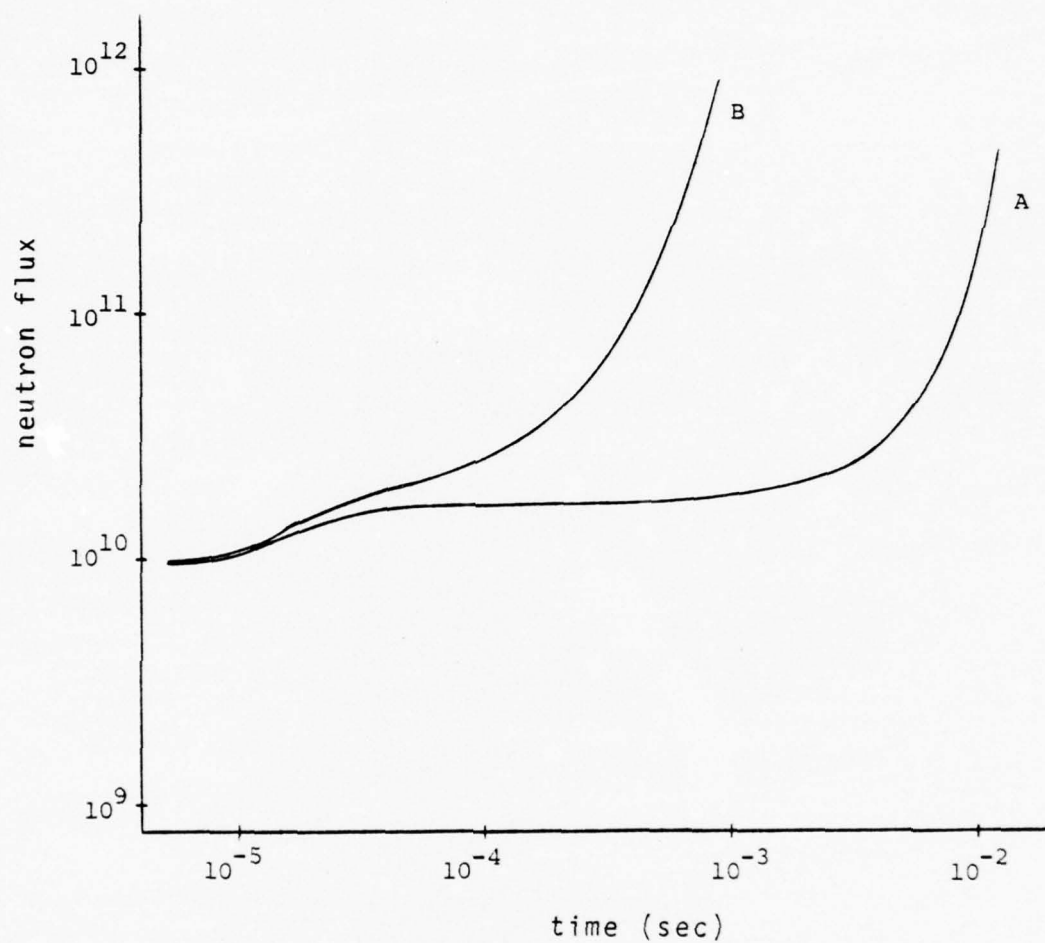
Figure 13. Neutron flux transient history at three test points with a uniform perturbation of 10 dollar of reactivity per second.



A - neutron flux at test point (0,0,0)  
 B - neutron flux at test point (60,0,0)  
 C - neutron flux at test point (-60,0,80)

Figure 14. Neutron flux transient history at various test points for a local central perturbation of 100 dollar/sec of reactivity.





A - nonlinear neutron response  
B - linear neutron response

Figure 15. Linear and nonlinear fluxes at (0,0,0) due to a local perturbation of 100 dollar/sec of reactivity at (0,60,40).

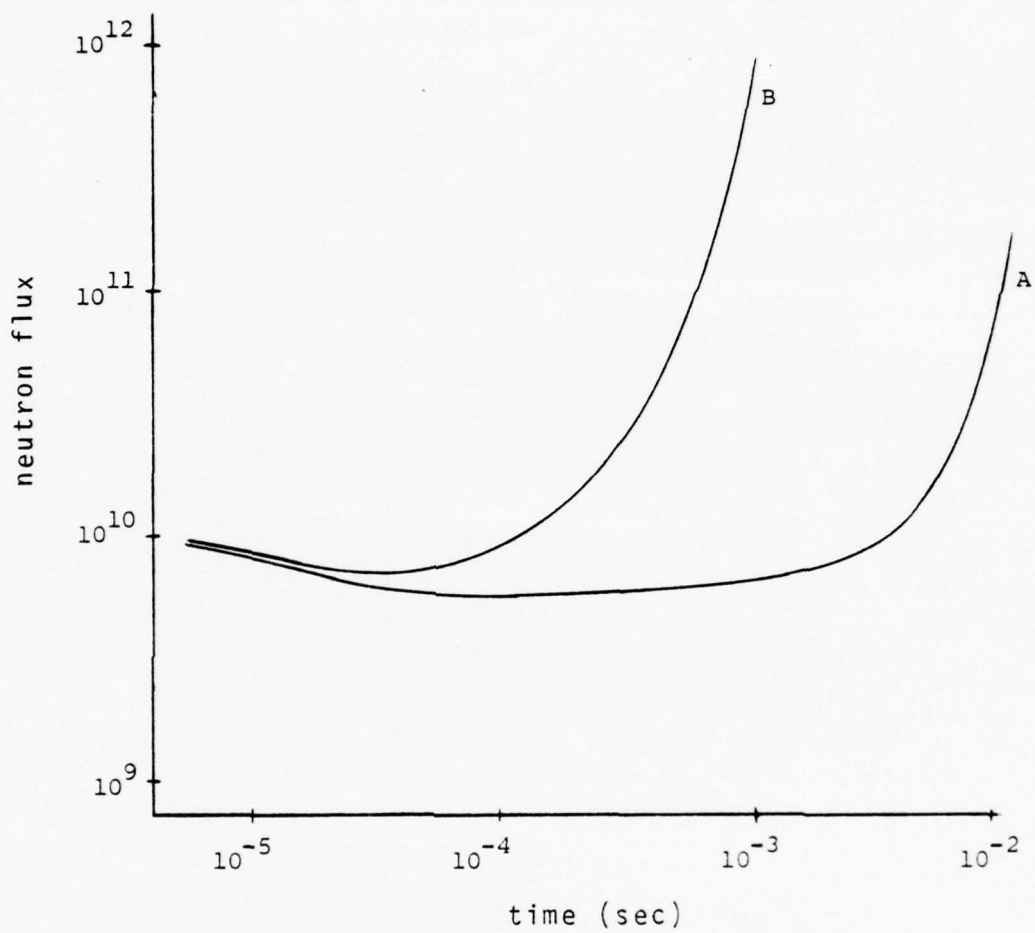
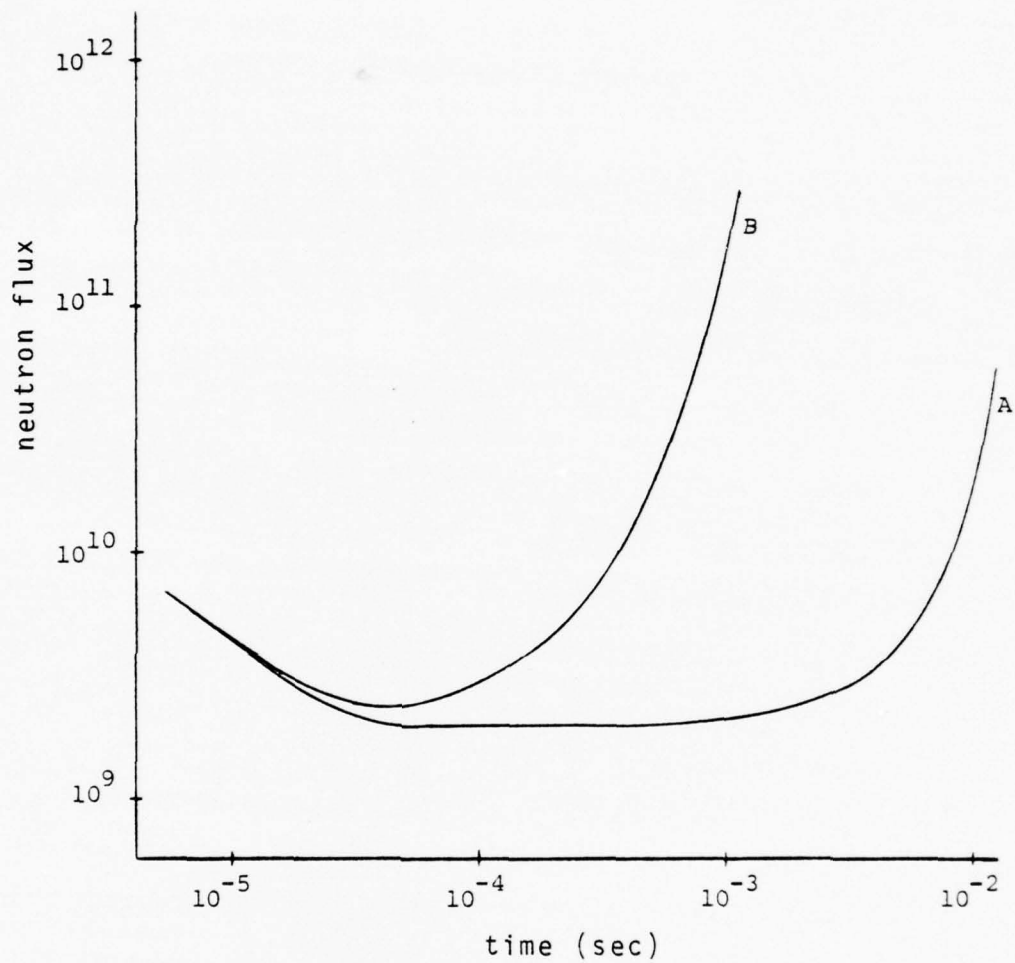
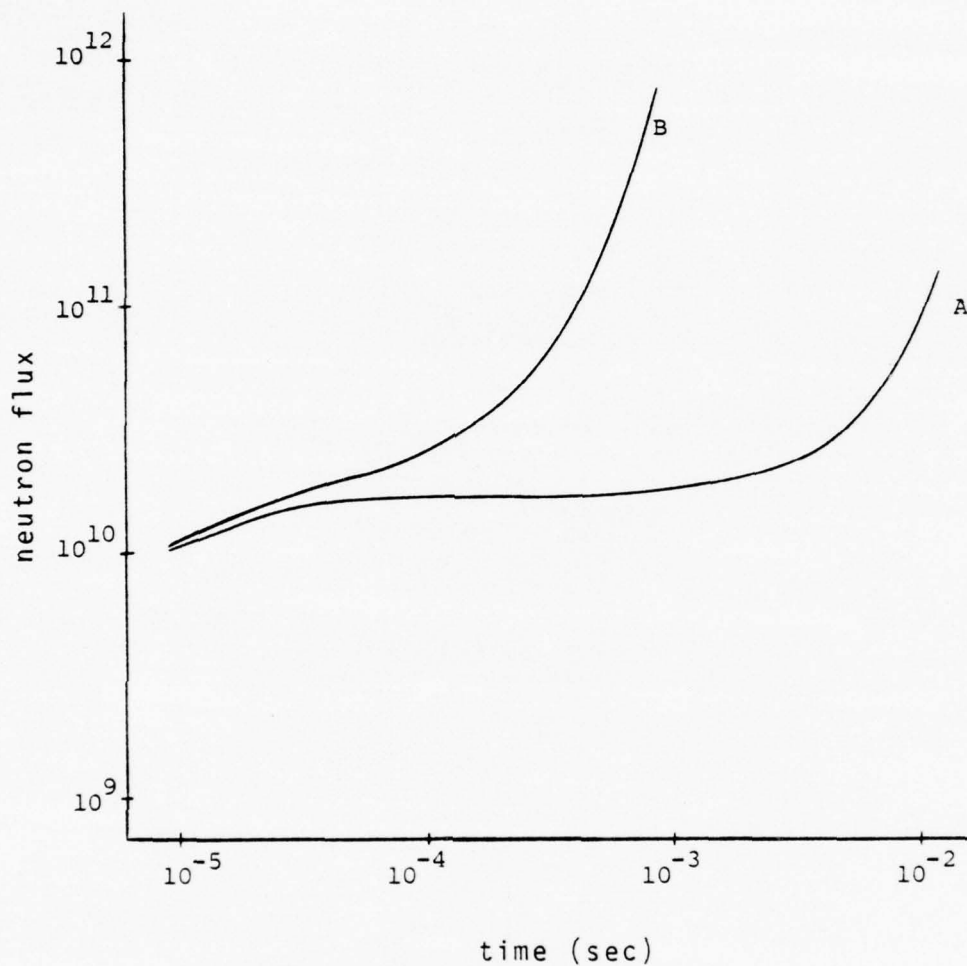


Figure 16. Linear and nonlinear fluxes at (60,0,0) due to a local perturbation of 100 dollar/sec at (0,60,40).



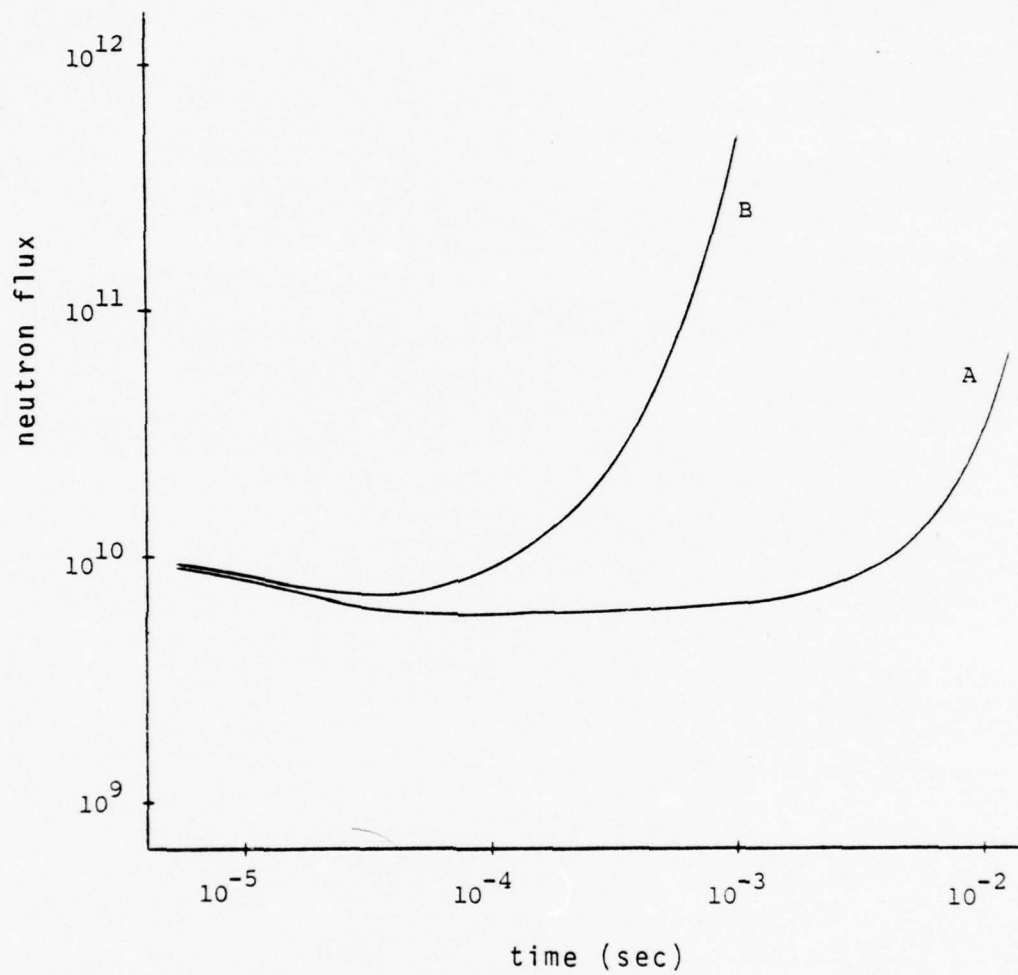
A - nonlinear neutron response  
B - linear neutron response

Figure 17. Linear and nonlinear fluxes at  $(-60, 0, 80)$  due to a local perturbation of 100 dollar/sec at  $(0, 60, 40)$ .



A - nonlinear neutron response  
B - linear neutron response

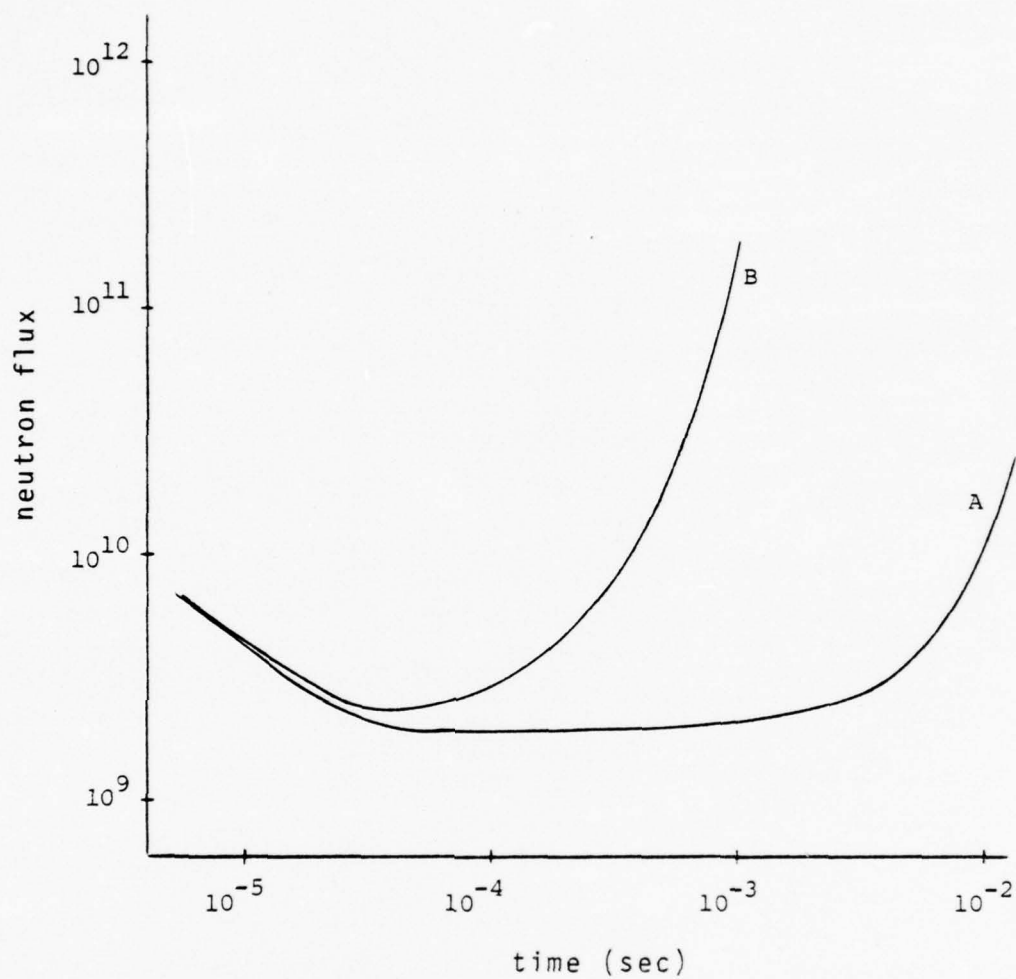
Figure 18. Linear and nonlinear fluxes at (0,0,0) due to a 50 dollar/sec local perturbation at (0,60,40).



A - nonlinear neutron response  
B - linear neutron response

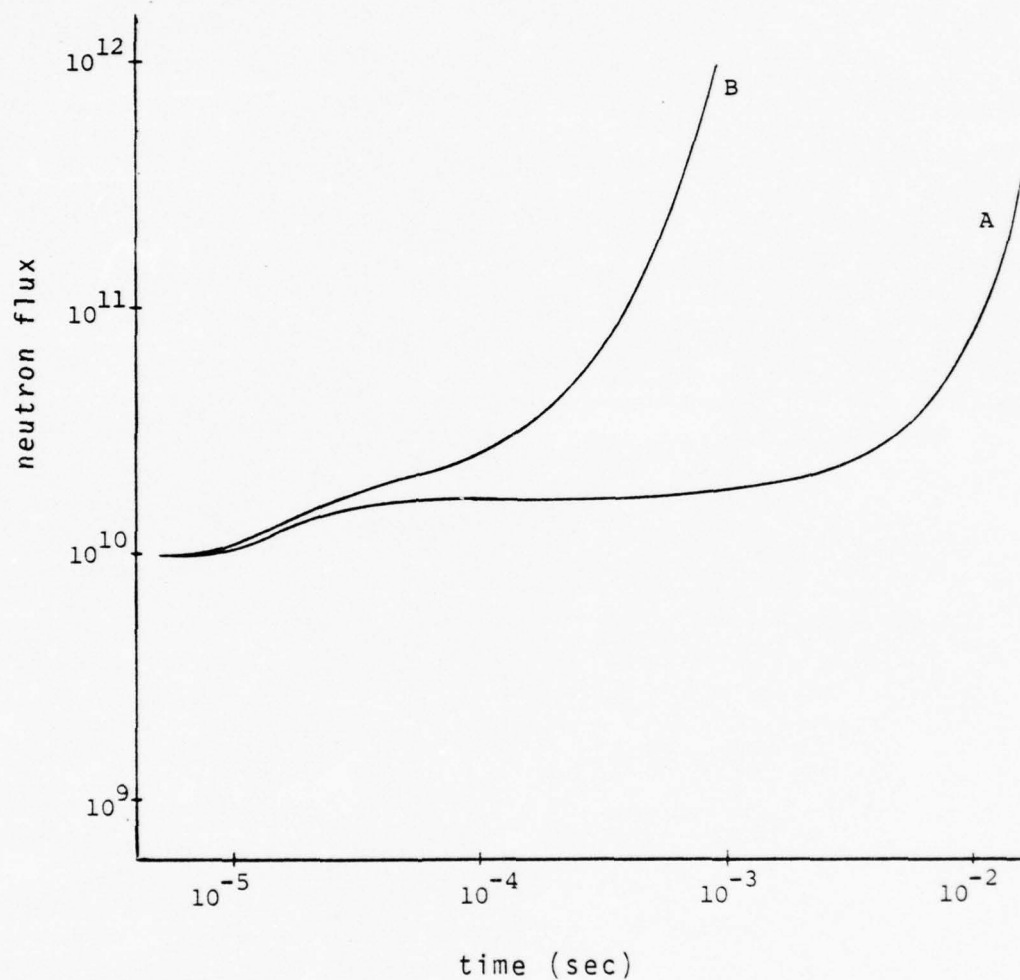
Figure 19. Linear and nonlinear fluxes at (60,0,0) due to a 50 dollar/sec local perturbation at (0,60,40).





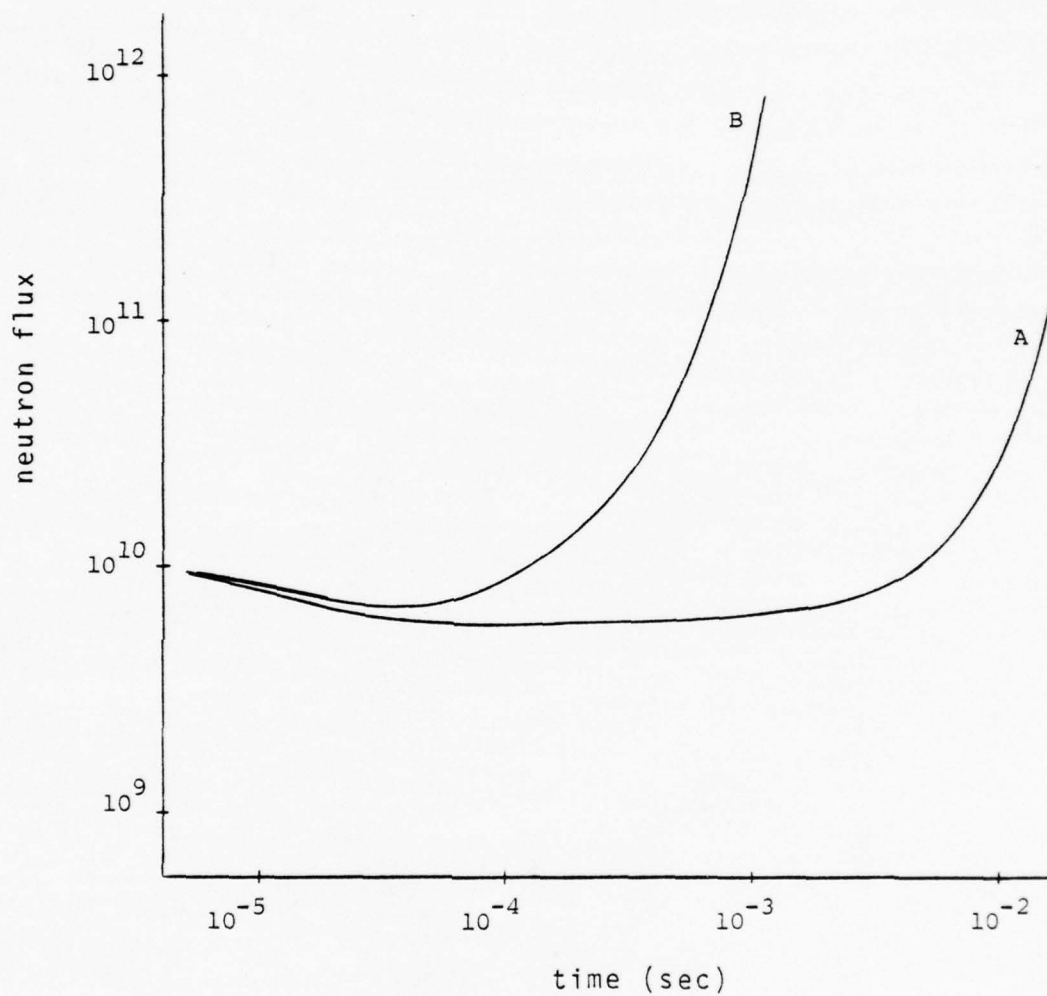
A - nonlinear neutron response  
 B - linear neutron response

Figure 20. Linear and nonlinear fluxes at  $(-60, 0, 80)$  due to a 50 dollar/sec local perturbation at  $(0, 60, 40)$ .



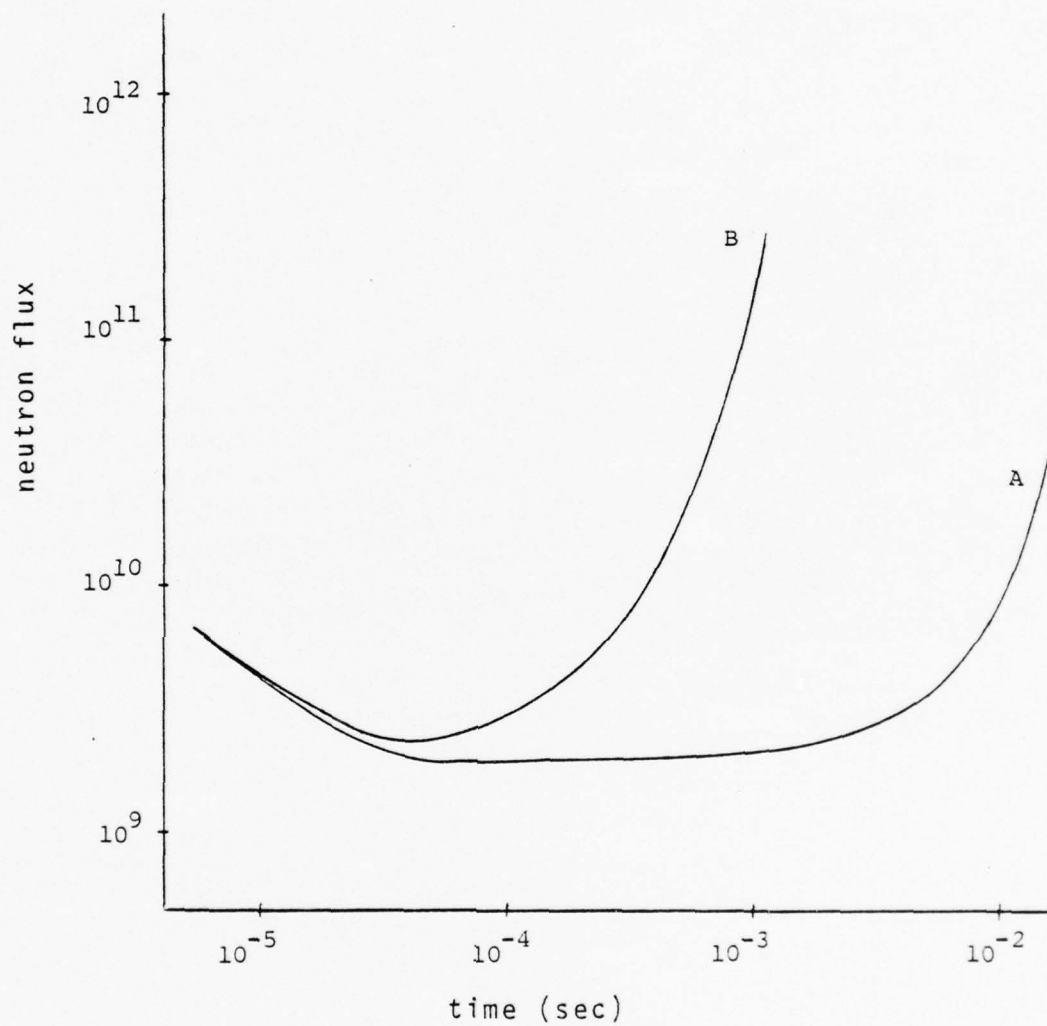
A - nonlinear neutron response  
B - linear neutron response

Figure 21. Linear and nonlinear fluxes at (0,0,0) due to a 10 dollar/sec local perturbation at (0,60,40).



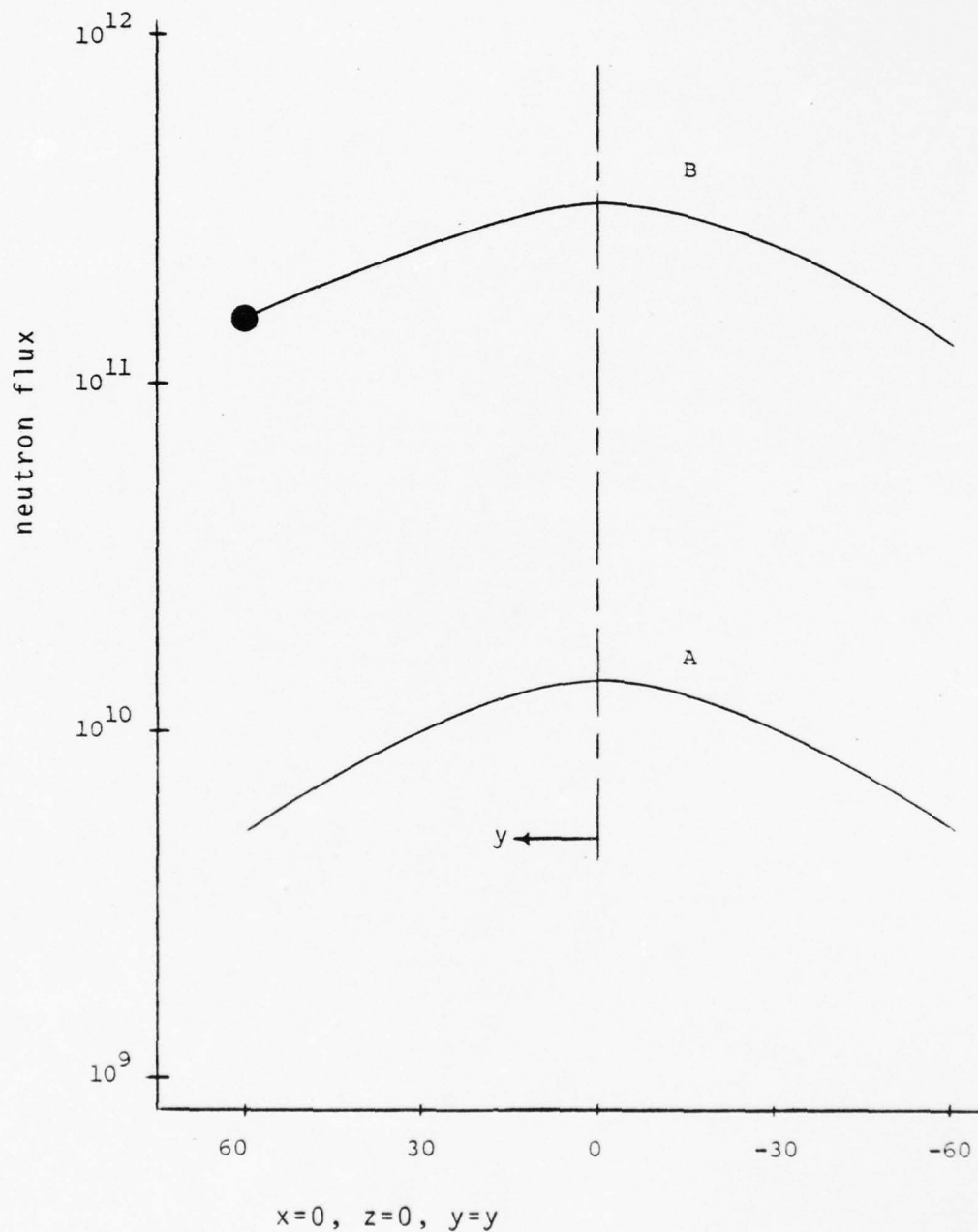
A - nonlinear neutron response  
B - linear neutron response

Figure 22. Linear and nonlinear fluxes at (60,0,0) due to a 10 dollar/sec local perturbation at (0,60,40).



A - nonlinear neutron response  
B - linear neutron response

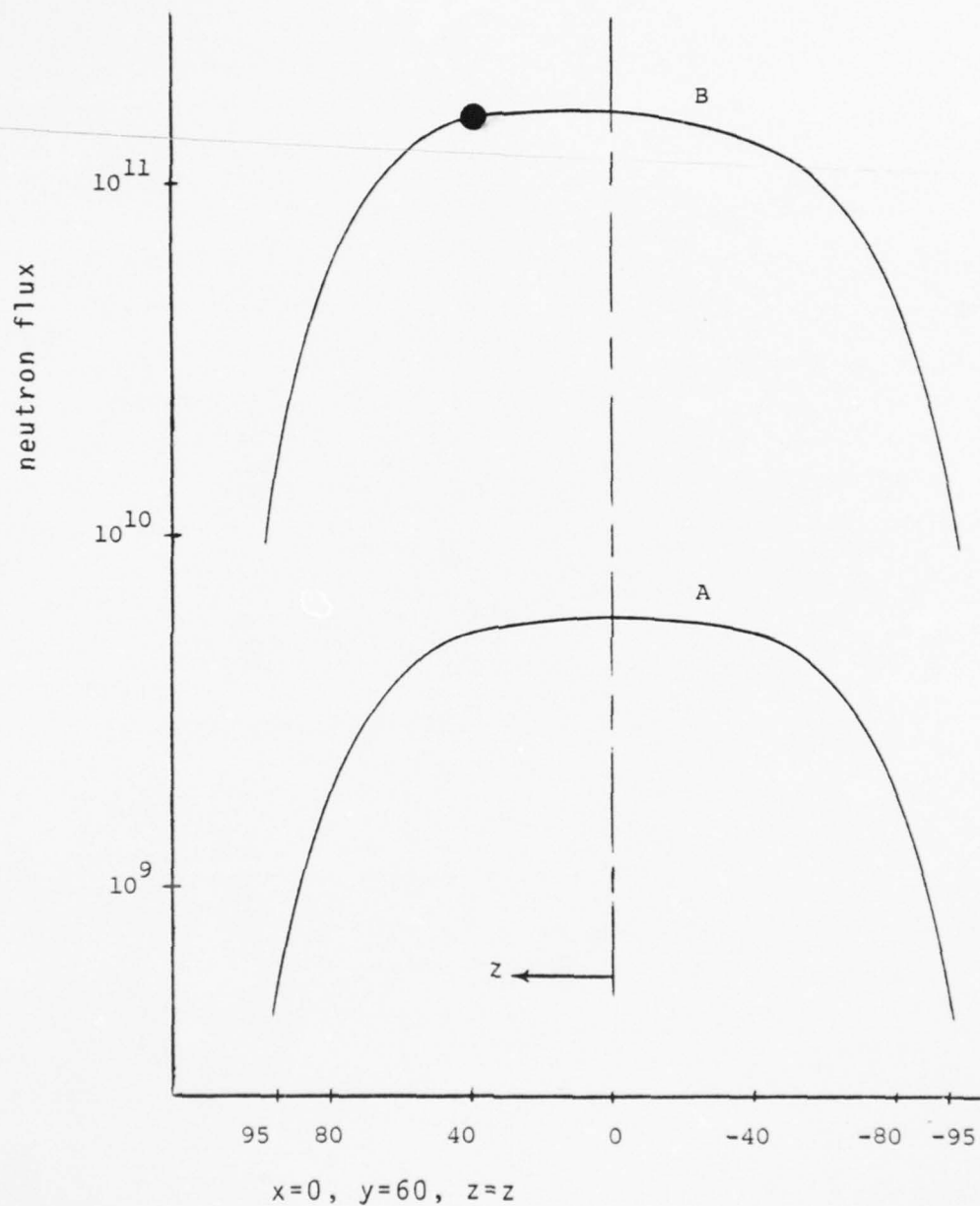
Figure 23. Linear and nonlinear fluxes at  $(-60, 0, 80)$  due to a 10 dollar/sec local perturbation at  $(0, 60, 40)$ .



- - point of local perturbation
- A - neutron flux at steady-state
- B - neutron flux under local perturbation

Figure 24. Radial flux distribution for the steady state and 100 dollar/sec local perturbation.





- - point of local perturbation
- A - axial flux distribution during steady state
- B - axial flux distribution during perturbation

Figure 25. Axial flux distribution for the steady state and 100 dollar/sec local perturbation.

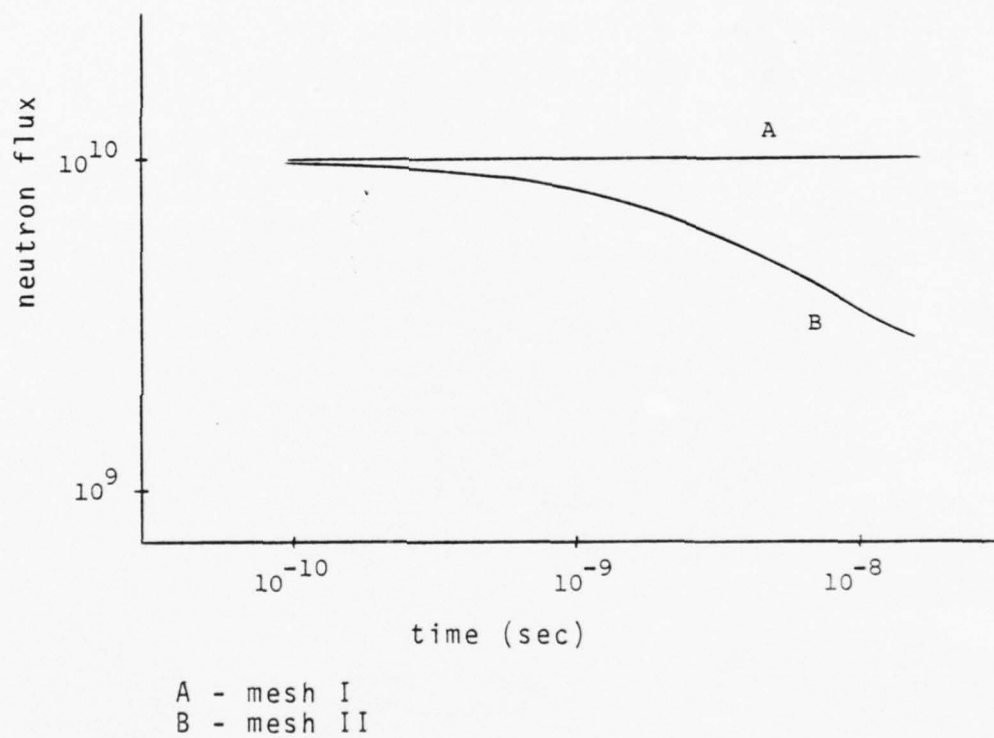


Figure 26. Early time history of the neutron flux at core center using mesh I and mesh II.

and delayed neutrons on the flux. To obtain an idea of the difference in magnitude between the linear and nonlinear flux for the 100 dollar local perturbation, at time  $t = 10^{-3}$  second, the linear case predicted a neutron flux at the core center of  $2.024 \times 10^{12}$  neutrons per  $\text{cm}^2$  per sec. The nonlinear reactor predicted  $1.85 \times 10^{10}$  neutrons per  $\text{cm}^2$  per sec. Although the numbers are not sufficiently accurate due to the crudeness of the finite element mesh, the significant difference in the order of magnitude between the linear and nonlinear neutron flux leads to the belief that the three-dimensional finite element model utilized is predicting the correct trend of neutron flux behavior.

The radial flux distribution for the steady state shown in figure 24 portrays the expected flux distribution. The radial flux distributions for the local perturbation case show a skew distribution at the point of perturbation. The axial flux distribution at steady state is very much symmetric about the center. Again, the expected skew at the point of perturbation is there, as shown in figure 25. Figure 26 gives an indication that the  $\Sigma_f^*$  for finer meshes is higher. However, curve B of figure 26 should be extended to longer times to verify this hypothesis. Curve B, as plotted in figure 26, used four hours of computer time employing the H-compiler of the IBM 360/67.

## VI. CONCLUSIONS AND RECOMMENDATIONS

The finite element mesh employed here is crude, and, thus, results that were obtained should be considered as positive indicators rather than numerically conclusive facts. The trend of neutron flux behavior is the major thrust of this work. From the results obtained, it is concluded that the expected patterns of neutron behavior as predicted by the three-dimensional finite element model used do occur. These patterns were best demonstrated by the differences between the linear and nonlinear flux responses and by the spatial flux distribution at steady state and during local perturbation. The three-dimensional quadratic finite element model utilized should produce better results by resorting to a finer mesh. The draw-back to a finer mesh, of course, is the significant increase in computer time and storage requirements. Once accurate results are obtained through finer element meshes, comparisons between three- and two-dimensional models can be attempted.

A mesh generator was not developed for this problem. It is recommended that this be done to ease the transition from one mesh to another and to minimize human error. In addition, a similar calculation using a three-dimensional linear element should be performed to corroborate the results obtained here. It should be particularly noted that this type of problem is highly sensitive to the fission cross-section.

In the search for  $\Sigma_f^*$ , it was necessary to adjust  $\Sigma_f$  to the sixth decimal place. There is no exact method of deriving  $\Sigma_f^*$  due to the highly nonlinear aspect of the problem; therefore, trial and error must be used. Finally, the Gaussian quadrature used to determine the element matrices should be investigated. The cause of the differences in values obtained by using different number of integration points should be established. Was it due to the integration points, the coordinate transformation, or the element shape functions? This is an important question upon which future numerical results could be based.



# APPENDIX A

## MESH I CONNECTIVITY AND COORDINATES

The connectivity matrix for the 128-element mesh is as follows:

ELEMENT NUMBER	1	2	3	4	5	6	7	8	9	10	11	12	13	14	15
1	1	3	12	11	10	2	26	28	27	35	37	46	45	44	36
2	1	4	15	13	12	3	26	29	28	35	38	48	47	46	37
3	1	5	18	15	14	4	26	30	29	35	39	50	49	48	38
4	1	6	22	17	16	5	26	31	30	35	40	52	51	50	39
5	1	7	24	19	18	6	26	32	31	35	42	54	53	52	40
6	1	8	27	22	21	7	26	33	32	35	43	56	55	54	41
7	1	9	30	25	24	8	26	34	33	35	43	58	57	56	42
8	1	10	33	28	27	9	26	35	34	35	43	61	60	58	43
9	1	11	36	31	30	36	26	36	35	35	43	62	61	59	44
10	35	37	40	45	44	37	60	62	61	69	71	80	79	78	70
11	35	38	41	46	45	38	60	63	62	69	72	82	81	80	71
12	35	39	42	49	48	39	60	64	63	69	73	84	83	82	72
13	35	40	43	51	50	40	60	65	64	69	74	86	85	84	73
14	35	41	44	53	52	41	60	66	65	69	75	88	87	86	74
15	35	42	45	55	54	42	60	67	66	69	76	90	89	88	75
16	35	43	46	57	56	43	60	68	67	69	77	92	91	90	76
17	35	44	47	59	58	44	60	69	68	69	78	93	92	91	77
18	69	71	80	79	78	70	118	120	119	425	427	436	435	434	426
19	69	72	81	80	79	71	118	121	120	425	428	437	436	435	427
20	69	73	82	81	80	72	118	122	121	425	429	438	437	436	428
21	69	74	83	82	81	73	118	123	122	425	430	439	438	437	429
22	69	75	84	83	82	74	118	124	123	425	431	440	439	438	430
23	69	76	85	84	83	75	118	125	124	425	432	441	440	439	431
24	69	77	86	85	84	76	118	126	125	425	433	442	441	440	432
25	69	78	87	86	85	77	118	127	126	425	434	443	442	441	433
26	69	79	88	87	86	78	118	128	127	425	435	444	443	442	434
27	379	95	92	93	92	94	410	411	409	436	436	445	444	443	435
28	80	97	94	93	92	96	410	412	410	436	437	446	445	444	436
29	80	98	95	94	93	97	411	413	411	436	438	447	446	445	437
30	82	98	96	95	94	99	412	414	412	438	439	448	447	446	438
31	82	99	97	96	95	100	413	415	413	438	440	449	448	447	439
32	87	100	98	97	96	102	414	416	414	438	441	450	449	448	440
33	84	101	99	98	97	103	415	417	415	440	442	451	450	449	441
34	84	102	100	99	98	105	416	418	416	440	443	452	451	450	442
35	89	103	101	100	99	106	417	419	417	442	444	453	452	451	443
36	86	104	102	101	100	106	418	420	418	442	445	454	453	452	444
37	86	107	105	104	103	106	419	421	419	442	446	455	454	453	445



89

The coordinates of the 128-element mesh are as follows:

NODE NUMBER	X	Y	Z
1	0.0	0.0	80.00
2	0.0	21.21	80.00
3	21.21	30.00	80.00
4	30.00	21.21	80.00
5	0.0	0.0	80.00
6	0.0	-21.21	80.00
7	21.21	-30.00	80.00
8	30.00	-21.21	80.00
9	-21.21	0.0	80.00
10	-30.00	21.21	80.00
11	-21.21	60.00	80.00
12	0.0	55.43	80.00
13	22.43	42.96	80.00
14	55.43	30.00	80.00
15	80.00	22.43	80.00
16	55.43	0.0	80.00
17	42.96	-22.43	80.00
18	30.00	-55.43	80.00
19	22.43	-80.00	80.00
20	0.0	-42.96	80.00
21	-22.43	-30.00	80.00
22	-55.43	-22.43	80.00
23	-80.00	-10.0	80.00
24	-55.43	22.43	80.00
25	-42.96	55.43	80.00
26	-30.00	80.00	80.00
27	-22.43	60.00	40.00
28	-10.0	42.96	40.00
29	0.0	30.00	40.00
30	22.43	22.43	40.00
31	42.96	10.0	40.00
32	55.43	0.0	40.00
33	80.00	10.0	40.00
34	55.43	30.00	40.00
35	42.96	55.43	40.00
36	30.00	80.00	40.00
37	22.43	60.00	0.0
38	10.0	42.96	0.0
39	0.0	30.00	0.0
40	22.43	21.21	0.0
41	42.96	10.0	0.0
42	55.43	0.0	0.0
43	80.00	10.0	0.0
44	55.43	30.00	0.0











[illegible]



AD-A038 775

NAVAL POSTGRADUATE SCHOOL MONTEREY CALIF  
FINITE ELEMENT SOLUTION OF A THREE-DIMENSIONAL NONLINEAR REACTO--ETC(U)  
DEC 76 E C BERMUDEZ

F/6 18/11

UNCLASSIFIED

NL

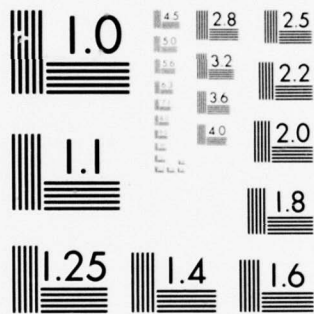
2 OF 2  
AD  
A038775



END

DATE  
FILMED  
5-77





63.64  
74.83  
83.15  
88.27  
90.00  
88.27  
83.15  
74.83  
63.64  
50.00  
34.44  
17.56  
0.00  
-17.56  
-34.44  
-50.00  
-63.64  
-74.83  
-83.15  
-88.27  
-90.00  
-88.27  
-83.15  
-74.83  
-63.64  
-50.00  
-34.44  
-17.56  
0.00  
34.44  
63.64  
83.15  
90.00  
88.27  
63.64  
34.44  
0.00  
-34.44  
-63.64  
-83.15  
-90.00  
-88.27  
-63.64  
-34.44  
0.00  
17.56  
34.44  
50.00

63.64  
50.00  
34.44  
17.56  
0.00  
-17.56  
-34.44  
-50.00  
-63.64  
-74.83  
-83.15  
-88.27  
-90.00  
-88.27  
-83.15  
-74.83  
-63.64  
-50.00  
-34.44  
-17.56  
0.00  
17.56  
34.44  
50.00  
63.64  
74.83  
83.15  
88.27  
90.00  
83.15  
63.64  
34.44  
0.00  
-34.44  
-63.64  
-83.15  
-90.00  
-83.15  
-63.64  
-34.44  
-3.00  
34.44  
63.64  
83.15  
90.00  
88.27  
83.15  
74.83



[illegible]

63.64  
50.00  
17.56  
0.00  
17.56  
34.44  
50.00  
63.64  
74.83  
88.27  
90.00  
88.27  
83.15  
74.83  
63.64  
50.00  
34.44  
17.56  
0.00  
17.56  
34.44  
50.00  
63.64  
74.83  
88.27  
90.00  
83.15  
63.64  
34.44  
0.00  
34.44  
63.64  
90.00  
83.15  
63.64  
34.44  
0.00  
34.44  
63.64  
83.15  
0.00  
30.00  
21.21  
0.00

[illegible]





[illegible]

# APPENDIX B

## MESH II CONNECTIVITY AND COORDINATES

The connectivity matrix for the 192-element mesh is as follows:

ELEMENT NUMBER	1	2	3	4	5	6	7	8	9	10	11	12	13	14	15
1	1	3	12	11	10	2	26	28	27	35	37	46	45	44	36
2	1	4	14	13	12	3	26	29	28	35	38	48	47	46	37
3	1	5	15	14	13	4	26	30	29	35	39	50	49	48	38
4	1	6	18	17	16	5	26	31	30	35	40	52	51	50	39
5	1	7	20	19	18	6	26	32	31	35	41	54	53	52	40
6	1	8	22	21	20	7	26	33	32	35	42	56	55	54	41
7	1	9	24	23	22	8	26	34	33	35	43	58	57	56	42
8	1	10	46	45	44	9	26	35	34	35	36	80	79	78	43
9	1	11	50	49	48	36	60	62	61	69	72	82	81	80	44
10	1	12	52	51	50	37	60	63	62	69	73	84	83	82	45
11	1	13	54	53	52	38	60	64	63	69	74	86	85	84	46
12	1	14	56	55	54	39	60	65	64	69	75	88	87	86	47
13	1	15	80	79	78	40	60	66	65	69	76	90	89	88	48
14	1	16	82	81	80	41	60	67	66	69	77	92	91	90	49
15	1	17	84	83	82	42	60	68	67	69	77	92	91	90	50
16	1	18	86	85	84	43	60	69	68	69	77	92	91	90	51
17	1	19	88	87	86	44	60	70	69	69	77	92	91	90	52
18	1	20	90	89	88	45	94	96	95	103	105	114	113	112	53
19	1	21	82	81	80	71	94	97	96	103	106	116	115	114	54
20	1	22	84	83	82	72	94	98	97	103	107	118	117	116	55
21	1	23	86	85	84	73	94	99	98	103	108	120	119	118	56
22	1	24	88	87	86	74	94	100	99	103	109	122	121	120	57
23	1	25	90	89	88	75	94	101	100	103	110	124	123	122	58
24	1	26	92	91	90	76	94	102	101	103	111	126	125	124	59
25	1	27	94	93	92	77	128	130	129	103	114	148	147	146	60
26	1	28	114	113	112	104	128	131	130	103	114	150	149	148	61
27	1	29	116	115	114	106	128	132	131	103	114	152	151	150	62
28	1	30	118	117	116	107	128	133	132	103	114	154	153	152	63
29	1	31	120	119	118	108	128	134	133	103	114	156	155	154	64
30	1	32	122	121	120	109	128	135	134	103	114	158	157	156	65
31	1	33	124	123	122	110	128	136	135	103	114	160	159	158	66
32	1	34	126	125	124	111	128	137	136	103	114	162	161	160	67
33	1	35	148	147	146	138	162	164	163	137	138	311	310	309	68
34	1	36	150	149	148	139	162	165	164	137	138	313	312	311	69
35	1	37	152	151	150	140	162	166	165	137	138	315	314	313	70

304	180	112	589	316	179	305	100	167	17	162	141	152	153	154	137	142	137	36
305	182	117	591	318	319	306	300	168	168	162	142	154	155	156	137	143	137	37
306	183	119	593	320	321	307	300	169	169	162	143	155	157	157	137	144	137	38
307	185	120	594	322	323	308	300	170	170	162	144	156	159	158	137	145	137	39
308	186	121	595	324	325	309	300	171	171	162	145	157	161	159	137	146	137	40
2	188	122	597	326	327	4	1	172	172	162	146	158	164	160	137	147	137	41
3	188	123	599	328	329	5	1	173	173	162	147	159	165	161	137	148	137	42
4	189	124	600	330	331	6	1	174	174	162	148	160	166	162	137	149	137	43
5	191	125	601	332	333	7	1	175	175	162	149	161	167	163	137	150	137	44
6	191	126	602	334	335	8	1	176	176	162	150	162	168	164	137	151	137	45
7	192	127	603	336	337	9	1	177	177	162	151	163	169	165	137	152	137	46
8	194	128	604	338	339	2	10	178	178	162	152	164	170	166	137	153	137	47
9	195	129	605	340	341	3	10	179	179	162	153	165	171	167	137	154	137	48
0	197	130	606	342	343	4	10	180	180	162	154	166	172	168	137	155	137	49
1	197	131	607	344	345	5	10	181	181	162	155	167	173	169	137	156	137	50
2	198	132	608	346	347	6	10	182	182	162	156	168	174	170	137	157	137	51
3	200	133	609	348	349	7	10	183	183	162	157	169	175	171	137	158	137	52
4	201	134	610	350	351	8	10	184	184	162	158	170	176	172	137	159	137	53
5	203	135	611	352	353	9	10	185	185	162	159	171	177	173	137	160	137	54
6	206	136	612	354	355	2	10	186	186	162	160	172	178	174	137	161	137	55
7	207	137	613	356	357	3	10	187	187	162	161	173	179	175	137	162	137	56
8	209	138	614	358	359	4	10	188	188	162	162	174	180	176	137	163	137	57
9	209	139	615	360	361	5	10	189	189	162	163	175	181	177	137	164	137	58
0	210	140	616	362	363	6	10	190	190	162	164	176	182	178	137	165	137	59
1	212	141	617	364	365	7	10	191	191	162	165	177	183	179	137	166	137	60
2	213	142	618	366	367	8	10	192	192	162	166	178	184	180	137	167	137	61
3	215	143	619	368	369	9	10	193	193	162	167	179	185	181	137	168	137	62
4	215	144	620	370	371	2	10	194	194	162	168	180	186	182	137	169	137	63
5	215	145	621	372	373	3	10	195	195	162	169	181	187	183	137	170	137	64
6	215	146	622	374	375	4	10	196	196	162	170	182	188	184	137	171	137	65
7	215	147	623	376	377	5	10	197	197	162	171	183	189	185	137	172	137	66
8	215	148	624	378	379	6	10	198	198	162	172	184	190	186	137	173	137	67
9	215	149	625	380	381	7	10	199	199	162	173	185	191	187	137	174	137	68
0	215	150	626	382	383	8	10	200	200	162	174	186	192	188	137	175	137	69
1	215	151	627	384	385	9	10	201	201	162	175	187	193	189	137	176	137	70
2	215	152	628	386	387	2	10	202	202	162	176	188	194	190	137	177	137	71
3	215	153	629	388	389	3	10	203	203	162	177	189	195	191	137	178	137	72
4	215	154	630	390	391	4	10	204	204	162	178	190	196	192	137	179	137	73
5	215	155	631	392	393	5	10	205	205	162	179	191	197	193	137	180	137	74
6	215	156	632	394	395	6	10	206	206	162	180	192	198	194	137	181	137	75
7	215	157	633	396	397	7	10	207	207	162	181	193	199	195	137	182	137	76
8	215	158	634	398	399	8	10	208	208	162	182	194	200	196	137	183	137	77
9	215	159	635	400	401	9	10	209	209	162	183	195	201	197	137	184	137	78
0	215	160	636	402	403	2	10	210	210	162	184	196	202	198	137	185	137	79
1	215	161	637	404	405	3	10	211	211	162	185	197	203	199	137	186	137	80
2	215	162	638	406	407	4	10	212	212	162	186	198	204	200	137	187	137	81
3	215	163	639	408	409	5	10	213	213	162	187	199	205	201	137	188	137	82
4	215	164	640	410	411	6	10	214	214	162	188	200	206	202	137	189	137	83
5	215	165	641	412	413	7	10	215	215	162	189	201	207	203	137	190	137	84
6	215	166	642	414	415	8	10	216	216	162	190	202	208	204	137	191	137	85
7	215	167	643	416	417	9	10	217	217	162	191	203	209	205	137	192	137	86
8	215	168	644	418	419	2	10	218	218	162	192	204	210	206	137	193	137	87
9	215	169	645	420	421	3	10	219	219	162	193	205	211	207	137	194	137	88
0	215	170	646	422	423	4	10	220	220	162	194	206	212	208	137	195	137	89
1	215	171	647	424	425	5	10	221	221	162	195	207	213	209	137	196	137	90
2	215	172	648	426	427	6	10	222	222	162	196	208	214	210	137	197	137	91
3	215	173	649	428	429	7	10	223	223	162	197	209	215	211	137	198	137	92
4	215	174	650	430	431	8	10	224	224	162	198	210	216	212	137	199	137	93
5	215	175	651	432	433	9	10	225	225	162	199	211	217	213	137	200	137	94
6	215	176	652	434	435	2	10	226	226	162	200	212	218	214	137	201	137	95
7	215	177	653	436	437	3	10	227	227	162	201	213	219	215	137	202	137	96
8	215	178	654	438	439	4	10	228	228	162	202	214	220	216	137	203	137	97
9	215	179	655	440	441	5	10	229	229	162	203	215	221	217	137	204	137	98
0	215	180	656	442	443	6	10	230	230	162	204	216	222	218	137	205	137	99
1	215	181	657	444	445	7	10	231	231	162	205	217	223	219	137	206	137	00
2	215	182	658	446	447	8	10	232	232	162	206	218	224	220	137	207	137	01
3	215	183	659	448	449	9	10	233	233	162	207	219	225	221	137	208	137	02
4	215	184	660	450	451	2	10	234	234	162	208	220	226	222	137	209	137	03
5	215	185	661	452	453	3	10	235	235	162	209	221	227	223	137	210	137	04
6	215	186	662	454	455	4	10	236	236	162	210	222	228	224	137	211	137	05
7	215	187	663	456	457	5	10	237	237	162	211	223	229	225	137	212	137	06
8	215	188	664	458	459	6	10	238	238	162	212	224	230	226	137	213	137	07
9	215	189	665	460	461	7	10	239	239	162	213	225	231	227	137	214	137	08
0	215	190	666	462	463	8	10	240	240	162	214	226	232	228	137	215	137	09
1	215	191	667	464	465	9	10	241	241	162	215	227	233	229	137	216	137	10
2	215	192	668	466	467	2	10	242	242	162	216	228	234	230	137	217	137	11
3	215	193	669	468	469	3	10	243	243	162	217	229	235	231	137	218	137	12
4	215	194	670	470	471	4	10	244	244	162	218	230	236	232	137	219	137	13
5	215	195	671	472	473	5	10	245	245	162	219	231	237	233	137	220	137	14
6	215	196	672	474	475	6	10	246	246	162	220	232	238	234	137	221	137	15
7	215	197	673	476	477	7	10	247	247	162	221	233	239	235	137	222	137	16
8	215	198	674	478	479	8	10	248	248	162	222	234						



84	18	193	605	604	603	192	31	582	580	522	216	557	558
85	17	193	603	606	605	192	32	31	32	529	217	552	553
86	20	193	609	608	607	194	58	58	58	544	219	561	560
87	11	196	611	610	609	195	32	33	33	543	220	563	562
88	61	196	612	611	610	197	58	58	58	566	222	565	564
89	22	198	615	614	613	197	33	33	33	567	223	567	566
90	22	199	615	614	613	198	33	33	33	567	223	567	566
91	22	201	622	621	620	200	58	58	58	567	226	569	568
92	24	202	627	626	625	201	34	34	34	588	226	571	570
93	24	202	627	626	625	201	34	34	34	588	226	571	570
94	24	205	628	627	626	203	38	38	38	571	229	578	577
95	10	205	643	642	641	204	27	27	27	478	229	494	493
96	44	207	645	644	643	206	62	62	62	495	231	498	497
97	54	207	645	644	643	206	62	62	62	495	231	498	497
98	46	208	649	648	647	209	62	62	62	495	232	499	498
99	47	208	649	648	647	209	62	62	62	495	232	499	498
100	48	211	651	650	649	210	63	63	63	499	233	501	500
101	55	211	651	650	649	210	63	63	63	499	233	501	500
102	55	213	655	654	653	212	64	64	64	503	235	504	503
103	55	213	655	654	653	212	64	64	64	503	235	504	503
104	55	214	655	654	653	213	64	64	64	503	235	504	503
105	55	214	655	654	653	213	64	64	64	503	235	504	503
106	55	216	657	656	655	215	65	65	65	507	238	508	507
107	55	216	657	656	655	215	65	65	65	507	238	508	507
108	55	217	659	658	657	216	65	65	65	507	240	509	508
109	55	217	659	658	657	216	65	65	65	507	240	509	508
110	54	219	662	661	660	218	66	66	66	511	241	512	511
111	54	220	662	661	660	218	66	66	66	511	241	512	511
112	56	222	667	666	665	221	66	66	66	511	244	513	512
113	56	222	667	666	665	221	66	66	66	511	244	513	512
114	56	223	667	666	665	221	66	66	66	511	244	513	512
115	56	223	667	666	665	221	66	66	66	511	244	513	512
116	56	225	669	668	667	222	67	67	67	519	246	518	517
117	56	225	669	668	667	222	67	67	67	519	246	518	517
118	57	226	671	670	669	224	68	68	68	519	247	521	520
119	57	226	671	670	669	224	68	68	68	519	247	521	520
120	44	229	678	677	676	227	68	68	68	519	249	522	521
121	44	229	678	677	676	227	68	68	68	519	249	522	521
122	45	231	680	679	678	230	69	69	69	523	251	524	523
123	45	231	680	679	678	230	69	69	69	523	251	524	523
124	45	232	681	680	679	231	69	69	69	523	251	524	523
125	45	232	681	680	679	231	69	69	69	523	251	524	523
126	45	233	681	680	679	233	69	69	69	523	255	525	524
127	45	233	681	680	679	233	69	69	69	523	255	525	524
128	45	235	682	681	680	236	69	69	69	523	255	525	524
129	45	235	682	681	680	236	69	69	69	523	255	525	524
130	45	238	683	682	681	236	69	69	69	523	255	525	524
131	45	238	683	682	681	236	69	69	69	523	255	525	524

132	133	134	135	136	137	138	139	140	141	142	143	144	145	146	147	148	149	150	151	152	153	154	155	156	157	158	159	160	161	162	163	164	165	166	167	168	169	170	171	172	173	174	175	176	177	178	179					
86	86	51	88	51	88	51	88	51	88	51	88	51	88	51	88	51	88	51	88	51	88	51	88	51	88	51	88	51	88	51	88	51	88	51	88	51	88	51	88	51	88	51	88	51	88	51	88	51	88			
240	241	242	243	244	245	246	247	248	249	250	251	252	253	254	255	256	257	258	259	260	261	262	263	264	265	266	267	268	269	270	271	272	273	274	275	276	277	278	279	280	281	282	283	284	285	286	287	288	289	290		
509	508	511	513	513	513	513	513	513	513	513	513	513	513	513	513	513	513	513	513	513	513	513	513	513	513	513	513	513	513	513	513	513	513	513	513	513	513	513	513	513	513	513	513	513	513	513	513	513	513	513		
239	240	242	243	244	245	246	247	248	249	250	251	252	253	254	255	256	257	258	259	260	261	262	263	264	265	266	267	268	269	270	271	272	273	274	275	276	277	278	279	280	281	282	283	284	285	286	287	288	289	290		
99	99	400	100	100	100	100	100	100	100	100	100	100	100	100	100	100	100	100	100	100	100	100	100	100	100	100	100	100	100	100	100	100	100	100	100	100	100	100	100	100	100	100	100	100	100	100	100	100	100	100	100	
486	486	487	488	489	490	491	492	493	494	495	496	497	498	499	500	501	502	503	504	505	506	507	508	509	510	511	512	513	514	515	516	517	518	519	520	521	522	523	524	525	526	527	528	529	530	531	532	533	534	535	536	537
485	486	487	488	489	490	491	492	493	494	495	496	497	498	499	500	501	502	503	504	505	506	507	508	509	510	511	512	513	514	515	516	517	518	519	520	521	522	523	524	525	526	527	528	529	530	531	532	533	534	535	536	537
485	486	487	488	489	490	491	492	493	494	495	496	497	498	499	500	501	502	503	504	505	506	507	508	509	510	511	512	513	514	515	516	517	518	519	520	521	522	523	524	525	526	527	528	529	530	531	532	533	534	535	536	537
120	123	122	127	124	124	127	124	127	124	127	124	127	124	127	124	127	124	127	124	127	124	127	124	127	124	127	124	127	124	127	124	127	124	127	124	127	124	127	124	127	124	127	124	127	124	127	124	127	124	127		
265	265	267	268	268	270	271	273	274	274	277	277	279	280	282	283	285	286	286	288	289	291	292	292	294	295	297	298	298	298	298	298	298	298	298	298	298	298	298	298	298	298	298	298	298	298	298	298	298	298	298	298	
461	463	460	465	462	469	471	473	474	475	476	477	478	479	480	481	482	483	484	485	486	487	488	489	490	491	492	493	494	495	496	497	498	499	500	501	502	503	504	505	506	507	508	509	510	511	512	513	514	515	516	517	
459	461	462	465	466	469	471	473	474	475	476	477	478	479	480	481	482	483	484	485	486	487	488	489	490	491	492	493	494	495	496	497	498	499	500	501	502	503	504	505	506	507	508	509	510	511	512	513	514	515	516	517	
264	266	267	269	269	270	272	273	275	275	276	278	279	281	281	282	284	285	287	288	290	291	293	294	296	296	297	299	299	299	299	299	299	299	299	299	299	299	299	299	299	299	299	299	299	299	299	299	299	299	299		



180	154	288	413	412	411	287	167	389	388	317	337	365	364
181	155	289	414	415	415	288	167	392	389	317	338	367	366
182	156	290	415	416	416	290	168	391	389	317	339	319	368
183	157	291	416	417	417	291	168	392	391	319	340	369	370
184	158	292	417	418	418	293	169	393	392	321	341	371	371
185	159	293	418	419	419	293	169	394	393	321	342	372	372
186	160	294	419	420	420	294	170	395	394	321	343	373	373
187	161	295	420	421	421	296	170	396	395	323	344	374	374
188	162	296	421	422	422	297	170	396	396	323	345	375	375
189	163	297	422	423	423	299	163	381	396	379	346	377	377
190	164	298	423	424	424	299	163	381	396	379	347	378	378
191	165	299	424	425	425	299	163	381	396	379	348	379	379
192	166	300	425	426	426	300	163	381	396	379	349	380	380

The coordinates of the 192-element mesh are as follows:

NODE NUMBER	X	Y	Z
1	0.0	0.0	80.00
2	0.0	30.21	80.00
3	0.0	21.00	80.00
4	1.0	0.0	80.00
5	1.0	21.00	80.00
6	1.0	-21.00	80.00
7	2.0	0.0	80.00
8	2.0	21.00	80.00
9	2.0	-21.00	80.00
10	3.0	0.0	80.00
11	3.0	21.00	80.00
12	3.0	-21.00	80.00
13	4.0	0.0	80.00
14	4.0	21.00	80.00
15	4.0	-21.00	80.00
16	5.0	0.0	80.00
17	5.0	21.00	80.00
18	5.0	-21.00	80.00
19	6.0	0.0	80.00
20	6.0	21.00	80.00
21	6.0	-21.00	80.00
22	7.0	0.0	80.00
23	7.0	21.00	80.00
24	7.0	-21.00	80.00
25	8.0	0.0	80.00
26	8.0	21.00	80.00
27	8.0	-21.00	80.00
28	9.0	0.0	80.00
29	9.0	21.00	80.00
30	9.0	-21.00	80.00
31	10.0	0.0	80.00
32	10.0	21.00	80.00
33	10.0	-21.00	80.00
34	11.0	0.0	80.00
35	11.0	21.00	80.00
36	11.0	-21.00	80.00
37	12.0	0.0	80.00
38	12.0	21.00	80.00
39	12.0	-21.00	80.00
40	13.0	0.0	80.00
41	13.0	21.00	80.00
42	13.0	-21.00	80.00
43	14.0	0.0	80.00
44	14.0	21.00	80.00
45	14.0	-21.00	80.00
46	15.0	0.0	80.00
47	15.0	21.00	80.00
48	15.0	-21.00	80.00
49	16.0	0.0	80.00
50	16.0	21.00	80.00
51	16.0	-21.00	80.00
52	17.0	0.0	80.00
53	17.0	21.00	80.00
54	17.0	-21.00	80.00
55	18.0	0.0	80.00
56	18.0	21.00	80.00
57	18.0	-21.00	80.00
58	19.0	0.0	80.00
59	19.0	21.00	80.00
60	19.0	-21.00	80.00
61	20.0	0.0	80.00
62	20.0	21.00	80.00
63	20.0	-21.00	80.00
64	21.0	0.0	80.00
65	21.0	21.00	80.00
66	21.0	-21.00	80.00
67	22.0	0.0	80.00
68	22.0	21.00	80.00
69	22.0	-21.00	80.00
70	23.0	0.0	80.00
71	23.0	21.00	80.00
72	23.0	-21.00	80.00
73	24.0	0.0	80.00
74	24.0	21.00	80.00
75	24.0	-21.00	80.00
76	25.0	0.0	80.00
77	25.0	21.00	80.00
78	25.0	-21.00	80.00
79	26.0	0.0	80.00
80	26.0	21.00	80.00
81	26.0	-21.00	80.00
82	27.0	0.0	80.00
83	27.0	21.00	80.00
84	27.0	-21.00	80.00
85	28.0	0.0	80.00
86	28.0	21.00	80.00
87	28.0	-21.00	80.00
88	29.0	0.0	80.00
89	29.0	21.00	80.00
90	29.0	-21.00	80.00
91	30.0	0.0	80.00
92	30.0	21.00	80.00
93	30.0	-21.00	80.00
94	31.0	0.0	80.00
95	31.0	21.00	80.00
96	31.0	-21.00	80.00
97	32.0	0.0	80.00
98	32.0	21.00	80.00
99	32.0	-21.00	80.00
100	33.0	0.0	80.00
101	33.0	21.00	80.00
102	33.0	-21.00	80.00
103	34.0	0.0	80.00
104	34.0	21.00	80.00
105	34.0	-21.00	80.00
106	35.0	0.0	80.00
107	35.0	21.00	80.00
108	35.0	-21.00	80.00
109	36.0	0.0	80.00
110	36.0	21.00	80.00
111	36.0	-21.00	80.00
112	37.0	0.0	80.00
113	37.0	21.00	80.00
114	37.0	-21.00	80.00
115	38.0	0.0	80.00
116	38.0	21.00	80.00
117	38.0	-21.00	80.00
118	39.0	0.0	80.00
119	39.0	21.00	80.00
120	39.0	-21.00	80.00
121	40.0	0.0	80.00
122	40.0	21.00	80.00
123	40.0	-21.00	80.00
124	41.0	0.0	80.00
125	41.0	21.00	80.00
126	41.0	-21.00	80.00
127	42.0	0.0	80.00
128	42.0	21.00	80.00
129	42.0	-21.00	80.00
130	43.0	0.0	80.00
131	43.0	21.00	80.00
132	43.0	-21.00	80.00
133	44.0	0.0	80.00
134	44.0	21.00	80.00
135	44.0	-21.00	80.00
136	45.0	0.0	80.00
137	45.0	21.00	80.00
138	45.0	-21.00	80.00
139	46.0	0.0	80.00
140	46.0	21.00	80.00
141	46.0	-21.00	80.00
142	47.0	0.0	80.00
143	47.0	21.00	80.00
144	47.0	-21.00	80.00
145	48.0	0.0	80.00
146	48.0	21.00	80.00
147	48.0	-21.00	80.00
148	49.0	0.0	80.00
149	49.0	21.00	80.00
150	49.0	-21.00	80.00
151	50.0	0.0	80.00
152	50.0	21.00	80.00
153	50.0	-21.00	80.00
154	51.0	0.0	80.00
155	51.0	21.00	80.00
156	51.0	-21.00	80.00
157	52.0	0.0	80.00
158	52.0	21.00	80.00
159	52.0	-21.00	80.00
160	53.0	0.0	80.00
161	53.0	21.00	80.00
162	53.0	-21.00	80.00
163	54.0	0.0	80.00
164	54.0	21.00	80.00
165	54.0	-21.00	80.00
166	55.0	0.0	80.00
167	55.0	21.00	80.00
168	55.0	-21.00	80.00
169	56.0	0.0	80.00
170	56.0	21.00	80.00
171	56.0	-21.00	80.00
172	57.0	0.0	80.00
173	57.0	21.00	80.00
174	57.0	-21.00	80.00
175	58.0	0.0	80.00
176	58.0	21.00	80.00
177	58.0	-21.00	80.00
178	59.0	0.0	80.00
179	59.0	21.00	80.00
180	59.0	-21.00	80.00
181	60.0	0.0	80.00
182	60.0	21.00	80.00
183	60.0	-21.00	80.00
184	61.0	0.0	80.00
185	61.0	21.00	80.00
186	61.0	-21.00	80.00
187	62.0	0.0	80.00
188	62.0	21.00	80.00
189	62.0	-21.00	80.00
190	63.0	0.0	80.00
191	63.0	21.00	80.00
192	63.0	-21.00	80.00





[illegible]



171  
172  
173  
174  
175  
176  
177  
178  
179  
180  
181  
182  
183  
184  
185  
186  
187  
188  
189  
190  
191  
192  
193  
194  
195  
196  
197  
198  
199  
200  
201  
202  
203  
204  
205  
206  
207  
208  
209  
210  
211  
212  
213  
214  
215  
216  
217  
218

[illegible][illegible][illegible]



-17.00  
 -38.60  
 -53.03  
 -62.90  
 -71.80  
 -75.00  
 -71.80  
 -62.80

16.80  
38.10  
53.03  
62.80  
71.30  
75.00  
71.80  
62.03  
38.10  
17.10  
10.90  
-16.90  
-38.50

253  
254  
255  
256  
257  
258  
259  
260  
261  
262  
263  
264  
265  
266

267  
268  
269  
270  
271  
272  
273  
274  
275  
276  
277  
278  
279  
280  
281  
282  
283  
284  
285  
286  
287  
288  
289  
290  
291  
292  
293  
294  
295  
296  
297  
298  
299  
300  
301  
302  
303  
304  
305  
306  
307  
308  
309  
310  
311  
312  
313  
314

-53.03
-62.70
-75.00
-71.30
-52.90
-58.60
-17.00
16.80
38.10
52.80
71.30
75.00
71.30
62.80
53.03
38.10
17.00
0.00
16.90
38.50
52.03
61.30
71.30
75.00
71.30
62.90
53.03
38.60
17.30
0.00
0.00
21.20
30.21
21.21
0.21
21.00
32.21
21.21
0.96
22.43
55.00
55.43

[illegible][illegible]



-110.00  
-110.00  
-110.00  
-110.00  
-110.00  
-110.00  
-110.00  
-110.00  
-110.00  
-110.00  
-95.00  
-95.00  
-95.00  
-95.00  
-95.00  
-95.00  
-95.00  
-95.00  
-80.00  
-80.00  
-80.00  
-80.00  
-80.00  
-80.00  
-80.00  
-80.00







459  
460  
461  
462  
463  
464  
465  
466  
467  
468  
469  
470  
471  
472  
473  
474  
475  
476  
477  
478  
479  
480  
481  
482  
483  
484  
485  
486  
487  
488  
489  
490  
491  
492  
493  
494  
495  
496  
497  
498  
499  
500  
501  
502  
503  
504  
505  
506

34.44  
17.56  
-17.56  
-34.44  
-50.00  
-74.83  
-88.27  
-90.00  
-88.27  
-74.83  
-63.64  
-50.00  
-34.44  
-17.56  
0.00  
34.44  
63.64  
83.15  
90.00  
63.64  
34.44  
0.00  
-34.44  
-63.64  
-83.15  
-90.00  
-63.64  
-34.44  
-34.44  
0.00  
17.56  
34.44  
50.00  
63.64  
74.83  
88.27  
90.00  
88.27  
83.15  
74.83  
50.00

-83.15  
 -88.27  
 -90.00  
 -88.27  
 -83.15  
 -74.83  
 -63.64  
 -50.00  
 -34.44  
 -17.56  
 0.00  
 17.56  
 34.44  
 50.00  
 63.64  
 74.83  
 83.15  
 88.27  
 90.00  
 83.15  
 63.64  
 34.44  
 0.00  
 -34.44  
 -63.64  
 -83.15  
 -90.00  
 -88.27  
 -83.15  
 -74.83  
 -63.64  
 -50.00  
 -34.44  
 -17.56  
 0.00  
 17.56  
 34.44  
 50.00  
 63.64  
 74.83  
 83.15  
 88.27  
 90.00  
 83.15  
 63.64  
 34.44  
 0.00  
 -34.44  
 -63.64  
 -83.15  
 -90.00  
 -88.27  
 -83.15  
 -74.83  
 -63.64  
 -50.00  
 -34.44  
 -17.56  
 0.00  
 17.56  
 34.44  
 50.00  
 63.64  
 74.83









651  
652  
653  
654  
655  
656  
657  
658  
659  
660  
661  
662  
663  
664  
665  
666  
667  
668  
669  
670  
671  
672  
673  
674  
675  
676  
677  
678  
679  
680  
681  
682  
683  
684  
685  
686  
687  
688  
689  
690  
691  
692  
693  
694  
695  
696  
697  
698

-83.15  
 -88.27  
 -90.00  
 -88.27  
 -83.15  
 -74.83  
 -73.64  
 -50.00  
 -44.44  
 -37.56  
 -17.00  
 17.56  
 30.44  
 50.00  
 63.64  
 74.83  
 88.27  
 75.00  
 62.90  
 53.03  
 38.60  
 17.00  
 0.00  
 17.00  
 38.60  
 53.03  
 62.90  
 75.00  
 88.27  
 71.80  
 71.80  
 62.03  
 52.80  
 38.60  
 17.10  
 17.10  
 38.30  
 52.80  
 60.30  
 71.30  
 55.43  
 42.43  
 22.96  
 -22.96



699  
700  
701  
702  
703  
704  
705  
706  
707  
708  
709  
710  
711  
712  
713  
714  
715  
716  
717

42.43  
22.96  
20.00  
-22.43  
-22.43  
-55.43  
-60.00  
-42.43  
-22.96  
0.00  
21.21  
30.00  
21.21  
21.00  
0.00  
-21.21  
-30.00  
-21.21  
0.00

-42.43  
-55.43  
-60.00  
-42.43  
-22.96  
0.00  
22.96  
42.43  
55.43  
30.00  
21.21  
0.00  
21.21  
-30.00  
-21.21  
0.00  
21.21  
0.00

110.00  
110.00  
110.00  
110.00  
110.00  
110.00  
110.00  
110.00  
110.00  
110.00  
110.00  
110.00  
110.00  
110.00  
110.00  
110.00  
110.00  
110.00



```

KK=CONN(I,K)
IF(KK.GT.183) GO TO 80
JA(JJ)=JA(JJ)+1
JAA=JA(JJ)
DO 70 L=2,JAA
JL=MAME(JJ,L)
IF(JJL.EQ.KK) JA(JJ)=JA(JJ)-1
IF(JJL.EQ.KK) GO TO 80
IF(JJL.EQ.0) MAME(JJ,JAA)=KK
70 CONTINUE
80 CONTINUE
90 CONTINUE
100 CONTINUE
C
JB(1)=1
JC=0
DO 200 I=1,183
JN=JA(I)
JB(I+1)=JB(I)+JA(I)
JC=JC+JA(I)
200 CONTINUE
WRITE(6,215) JC
DO 250 I=1,183
JAA=JA(I)
JBL=JB(I)
DO 240 J=1,JAA
JJ=JBL+J-1
NAME(JJ)=MAME(I,J)
240 CONTINUE
250 CONTINUE
WRITE(6,204)
WRITE(6,205) (JA(I),I=1,183)
WRITE(6,207)
WRITE(6,208) (JB(I),I=1,183)
WRITE(6,208)
WRITE(6,205) (NAME(I),I=1,JC)
STOP
END

```

```

C-----
C THIS IS THE MAIN PROGRAM WHICH CALCULATES THE BIGG AND BIGGG
C SYSTEM MATRICES BY USING SUBROUTINES FLOWIE AND TANYA. THE SYSTEM
C MATRICES ARE THEN PUT ON TAPE NUMBER NPS182.
C-----
      REAL*8 G,GG,BIGG,BIGGG
      REAL*8 WL,WS,S,CL1,CL2,CL3,FN,DL1,DL2,DL3,DS,DETJ
      INTEGER*2 NAME,JA,JB,NNZ,JC,NUMNP,NUMEL,NELDOF,CONN
      COMMON/STRY2/NAME(4615),JA(183),JB(183),NNZ,JC,NUMNP,NUMEL,NELDOF,
1     CONN(128,15)
      COMMON/STRY1/X(505),P(505),Z(505)
      COMMON/XCAL/XX(15),YY(15),ZZ(15),PPSI(15)
      COMMON/GMAT/G(15,15)
      COMMON/GMAT/GG(15,15)
      COMMON/SYST1/BSMT1(4615)
      COMMON/SYST2/BSMT2(4615)
      COMMON/GAJSS/WL(7),WS(5),CL1(7),CL2(7),CL3(7),FN(15,21),DL1(1
15,21),DL2(15,21),DL3(15,21),DS(15,21),DETJ(21)
      FORMAT(16I5)
150  FORMAT(25I5)
160  FORMAT(8E16.8)
211  FORMAT(12F10.4)
702  FORMAT(20I6)
800  FORMAT(10F8.2)
952  FORMAT(20I4)
      NNZ=183
      NUMEL=128
      NUMNP=505
      JC=4615
      NELDOF=15
      DO 455 I=1,NUMEL
        READ(5,150)I,(CONN(I,J),J=1,NELDOF)
      CONTINUE
455  READ(5,952)(JA(I),I=1,NNZ)
      READ(5,952)(JB(I),I=1,NNZ)
      READ(5,952)(NAME(I),I=1,JC)
      READ(5,800)(X(I),I=1,NUMNP)
      READ(5,800)(P(I),I=1,NUMNP)
      READ(5,800)(Z(I),I=1,NUMNP)
      DO 465 I=1,JC
        BIGG(I)=0.0
        BIGGG(I)=0.0
      CONTINUE
465  CALL TANYA
      CALL FLOWIE
      STOP

```

M-010  
M-015

M-060

M-100

M-120  
M-125  
M-130

M-160  
M-140  
M-145

M-355  
M-360  
M-365  
M-370  
M-405  
M-415  
M-615



M-620

END

-----  
 THIS SUBROUTINE EVALUATES THE GG ELEMENT MATRIX USING 20 POINTS OF  
 INTEGRATION. THE GG ELEMENT MATRIX IS THEN INSERTED INTO THE BIGGG  
 SYSTEM MATRIX.  
 -----

-----  
 SUBROUTINE TANYA  
 REAL\*8 GG,BIGGG  
 INTEGER\*8 WL,WS,S,CL1,CL2,CL3,FN,DL1,DL2,DL3,DS,DETJ  
 INTEGER\*2 NAME,JA,JB,NNZ,JC,NJMNP,NUMEL,NELDOF,CONN  
 COMMON/GTRY2/NAME(8199),JA(299),JB(299),NNZ,JC,NUMNP,NUMEL,NELDOF,  
 ICONN(192,15)  
 COMMON/GTRY1/X(717),P(717),Z(717)  
 COMMON/XOCAL/KX(15),YY(15),ZZ(15),PPSI(15)  
 COMMON/GGMAT/G3(15,15)  
 COMMON/SYSMT2/BIGGG(8199)  
 COMMON/GAUSS/WL(7),WS(5),S(5),CL1(7),CL2(7),CL3(7),FN(15,21),DL1(1  
 5,21),DL2(15,21),DL3(15,21),DS(15,21),DETJ(21)  
 WS(1)=0.236926885056189  
 WS(2)=0.478628670499366  
 WS(3)=0.568888888888889  
 WS(4)=0.478628670499366  
 WS(5)=0.236926885056189  
 S(1)=0.906179845938664  
 S(2)=0.538469310105683  
 S(3)=0.  
 S(4)=-.538469310105683  
 S(5)=-.906179845938664  
 WL(1)=-0.281250  
 WL(2)=0.260416666666667  
 WL(3)=0.260416666666667  
 WL(4)=0.260416666666667  
 CL1(1)=0.333333333333333  
 CL1(2)=0.60  
 CL1(3)=0.20  
 CL1(4)=0.20  
 CL2(1)=0.333333333333333  
 CL2(2)=0.20  
 CL2(3)=0.60  
 CL2(4)=0.20  
 CL3(1)=0.333333333333333  
 CL3(2)=0.20  
 CL3(3)=0.20  
 CL3(4)=0.60  
 DO 80 K=1,5  
 DO 90 M=1,4

T-015



```

IF(K.EQ.1) GO TO 10
IF(K.EQ.2) GO TO 20
IF(K.EQ.3) GO TO 30
IF(K.EQ.4) GO TO 40
IF(K.EQ.5) GO TO 50
N=M
10 GO TO 60
20 N=M+4
   GO TO 60
30 N=M+8
   GO TO 60
40 N=M+12
   GO TO 60
50 N=M+16
   GO TO 60
60 CONTINUE
FN(1,V)=0.50*CL1(M)*((2.0*CL1(M)-1.0)*(1.0+S(K))-(1.0-S(K)**2))
FN(2,N)=2.0*CL1(M)*CL2(M)*(1.0+S(K))
FN(3,V)=0.50*CL2(M)*((2.0*CL2(M)-1.0)*(1.0+S(K))-(1.0-S(K)**2))
FN(4,V)=2.0*CL2(M)*CL3(M)*(1.0+S(K))
FN(5,N)=0.50*CL3(M)*((2.0*CL3(M)-1.0)*(1.0+S(K))-(1.0-S(K)**2))
FN(6,V)=2.0*CL1(M)*CL3(M)*(1.0+S(K))
FN(7,N)=CL1(M)*(1.0-S(K)**2)
FN(8,N)=CL3(M)*((1.0-S(K))**2)
FN(9,V)=CL3(M)*((1.0-S(K))**2)
FN(11,N)=0.50*CL1(M)*((2.0*CL1(M)-1.0)*(1.0-S(K))-(1.0-S(K)**2))
FN(12,V)=2.0*CL1(M)*CL2(M)*(1.0-S(K))
FN(13,N)=0.50*CL2(M)*((2.0*CL2(M)-1.0)*(1.0-S(K))-(1.0-S(K)**2))
FN(14,V)=2.0*CL2(M)*CL3(M)*(1.0-S(K))
FN(15,V)=0.50*CL3(M)*((2.0*CL3(M)-1.0)*(1.0-S(K))-(1.0-S(K)**2))
FN(1,V)=2.0*CL1(M)*CL3(M)*(1.0-S(K))
DL1(1,V)=0.50*((1.0+S(K))*(4.0*CL1(M)-1.0)-(1.0-S(K)**2))
DL1(2,V)=2.0*CL2(M)*(1.0+S(K))
DL1(3,N)=0.0
DL1(4,V)=0.0
DL1(5,N)=0.0
DL1(6,N)=2.0*CL3(M)*(1.0+S(K))
DL1(7,N)=1.0-S(K)**2
DL1(8,N)=0.0
DL1(9,N)=0.0
DL1(10,N)=0.50*((1.0-S(K))*(4.0*CL1(M)-1.0)-(1.0-S(K)**2))
DL1(11,N)=2.0*CL2(M)*(1.0-S(K))
DL1(12,N)=0.0
DL1(13,N)=0.0
DL1(14,N)=0.0
DL1(15,N)=2.0*CL3(M)*(1.0-S(K))
DL2(1,V)=0.0
DL2(2,V)=2.0*CL1(M)*(1.0+S(K))
DL2(3,V)=0.50*((1.0+S(K))*(4.0*CL2(M)-1.0)-(1.0-S(K)**2))

```

```

DL2(4,N)=2.0*CL3(M)*(1.0+S(K))
DL2(5,N)=0.0
DL2(6,N)=0.0
DL2(7,N)=0.0
DL2(8,N)=(1.0-S(K)**2)
DL2(9,N)=0.0
DL2(10,N)=0.0
DL2(11,N)=2.0*CL1(M)*(1.0-S(K))
DL2(12,N)=0.50*{(1.0-S(K))*(4.0*CL2(M)-1.0)-(1.0-S(K)**2)}
DL2(13,N)=2.0*CL3(M)*(1.0-S(K))
DL2(14,N)=0.0
DL2(15,N)=0.0
DL3(1,N)=0.0
DL3(2,N)=0.0
DL3(3,N)=0.0
DL3(4,N)=2.0*CL2(M)*(1.0+S(K))
DL3(5,N)=0.50*{(1.0+S(K))*(4.0*CL3(M)-1.0)-(1.0-S(K)**2)}
DL3(6,N)=2.0*CL1(M)*(1.0+S(K))
DL3(7,N)=0.0
DL3(8,N)=0.0
DL3(9,N)=(1.0-S(K)**2)
DL3(10,N)=0.0
DL3(11,N)=0.0
DL3(12,N)=0.0
DL3(13,N)=2.0*CL2(M)*(1.0-S(K))
DL3(14,N)=0.50*{(1.0-S(K))*(4.0*CL3(M)-1.0)-(1.0-S(K)**2)}
DL3(15,N)=2.0*CL1(M)*(1.0-S(K))
DS(1,N)=0.50*(2.0*CL1(M)**2-CL1(M))+CL1(M)*S(K)
DS(2,N)=2.0*CL1(M)*CL2(M)
DS(3,N)=0.50*(2.0*CL2(M)**2-CL2(M))+CL2(M)*S(K)
DS(4,N)=2.0*CL2(M)*CL3(M)
DS(5,N)=0.50*(2.0*CL3(M)**2-CL3(M))+CL3(M)*S(K)
DS(6,N)=2.0*CL1(M)*CL3(M)
DS(7,N)=-2.0*CL1(M)*S(K)
DS(8,N)=-2.0*CL2(M)*S(K)
DS(9,N)=-2.0*CL3(M)*S(K)
DS(10,N)=-0.50*(2.0*CL1(M)**2-CL1(M))+CL1(M)*S(K)
DS(11,N)=-0.50*(2.0*CL2(M)**2-CL2(M))+CL2(M)*S(K)
DS(12,N)=-0.50*(2.0*CL3(M)**2-CL3(M))+CL3(M)*S(K)
DS(13,N)=-0.50*(2.0*CL1(M)*CL2(M))
DS(14,N)=-0.50*(2.0*CL2(M)*CL3(M))
DS(15,N)=-0.50*(2.0*CL1(M)*CL3(M))
90 CONTINUE
80 CONTINUE
DO 510 L=1,NUMEL
DO 475 I=1,NELDOF
DO 470 J=1,NELDOF
GG(I,J)=0.0

```

```

470 CONTINUE
475 DO 480 JJ=1,NELDOF
    NN=CONN(L,JJ)
    XX(JJ)=X(NN)
    YY(JJ)=P(NN)
    ZZ(JJ)=Z(NN)
480 CONTINUE
    A5=2.0/(ZZ(1)-ZZ(15))
    DETJJ=0.0
    DO 200 K=1.5
    DETJ1=0.0
    DO 210 M=1.4
    IF(K.EQ.1) GO TO 11
    IF(K.EQ.2) GO TO 21
    IF(K.EQ.3) GO TO 31
    IF(K.EQ.4) GO TO 41
    IF(K.EQ.5) GO TO 51
11 N=M
    GO TO 61
21 N=M+4
    GO TO 61
31 N=M+8
    GO TO 61
41 N=M+12
    GO TO 61
51 N=M+16
    GO TO 61
61 CONTINUE
    T1=DL1(1,N)*XX(1)+DL1(2,N)*XX(2)-DL3(4,N)*XX(4)-DL3(5,N)*XX(5)
    T2=DL1(7,N)*XX(7)-DL3(9,N)*XX(9)+DL1(13,N)*XX(10)+DL1(11,N)*XX(11)
    T3=(DL1(6,N)-DL3(6,N))*XX(6)-DL3(13,N)*XX(13)-DL3(14,N)*XX(14)
    T4=(DL1(15,N)-DL3(15,N))*XX(15)
    DJ11=T1+T2+T3+T4
    D1=DL1(1,N)*YY(1)+DL1(2,N)*YY(2)-DL3(4,N)*YY(4)-DL3(5,N)*YY(5)
    D2=DL1(7,N)*YY(7)-DL3(9,N)*YY(9)+DL1(10,N)*YY(10)+DL1(11,N)*YY(11)
    D3=(DL1(6,N)-DL3(6,N))*YY(6)-DL3(13,N)*YY(13)-DL3(14,N)*YY(14)
    D4=(DL1(15,N)-DL3(15,N))*YY(15)
    DJ12=D1+D2+D3+D4
    T5=DL2(2,N)*XX(2)+DL2(3,N)*XX(3)-DL3(5,N)*XX(5)-DL3(6,N)*XX(6)
    T6=DL2(8,N)*XX(8)-DL3(9,N)*XX(9)+(DL2(4,N)-DL3(4,N))*XX(4)
    T7=DL2(11,N)*XX(11)+DL2(12,N)*XX(12)+(DL2(13,N)-DL3(13,N))*XX(13)
    T8=-DL3(14,N)*XX(14)-DL3(15,N)*XX(15)
    DJ21=T5+T6+T7+T8
    D5=DL2(2,N)*YY(2)+DL2(3,N)*YY(3)-DL3(5,N)*YY(5)-DL3(6,N)*YY(6)
    D6=DL2(8,N)*YY(8)-DL3(9,N)*YY(9)+(DL2(4,N)-DL3(4,N))*YY(4)
    D7=DL2(11,N)*YY(11)+DL2(12,N)*YY(12)+(DL2(13,N)-DL3(13,N))*YY(13)
    D8=-DL3(14,N)*YY(14)-DL3(15,N)*YY(15)
    DJ22=D5+D6+D7+D8

```

```

210 DETJ(N)=DJ11*2J22-DJ12*DJ21
    DETJ1=DETJ1+DETJ(N)*WL(M)
200 CONTINUE
    DETJJ=DETJJ+WS(K)*DETJ1
    DO 600 J=1,15
    DO 610 I=1,15
    FGG=0.0
    DO 660 K=1,5
    FFG=0.0
    DO 670 M=1,4
    IF(K.EQ.1) GO TO 12
    IF(K.EQ.2) GO TO 22
    IF(K.EQ.3) GO TO 32
    IF(K.EQ.4) GO TO 42
    IF(K.EQ.5) GO TO 52
12 N=M
    GO TO 62
22 N=M+4
    GO TO 62
32 N=M+8
    GO TO 62
42 N=M+12
    GO TO 62
52 N=M+16
    GO TO 62
62 CONTINUE
    DXDL5=DL1(1,N)*XX(1)+(DL1(2,N)-DL2(2,N))*XX(2)-DL2(3,N)*XX(3)
    DXDL6=-(DL2(4,N)+DL3(4,N))*XX(4)-DL3(5,N)*XX(5)
    DXDL7=-(DL1(6,N)-DL3(6,N))*XX(6)+DL1(7,N)*XX(7)-DL2(8,N)*XX(8)
    DXDL9=-DL3(9,N)*XX(9)+DL1(10,N)*XX(10)+(DL1(11,N)-DL2(11,N))*XX(11)
1)
    DXDL9=-DL2(12,N)*XX(12)-(DL2(13,N)+DL3(13,N))*XX(13)-DL3(14,N)*XX(14)
    114)+(DL1(15,N)-DL3(15,N))*XX(15)
    DXDL1=DXDL5+DXDL6+DXDL7+DXDL8+DXDL9
    DYDL5=DL1(1,N)*YY(1)+(DL1(2,N)-DL2(2,N))*YY(2)-DL2(3,N)*YY(3)
    DYDL6=-(DL2(4,N)+DL3(4,N))*YY(4)-DL3(5,N)*YY(5)
    DYDL7=-(DL1(6,N)-DL3(6,N))*YY(6)+DL1(7,N)*YY(7)-DL2(8,N)*YY(8)
    DYDL8=-DL3(9,N)*YY(9)+DL1(10,N)*YY(10)+(DL1(11,N)-DL2(11,N))*YY(11)
1)
    DYDL9=-DL2(12,N)*YY(12)-(DL2(13,N)+DL3(13,N))*YY(13)-DL3(14,N)*YY(14)
    114)+(DL1(15,N)-DL3(15,N))*YY(15)
    DYDL1=DYDL5+DYDL6+DYDL7+DYDL8+DYDL9
    DXDL55=-DL1(1,N)*XX(1)+(DL2(2,N)-DL1(2,N))*XX(2)+DL2(3,N)*XX(3)
    DXDL56=-(DL2(4,N)-DL3(4,N))*XX(4)-DL3(5,N)*XX(5)-DL1(7,N)*XX(7)
    DXDL77=-(DL1(6,N)+DL3(6,N))*XX(6)+DL2(8,N)*XX(8)-DL3(9,N)*XX(9)
    DXDL88=-DL1(10,N)*XX(10)+(DL2(11,N)-DL1(11,N))*XX(11)
    DXDL99=DL2(12,N)*XX(12)+(DL2(13,N)-DL3(13,N))*XX(13)-DL3(14,N)*XX(14)
    114)-(DL1(15,N)+DL3(15,N))*XX(15)

```



```

DXDL2=DXDL55+DXDL66+DXDL77+DXDL88+DXDL99
DYDL55=-DL1(1,N)*YY(1)+(DL2(2,N)-DL1(2,N))*YY(2)+DL2(3,N)*YY(3)
DYDL66=(DL2(4,N)-DL3(4,N))*YY(4)-DL3(5,N)*YY(5)-DL1(7,N)*YY(7)
DYDL77=-((DL1(6,N)+DL3(6,N))*YY(6)+DL2(8,N)*YY(8)-DL3(9,N)*YY(9)
DYDL88=-DL1(13,N)*YY(10)+(DL2(11,N)-DL1(11,N))*YY(11)
DYDL99=DL2(12,N)*YY(12)+(DL2(13,N)-DL3(13,N))*YY(13)-DL3(14,N)*YY(
114)-(DL1(15,N)+DL3(15,N))*YY(15)
DYDL2=DYDL55+DYDL66+DYDL77+DYDL88+DYDL99
DL1DY=1.0/DYDL1
DL2DX=1.0/DXDL2
DL1DX=1.0/DXDL1
DL2DY=1.0/DYDL2
BB11=(DL1DX**2)+(DL1DY**2)
BB12=DL1DX*DL2DX+DL1DY*DL2DY
BB22=(DL2DX**2)+(DL2DY**2)
H1=BB11*((DL1(J,N)-DL3(J,N))*((DL1(I,N)-DL3(I,N)))
H2=BB12*((DL2(J,N)-DL3(J,N))*((DL1(I,N)-DL3(I,N)))
H3=BB12*((DL1(J,N)-DL3(J,N))*((DL2(I,N)-DL3(I,N)))
H4=BB22*((DL2(J,N)-DL3(J,N))*((DL2(I,N)-DL3(I,N)))
H5=(A5**2)*DS(J,N)*DS(I,N)
H6=(H1+H2+H3+H4+H5)*DETJ(N)
FFG=FFG+WL(M)*H6
670 CONTINUE
EGG=WS(K)*FFG+FGG
660 CONTINUE
GG(J,I)=FGG/A5
610 CONTINUE
600 CONTINUE
*** INSERT ELEMENT MATRIX INTO SYSTEM MATRIX *****
DO 505 K=1,NELDOF
KK=CONN(L,K)
IF(KK.GT.NNZ) GO TO 505
KKK=JA(KK)
LLL=JB(KK)-1
DO 500 I=1,NELDOF
II=CONN(L,I)
IF(II.GT.NNZ) GO TO 500
DO 490 M=1,KKK
MM=LLL+M
KKM=NAME(MM)
IF(II.EQ.KKM) GO TO 495
490 CONTINUE
495 BIGGG(MM)=BIGGG(MM)+GG(K,I)
500 CONTINUE
505 CONTINUE
510 RETURN

```



```

CC-----
CC      THIS SUBROUTINE EVALUATES THE G ELEMENT MATRIX USING 21 POINTS OF
CC      INTEGRATION. THE G ELEMENT MATRIX IS THEN INSERTED INTO THE BIGG
CC      SYSTEM MATRIX.
CC-----
END

SUBROUTINE FLOWIE
REAL*8 G,BIGG
REAL*8 WL,WS,S,CL1,CL2,CL3,FN,DL1,DL2,DL3,DS,DETJ
INTEGER*2 NAME,JA,JB,NNZ,JC,NJMNP,NUMEL,NELCOF,CONN
COMMON/GTRY2/NAME(8199),JA(299),JB(299),NNZ,JC,NUMNP,NUMEL,NELDOF,
1 CONN(192,15)
COMMON/GTRY1/X(717),P(717),Z(717)
COMMON/XOCAL/XX(15),YY(15),ZZ(15),PPSI(15)
COMMON/GMAT/G(15,15)
COMMON/GYSMT1/BIGG(8199)
COMMON/GAUSS/WL(7),WS(5),S(5),CL1(7),CL2(7),CL3(7),FN(15,21),DL1(1
15,21),DL2(15,21),DL3(15,21),DS(15,21),DETJ(21)
WS(1)=0.5555555555555556
WS(2)=0.888888888888889
WS(3)=0.5555555555555556
S(1)=0.774596669241483
S(2)=0.0
S(3)=-.774596669241483
WL(1)=0.112500
WL(2)=0.06619707500
WL(3)=0.06619707500
WL(4)=0.06619707500
WL(5)=0.0629695900
WL(6)=0.0629695900
WL(7)=0.0629695900
CL1(1)=0.333333333333333
CL1(2)=0.059615870
CL1(3)=0.470142060
CL1(4)=0.470142060
CL1(5)=0.797426990
CL1(6)=0.101286510
CL1(7)=0.101286510
CL2(1)=0.333333333333333
CL2(2)=0.470142060
CL2(3)=0.059615870
CL2(4)=0.470142060
CL2(5)=0.101286510
CL2(6)=0.797426990
CL2(7)=0.101286510
CL3(1)=0.333333333333333

```

```

CL3(2)=0.470142060
CL3(3)=0.470142060
CL3(4)=0.059515870
CL3(5)=0.101286510
CL3(6)=0.101286510
CL3(7)=0.797426990
DO 10 K=1,3
DO 20 M=1,7
C THE 3 X 7 MATRICES ARE BEING CONVERTED TO 1 X 21 VECTORS
IF(K-2)30,40,50
30 N=M
GO TO 60
40 N=M+7
GO TO 60
50 N=M+14
GO TO 60
60 CONTINUE
FN(1,N)=0.50*CL1(M)*((2.0*CL1(M)-1.0)*(1.0+S(K))-(1.0-S(K)**2))
FN(2,N)=2.0*CL1(M)*CL2(M)*(1.0+S(K))
FN(3,N)=0.50*CL2(M)*((2.0*CL2(M)-1.0)*(1.0+S(K))-(1.0-S(K)**2))
FN(4,N)=2.0*CL2(M)*CL3(M)*(1.0+S(K))
FN(5,N)=0.50*CL3(M)*((2.0*CL3(M)-1.0)*(1.0+S(K))-(1.0-S(K)**2))
FN(6,N)=2.0*CL3(M)*CL3(M)*(1.0+S(K))
FN(7,N)=CL1(M)*(1.0-S(K)**2)
FN(8,N)=CL2(M)*(1.0-S(K)**2)
FN(9,N)=CL3(M)*(1.0-S(K)**2)
FN(10,N)=0.50*CL1(M)*((2.0*CL1(M)-1.0)*(1.0-S(K))-(1.0-S(K)**2))
FN(11,N)=2.0*CL1(M)*CL2(M)*(1.0-S(K))
FN(12,N)=0.50*CL2(M)*((2.0*CL2(M)-1.0)*(1.0-S(K))-(1.0-S(K)**2))
FN(13,N)=2.0*CL2(M)*CL3(M)*(1.0-S(K))
FN(14,N)=0.50*CL3(M)*((2.0*CL3(M)-1.0)*(1.0-S(K))-(1.0-S(K)**2))
FN(15,N)=2.0*CL3(M)*CL3(M)*(1.0-S(K))
DL1(1,N)=0.50*((1.0+S(K))*(4.0*CL1(M)-1.0)-(1.0-S(K)**2))
DL1(2,N)=2.0*CL2(M)*(1.0+S(K))
DL1(3,N)=0.0
DL1(4,N)=0.0
DL1(5,N)=0.0
DL1(6,N)=2.0*CL3(M)*(1.0+S(K))
DL1(7,N)=(1.0-S(K)**2)
DL1(8,N)=0.0
DL1(9,N)=0.0
DL1(10,N)=0.5*((1.0-S(K))*(4.0*CL1(M)-1.0)-(1.0-S(K)**2))
DL1(11,N)=2.0*CL2(M)*(1.0-S(K))
DL1(12,N)=0.0
DL1(13,N)=0.0
DL1(14,N)=0.0
DL1(15,N)=2.0*CL3(M)*(1.0-S(K))
DL2(1,N)=0.0
DL2(2,N)=2.0*CL1(M)*(1.0+S(K))

```

```

DL2(3,N)= 0.50*((1.0+S(K))*(4.0*CL2(M)-1.0)-(1.0-S(K)**2))
DL2(4,V)= 2.0*CL3(M)*(1.0+S(K))
DL2(5,N)= 0.0
DL2(6,N)= 0.0
DL2(7,N)= 0.0
DL2(8,N)= (1.0-S(K)**2)
DL2(9,N)= 0.0
DL2(10,N)= 0.0
DL2(11,N)= 2.0*CL1(M)*(1.0-S(K))
DL2(12,N)= 0.50*((1.0-S(K))*(4.0*CL2(M)-1.0)-(1.0-S(K)**2))
DL2(13,N)= 2.0*CL3(M)*(1.0-S(K))
DL2(14,N)= 0.0
DL2(15,N)= 0.0
DL3(1,N)= 0.0
DL3(2,N)= 0.0
DL3(3,N)= 0.0
DL3(4,N)= 2.0*CL2(M)*(1.0+S(K))
DL3(5,N)= 0.50*((1.0+S(K))*(4.0*CL3(M)-1.0)-(1.0-S(K)**2))
DL3(6,V)= 2.0*CL1(M)*(1.0+S(K))
DL3(7,N)= 0.0
DL3(8,N)= 0.0
DL3(9,N)= (1.0-S(K)**2)
DL3(10,N)= 0.0
DL3(11,N)= 0.0
DL3(12,N)= 0.0
DL3(13,N)= 2.0*CL2(M)*(1.0-S(K))
DL3(14,N)= 0.50*((1.0-S(K))*(4.0*CL3(M)-1.0)-(1.0-S(K)**2))
DL3(15,N)= 2.0*CL1(M)*(1.0-S(K))
DS(1,N)= 0.50*(2.0*CL1(M)**2-CL1(M))+CL1(M)*S(K)
DS(2,N)= 0.50*(2.0*CL2(M)**2-CL2(M))+CL2(M)*S(K)
DS(3,N)= 0.50*(2.0*CL3(M)**2-CL3(M))+CL3(M)*S(K)
DS(4,N)= 0.50*(2.0*CL1(M)*CL3(M)-2.0*CL1(M)*CL3(M))+CL1(M)*S(K)
DS(5,N)= 0.50*(2.0*CL2(M)*CL3(M)-2.0*CL2(M)*CL3(M))+CL2(M)*S(K)
DS(6,N)= -2.0*CL1(M)*S(K)
DS(7,N)= -2.0*CL2(M)*S(K)
DS(8,N)= -2.0*CL3(M)*S(K)
DS(9,N)= -2.0*CL1(M)*S(K)
DS(10,V)= -50*(2.0*CL1(M)**2-CL1(M))+CL1(M)*S(K)
DS(11,N)= -2.0*CL1(M)*CL2(M)
DS(12,V)= -50*(2.0*CL2(M)**2-CL2(M))+CL2(M)*S(K)
DS(13,N)= -2.0*CL2(M)*CL3(M)
DS(14,N)= -50*(2.0*CL3(M)**2-CL3(M))+CL3(M)*S(K)
DS(15,N)= -2.0*CL1(M)*CL3(M)
20 CONTINUE
10
DO 510 L=1,NUMEL
DO 475 I=1,NELDOF
DO 470 J=1,NELDOF

```

```

470 G(I,J)=0.0
475 CONTINUE
DO 480 JJ=1,NELDOF
NN=CONN(L,JJ)
XX(JJ)=X(NN)
YY(JJ)=P(NN)
ZZ(JJ)=Z(NN)
480 CONTINUE
A5=2.0/(ZZ(1)-ZZ(15))
DETJJ=0.0
DO 200 K=1,3
DETJ1=0.0
DO 210 M=1,7
IF(K-2)31,41,51
31 N=M
GO TO 61
41 N=M+7
GO TO 61
51 N=M+14
61 CONTINUE
T1=DL1(1,N)*XX(1)+DL1(2,N)*XX(2)-DL3(4,N)*XX(4)-DL3(5,N)*XX(5)
T2=DL1(7,N)*XX(7)-DL3(6,N)*XX(6)-DL3(13,N)*XX(13)-DL3(14,N)*XX(14)
T3=(DL1(6,N)-DL3(6,N))*XX(6)-DL3(13,N)*XX(13)-DL3(14,N)*XX(14)
T4=(DL1(15,N)-DL3(15,N))*XX(15)
DJ1=T1+T2+T3+T4
D1=DL1(1,N)*YY(1)+DL1(2,N)*YY(2)-DL3(4,N)*YY(4)-DL3(5,N)*YY(5)
D2=DL1(7,N)*YY(7)-DL3(6,N)*YY(6)-DL3(13,N)*YY(13)-DL3(14,N)*YY(14)
D3=(DL1(6,N)-DL3(6,N))*YY(6)-DL3(13,N)*YY(13)-DL3(14,N)*YY(14)
D4=(DL1(15,N)-DL3(15,N))*YY(15)
DJ2=D1+D2+D3+D4
T5=DL2(2,N)*XX(2)+DL2(3,N)*XX(3)-DL3(5,N)*XX(5)-DL3(6,N)*XX(6)
T6=DL2(8,N)*XX(8)-DL3(9,N)*XX(9)+DL2(4,N)-DL3(4,N)*XX(4)
T7=DL2(11,N)*XX(11)+DL2(12,N)*XX(12)+(DL2(13,N)-DL3(13,N))*XX(13)
T8=-DL3(14,N)*XX(14)-DL3(15,N)*XX(15)
DJ21=T5+T6+T7+T8
D5=DL2(2,N)*YY(2)+DL2(3,N)*YY(3)-DL3(5,N)*YY(5)-DL3(6,N)*YY(6)
D6=DL2(8,N)*YY(8)-DL3(9,N)*YY(9)+DL2(4,N)-DL3(4,N)*YY(4)
D7=DL2(11,N)*YY(11)+DL2(12,N)*YY(12)+(DL2(13,N)-DL3(13,N))*YY(13)
D8=-DL3(14,N)*YY(14)-DL3(15,N)*YY(15)
DJ22=D5+D6+D7+D8
DETJ(N)=DJ1#DJ22-DJ12#DJ21
DETJ1=DETJ(N)*WL(M)+DETJ1
210 CONTINUE
DETJJ=DETJJ+WS(K)*DETJ1
200 CONTINUE
DO 600 J=1,15
DO 610 I=1,15

```



```

FG=0.0      DO 660 K=1,3
F=0.0
DO 670 M=1,7
IF(K-2) 620,630,640
620 N=M      GO TO 650
630 N=M+7    GO TO 650
640 N=M+14
650 CONTINUE
F=F+WL(M)*FN(J,N)*FN(I,N)*DETJ(N)
670 CONTINUE
FG=FG+WS(K)*F
660 CONTINUE
G(J,I)=FG/A5
610 CONTINUE
600 C
** INSERT ELEMENT MATRIX INTO SYSTEM MATRIX *****
DO 505 K=1,NELDOF
KK=CONN(L,K)
IF(KK.GT.NNZ) GO TO 505
KKK=JA(KK)
LLL=JB(KK)-1
DO 500 I=1,NELDOF
II=CONN(L,I)
IF(II.GT.NNZ) GO TO 500
DO 490 M=1,KK<
MM=LLL+M
KKM=NAME(MM)
IF(II.EQ.KKM) GO TO 495
490 CONTINUE
495 BIGG(MM)=BIGG(MM)+G(K,I)
500 CONTINUE
505 CONTINUE
510 RETURN
END

```



```

C-----
C      THIS IS THE MAIN PROGRAM FOR THE SOLUTION OF THE FIELD EQUATIONS.
C      THE DATA FROM THE TAPE IS READ OUT, VODAL CONSTANTS ARE EVALUATED,
C      THE INTEGRATION PACKAGE IS INITIATED, ETC.
C-----
C
C
C
C

```

```

REAL*8 SIGF, SIGA, C1, C2, C4, C5
REAL*8 GGG, BIGG, BIGGG, BIGH
REAL*8 WL, WS, S, CL1, CL2, CL3, FN, DL1, DL2, DL3, DS, DETJ
INTEGER*2 NAME, JA, JB, NNZ, JC, NUMNP, NUMEL, NELDOF, CONN
COMMON/GTRY2/NAME(4615), JA(183), JB(184), NNZ, JC, NUMNP, NUMEL, NELDOF,
1CONN(128,15)
COMMON/GTRY1/X(505), P(505), Z(505)
COMMON/XOCAL/XX(15), YY(15), ZZ(15), PPSI(15)
DIMENSION W(7000), Y(7,183)
COMMON/DELAY/SUM(183), PSI(93)
COMMON/TEMP/C3(183), C6(15)
DIMENSION SIGF(93), SIGA(183)
COMMON/COEF/CL(183), C2(183), C4(183), C5(183)
COMMON/GGGMAT/GGG(15,15)
COMMON/SYSMT1/BIGG(4615)
COMMON/SYSMT2/BIGGG(4615)
COMMON/SYSMT3/BIGH(4615)
COMMON/GAUSS/WL(7), WS(5), S(5), CL1(7), CL2(7), CL3(7), FN(15,21), DL1(1
15,21), DL2(15,21), DL3(15,21), DETJ(21)
NNZ=183
NUMEL=128
NUMNP=505
NELDOF=15
JC=4615
FMAX=1.0E10
DO 771 I=1, NUMEL
  READ(4) (CONN(I, J), J=1, NELDOF)

```

M-010  
M-015  
M-020  
M-025  
M-055  
M-060

M-075  
M-080  
M-085  
M-095  
M-100

M-105

```

771 CONTINUE
  READ(4) (JA(I), I=1, NNZ)
  READ(4) (JB(I), I=1, NNZ)
  READ(4) (NAME(I), I=1, JC)
  READ(4) (X(I), I=1, NUMNP)
  READ(4) (P(I), I=1, NUMNP)
  READ(4) (Z(I), I=1, NUMNP)
  READ(4) (BIGG(I), I=1, JC)
  READ(4) (BIGGG(I), I=1, JC)
  DO 772 I=1, 3
    READ(4) WS(I), S(I)
772 CONTINUE

```

```

DO 773 I=1,7
READ(4) WL(I),CL1(I),CL2(I),CL3(I)
CONTINUE
773 DO 781 I=1,NELDOF
DO 782 J=1,21
READ(4) FN(I,J),DL1(I,J),DL2(I,J),DL3(I,J),DS(I,J)
782 CONTINUE
781 CONTINUE
DO 460 I=1,NNZ
Y(1,I)=FMAX
Y(2,I)=0.0
SUM(I)=0.0
IF(I.GT.93) GO TO 460
PSI(I)=FMAX
460 CONTINUE
WRITE(6,3) SIGF(I)=0.0057450, SIGA(I)=0.014010,0.0080 ' )
3 FORMAT(1,3)
V=4.800E07
Q=0.4349710
BETA=0.006420
B=-0.00400
DO 445 I=1,NNZ
IF(I.GT.93) GO TO 420
D=0.9130
SIGF(I)=0.0057450
SIGA(I)=0.014010
ZNU=2.54
C1(I)=V*D
C2(I)=V*SIGA(I)-V*(1.0-BETA)*SIGF(I)*ZNU
C3(I)=(2.0179325E-13)*SIGF(I)
C4(I)=-V*(1.0-BETA)*SIGA(I)*B
C5(I)=-V*BETA*Q*ZNU*SIGF(I)
GO TO 445
420 D=1.200
SIGA(I)=0.00800
C1(I)=V*D
C2(I)=V*SIGA(I)
C3(I)=0.0
C4(I)=0.0
C5(I)=0.0
445 CONTINUE
TEND=0.0010
NY=NNZ
NL=0
H=1.0E-19
T=0.0
HMIN=1.0E-20
HMAX=0.10

```

M-520  
M-535  
M-545  
M-540  
M-550

M-565  
M-570  
M-575  
M-580  
M-585  
M-590



```

SDESOL. JSKF > 0 INDICATES A CONTINUATION OF THE
PREVIOUS CALL TO SDESOL. JSKF < -1 MAY HAVE RESULTED
FROM THE USER NEGLECTING TO TEST FOR ERROR RETURNS
FROM SDESOL. BECAUSE OF THIS POSSIBILITY, JSKF < -1
RESULTS IN TERMINATION OF THE RUN WITH THE
APPROPRIATE COMMENT.
ON OUTPUT, JSKF CONSISTS OF TWO DIGITS AND SIGN,
+ OR - OP. Q IS THE ORDER OF THE FORMULA CURRENTLY
BEING USED. P INDICATES THE TYPE OF RETURN, AS
FOLLOWS.
JSKF > 0, P = 1 IS THE NORMAL RETURN
JSKF < 0 IS AN ERROR RETURN, WITH THE FOLLOWING
MEANINGS.
P = 1 ERROR TEST FAILURE FOR H > HMIN
P = 3 CORRECTOR FAILED TO CONVERGE FOR H > HMIN
P = 4 CORRECTOR FAILED TO CONVERGE FOR FIRST
ORDER METHOD
P = 5 ERROR RETURN FROM SUBROUTINE NUTSL
P = 6 ERROR RETURN FROM SUBROUTINE Derval
MAXDER - MAXIMUM ORDER DERIVATIVE THAT SHOULD BE USED IN
METHOD. IT MUST BE NO GREATER THAN SIX.
IPRT - INTERNAL PRINT CONTROL INDICATOR FOR LDASUB.
IPRT = 0 NO PRINT
IPRT > 0 PRINT COUNTERS, STEPSIZE, CURRENT TIMES
AND VALUES OF DEPENDENT VARIABLES AT
EACH STEP.
H - CURRENT STEPSIZE. AN INITIAL VALUE MUST BE SUPPLIED
BUT NEED NOT BE THE ONE WHICH MUST BE USED, SINCE THE
SUBROUTINE WILL CHOOSE A SMALLER ONE IF NECESSARY TO
KEEP THE ERROR PER STEP SMALLER THAN THE SPECIFIED
VALUE. IT IS BETTER TO UNDERESTIMATE THE INITIAL
STEPSIZE THAN TO OVERESTIMATE IT. THE STEPSIZE IS
VARIABLELY NOT CHANGED BY THE USER.
HMIN - MINIMUM STEPSIZE ALLOWED
HMAX - MAXIMUM STEPSIZE ALLOWED
RMSEPS - THE ERROR TEST CONSTANT. THE ROOT-MEAN-SQUARE OF
TIMES,  $ER(I)$ , DIVIDED BY
YMAX(I) = (MAXIMUM CURRENT TIME OF Y(I)) MUST BE
LESS THAN EPS. THE STEPSIZE AND/OR THE ORDER
ARE VARIED TO ACHIEVE THIS.
W - SCRATCH STORAGE ARRAY. MUST BE AT LEAST 13*NY + 5*NL
LOCATIONS, PLUS THOSE REQUIRED FOR STORAGE OF THE
MATRIX PW (SEE DESCRIPTION OF SUBROUTINE JACMAT).
THE STORAGE OF PW WILL NORMALLY REQUIRE NO MORE THAN
N*2 + 2*N LOCATIONS, AND IF COMPACT STORAGE TECH-
NIQUES ARE USED, CAN BE MUCH FEWER.

```

440 SDE  
450 SDE  
460 SDE  
470 SDE  
480 SDE  
490 SDE  
500 SDE  
510 SDE  
520 SDE  
530 SDE  
540 SDE  
550 SDE  
560 SDE  
570 SDE  
580 SDE  
590 SDE  
600 SDE  
610 SDE  
620 SDE  
630 SDE  
640 SDE  
650 SDE  
660 SDE  
670 SDE  
680 SDE  
690 SDE  
700 SDE  
710 SDE  
720 SDE  
730 SDE  
740 SDE  
750 SDE  
760 SDE  
770 SDE  
780 SDE  
790 SDE  
800 SDE  
810 SDE  
820 SDE  
830 SDE  
840 SDE  
850 SDE  
860 SDE  
870 SDE  
880 SDE  
890 SDE  
900 SDE  
910 SDE

CC







```

1HMIN,HMAX,RMSEPS,SAVE,YLSV,YMAX,ER,ESV,FL,DY,PW)
SUBROUTINE LOASUB IS A MODIFICATION OF SUBROUTINE DFASUB
WHICH IS DUE TO R. L. BROWN AND C. W. GEAR. DFASUB IS DOCUMENTED
IN THE REPORT
DOCUMENTATION FOR DFASUB--
BY R. L. BROWN AND C. W. GEAR
REPORT UIUCDCS-R-73-575, JULY 1973
UNIVERSITY OF ILLINOIS AT URBANA-CHAMPAIGN
URBANA, ILLINOIS 61801
THIS REPORT IS AVAILABLE FROM THE NATIONAL TECHNICAL INFORMATION
SERVICE OF THE U. S. DEPARTMENT OF COMMERCE UNDER ACCESSION NUMBER
COO-1459-225.
THE MODIFICATION HERE IS DOCUMENTED IN THE REPORT
A PROGRAM FOR THE NUMERICAL SOLUTION OF LARGE SPARSE SYSTEMS OF
ALGEBRAIC AND IMPLICITLY DEFINED STIFF DIFFERENTIAL EQUATIONS
BY RICHARD FRANK
REPORT NPS53FE76051, MAY 1976
NAVAL POSTGRADUATE SCHOOL
MONTEREY, CALIFORNIA 93940
-----
THE CALLING SEQUENCE FOR LDASUB IS
CALL LDASUB(Y,VL,T,TEND,V,NY,M,JSTART,KFLAG,MAXOR,IPRT,H,HMIN,
HMAX,RMSEPS,SAVE,YLSV,YMAX,ER,ESV,FL,DY,PW)
WHERE THE PARAMETERS ARE DEFINED AS FOLLOWS.
Y - ARRAY DIMENSIONED (7,NY). THIS ARRAY CONTAINS THE
DEPENDENT VARIABLES AND THEIR SCALED DERIVATIVES.
Y(J+1,I) CONTAINS THE J-TH DERIVATIVE OF THE I-TH VARIABLE.
TABLE TIMES H*J/J-FACTORIAL, WHERE H IS THE CURRENT
STEP SIZE. ON FIRST ENTRY THE CALLER SUPPLIES THE
INITIAL VALUES OF EACH VARIABLE IN Y(1,I) AND AN
ESTIMATE OF THE INITIAL VALUES OF THE DERIVATIVES
IN Y(2,I). ON SUBSEQUENT ENTRIES IT IS ASSUMED THAT
THE ARRAY Y HAS NOT BEEN CHANGED. TO INTERPOLATE TO
NON-MESH POINTS, THESE VALUES CAN BE USED AS FOLLOWS.
IF H IS THE CURRENT STEP SIZE AND VALUES AT TIME T+T*E
NEEDED, LET S = E/H AND THEN
NQ SUM Y(J+1,I)*S**J
I-TH VARIABLE AT T+T*E IS
J=0
THE VALUE OF NQ IS OBTAINED IN THE CALLING PROGRAM

```

```

20 LDA
30 LDA
40 LDA
50 LDA
60 LDA
70 LDA
80 LDA
90 LDA
100 LDA
110 LDA
120 LDA
130 LDA
140 LDA
150 LDA
160 LDA
170 LDA
180 LDA
190 LDA
200 LDA
210 LDA
220 LDA
230 LDA
240 LDA
250 LDA
260 LDA
270 LDA
280 LDA
290 LDA
300 LDA
310 LDA
320 LDA
330 LDA
340 LDA
350 LDA
360 LDA
370 LDA
380 LDA
390 LDA
400 LDA
410 LDA
420 LDA
430 LDA
440 LDA
450 LDA
460 LDA
470 LDA
480 LDA
490 LDA

```

CC







```

C          DATA PERT/4.,9.,16.,25.,36.,49.,9.,16.,25.,36.,49.,64.,1.,1.,.25,
C          12.7889E-2,1.70569E-3,6.83929E-5/
C          -----
C          THE ENTRIES IN THE COF ARRAY ARE THE CJEFFICIENTS FOR THE STIFFLY
C          STABLE METHODS USED IN THIS PROGRAM AND ARE TO BE THE MACHINE
C          PRECISION EQUIVALENTS OF THE FOLLOWING CONSTANTS.
C          -----
C          -1
C          -3/2 , -1/2
C          -11/6 , -1 , -1/6
C          -25/12 , -35/24 , -5/12 , -1/24
C          -137/60 , -15/8 , -17/24 , -1/8 , -1/120
C          -147/60 , -203/90 , -49/48 , -35/144 , -7/240 , -1/720
C          -----
C          DATA CJF/-1.,-1.5,-.5,-1.833333,-1.,-.1666667,-2.083333,-1.458333,
C          1-.4166667,-.04166667,-2.283333,-1.875,-.7083333,-.125,-.008333333,
C          2-2.45,-2.255556,-1.020833,-.2430556,-.32916667,-.001388889/
C          IF (JSTART) 100,110,150
C          -----
C          IF THIS IS A RESTART ENTRY, RESTORE Y AND YL FROM THE SAVE AND
C          YLSV ARRAYS, WHERE THEY WERE SAVED BY A PREVIOUS CALL TO LDASAV.
C          -----
C          100 CALL COPYZ (Y,SAVE,LCOPYY)
C          CALL COPYZ (YL,YLSV,LCOPYL)
C          GO TO 150
C          -----
C          IF THIS IS THE FIRST CALL, INITIALIZE YMAX, SCALE DERIVATIVES, AND
C          INITIALIZE INDICATORS AND SET ORDER TO ONE.
C          FOR DOUBLE PRECISION, SET LCOPYL = 14*NY AND LCOPYL = 2*NL IF
C          SUBROUTINE COPYZ IS IN SINGLE PRECISION.
C          -----
C          110 NL = N-NY
C          LCOPYY = 7*NY
C          LCOPYL = NL
C          M1 = MINO(M,NY)
C          EPS = SQRT(FLJDAT(M1))*RMSEPS
C          MAXDER = MINO(MAXOR,6)
C          IF (IPRT.LE.0) GO TO 120
C          PRINT 3, N,NL,RMSEPS,TEND,H
C          PRINT 4
C          120 NS = 0
C          NW = 0
C          DO 130 J=1,NY

```

```

C      YMAX(J) = AMAX1(1.,ABS(Y(1,J)))
130  Y(2,J) = Y(2,J)*H
C      NQ = 1
C      BR = 1.
C      ASSIGN 190 TO IRET
C      SET COEFFICIENTS FOR THE ORDER CURRENTLY BEING USED.
C      E IS A TEST FOR ERRORS OF THE CURRENT ORDER NQ
C      EUP IS TO TEST FOR INCREASING THE ORDER, EDWN FOR DECREASING THE
C      ORDER.
C      K = NQ*(NQ-1)/2
140  CALL COPYZ (A(2),COF(K+1),NQ)
C      K = NQ+1
C      IDOUB = NQ
C      ENQ1 = .5/NQ
C      ENQ2 = .5/K
C      ENQ3 = .5/(NQ+2)
C      PEP SH = EPS*#2
C      E = PERT(NQ,1)*PEP SH
C      EUP = PERT(NQ,2)*PEP SH
C      EDWN = PERT(NQ,3)*PEP SH
C      BND = (EPS*ENQ3)**2
C      IWEVAL = 1
C      GO TO IRET, (190,200,490,570)
150  IF (H.EQ.HNEW) GO TO 190
C      IF CALLER HAS CHANGED H, RESCALE DERIVATIVES TO REFLECT THAT HNEW
C      WAS USED ON THE LAST CALL.
C      R = H/HNEW
C      ASSIGN 190 TO IRET
C      GO TO 610
C      SET JSTART TO NQ, THE CURRENT ORDER OF THE METHOD, BEFORE EXIT,
C      AND SAVE THE CURRENT STEP SIZE IN HNEW.
160  JSTART = NQ
C      HNEW = H
C      RETURN
170  NS = NS+1
C      IF (IPRT.LE.0) GO TO 180
C      PRINT DATA IF DESIRED BY USER
C      PRINT 1, NS, NQ, VQ, H, T, (Y(1,I), I=1,NY)
C      IF (NL.GT.0) PRINT 2, (YL(I), I=1,NL)

```

```

LDA 1940
LDA 1950
LDA 1960
LDA 1970
LDA 1980
LDA 1990
LDA 2000
LDA 2010
LDA 2020
LDA 2030
LDA 2040
LDA 2050
LDA 2060
LDA 2070
LDA 2080
LDA 2090
LDA 2100
LDA 2110
LDA 2120
LDA 2130
LDA 2140
LDA 2150
LDA 2160
LDA 2170
LDA 2180
LDA 2190
LDA 2200
LDA 2210
LDA 2220
LDA 2230
LDA 2240
LDA 2250
LDA 2260
LDA 2270
LDA 2280
LDA 2290
LDA 2300
LDA 2310
LDA 2320
LDA 2330
LDA 2340
LDA 2350
LDA 2360
LDA 2370
LDA 2380
LDA 2390
LDA 2400
LDA 2410

```







```

310 KFLAG = -3
320 CALL COPYZ (Y,SAVE,LCOPYZ)
    CALL COPYZ (YL,YLSV,LCOPYL)
    H = HOLD
    NQ = NQOLD
    GO TO 170
330 D = 0.
    DO 340 I=1,M1
        YM = AMAX1(ABS(Y(I,I)),YMAX(I))
        D = D+(ER(I)/YM)**2
    MEVAL = 0
    IF (D.GT.E) GO TO 380
    THE ERROR TEST IS OKAY, SO THE STEP IS ACCEPTED. IF IDOUB
    NOW BECOMES NEGATIVE, A TEST IS MADE TO SEE IF THE STEP SIZE
    CAN BE INCREASED AT THIS ORDER OR ONE HIGHER OR ONE LOWER.
    THE CHANGE IS MADE ONLY IF THE STEP CAN BE INCREASED BY AT
    LEAST 10%. IDOUB IS SET TO NQ TO PREVENT FURTHER TESTING
    FOR A WHILE. IF NO CHANGE IS MADE, IDOUB IS SET TO 9.
    IF (K.LT.3) GO TO 360
    DO 350 J=3,K
    DO 350 I=1,NY
        Y(J,I) = Y(J,I)+A(J)*ER(I)
    KFLAG = 1
    IDOUB = IDOUB-1
    IF (IDOUB) 410,370,510
    CALL COPYZ (ESV,ER,M1)
    GO TO 510
    THE ERROR TEST FAILED. IF JSTART = 0, THE DERIVATIVES IN THE
    SAVE ARRAY ARE UPDATED. TESTS ARE THEN MADE TO FIX THE STEP SIZE
    AND PERHAPS REDUCE THE ORDER. AFTER RESTORING AND SCALING THE
    Y VARIABLES, THE STEP IS RETRIED.
380 IF (JSTART.GT.0) GO TO 400

```

```

C      DO 390 I=1,NY
C      390 SAVE(2,I) = Y(2,I)
C      400 KFLAG = KFLAG-2
C      IF (H.LE.HMIN) GO TO 550
C      I = TOLD
C      IF (KFLAG.LE.-5) GO TO 530
C      410 PR2 = (D/E)**NQ2*1.2
C      L = 0
C      IF (NQ.LE.1) GO TO 430
C      D = 0.
C      DO 420 J=1,M1
C      YM = AMAX1(ABS(Y(1,J)),YMAX(J))
C      420 D = D+(Y(K,J)/YM)**2
C      PR1 = (D/EDWN)**ENQ1*1.3
C      IF (PR1.GE.PR2) GO TO 430
C      PR2 = PR1
C      L = -1
C      430 IF (KFLAG.LT.0.JR.NQ.GE.MAXDER) GO TO 450
C      D = 0
C      DO 440 J=1,M1
C      YM = AMAX1(ABS(Y(1,J)),YMAX(J))
C      440 D = D+((ER(J)-ESV(J))/YM)**2
C      PR1 = (D/EUP)**ENQ3*1.4
C      IF (PR1.GE.PR2) GO TO 450
C      PR2 = PR1
C      L = 1
C      450 R = 1./AMAX1(PR2,1.E-5)
C      IF (KFLAG.LT.0.JR.R.GE.1.1) GO TO 460
C      IDOUB = 9
C      GO TO 510
C      460 NEWQ = NQ+L
C      K = NEWQ+1
C      IF (NEWQ.LE.NQ) GO TO 480
C      R1 = A(NEWQ)/FLOAT(NEWQ)
C      DO 470 J=1,NY
C      470 Y(K,J) = ER(J)*R1
C      480 CONTINUE
C      IF THE STEP WAS OKAY, SCALE THE Y VARIABLES IN ACCORDANCE
C      WITH THE NEW VALUE OF H. IF KFLAG < 0, HOWEVER, USE THE
C      SAVED VALUES (IN SAVE AND YLSV). IN EITHER CASE, IF THE ORDER

```

```

LDA 3850
LDA 3860
LDA 3870
LDA 3880
LDA 3890
LDA 3900
LDA 3910
LDA 3920
LDA 3930
LDA 3940
LDA 3950
LDA 3960
LDA 3970
LDA 3980
LDA 3990
LDA 4000
LDA 4010
LDA 4020
LDA 4030
LDA 4040
LDA 4050
LDA 4060
LDA 4070
LDA 4080
LDA 4090
LDA 4100
LDA 4110
LDA 4120
LDA 4130
LDA 4140
LDA 4150
LDA 4160
LDA 4170
LDA 4180
LDA 4190
LDA 4200
LDA 4210
LDA 4220
LDA 4230
LDA 4240
LDA 4250
LDA 4260
LDA 4270
LDA 4280
LDA 4290
LDA 4310
LDA 4320
LDA 4330

```







```

C      DO 580 I=1,NY
580   Y(J,I) = SAVE(J,I)*R1
C
C      DO 590 I=1,NY
590   Y(I,I) = SAVE(I,I)
C      CALL COPYZ (YL,YLSV,LCOPYL)
      IWEVAL = 1
      GO TO 200
600   KFLAG = -5
      GO TO 160
C
C      ----- THIS SECTION SCALES THE Y DERIVATIVES BY R**J -----
C      DO 610 R1 = 1.
610
C      DO 620 J=2,K
      R1 = R1*R
C
C      DO 620 I=1,NY
620   Y(J,I) = Y(J,I)*R1
C      GO TO IRET, (190,510)
C
C      ----- THIS SECTION ALLOWS FOR RESTARTS AFTER SOLVING ANOTHER PROBLEM, OR
C      ----- HAVING TERMINATED THE CURRENT COMPUTER RUN. SUBROUTINE LDASAV
C      ----- SAVES THE NECESSARY VALUES WHICH ARE INTERNAL TO LDASUB. FOR
C      ----- DOUBLE PRECISION, WITH COPYZ IN SINGLE PRECISION, THE NUMBER OF
C      ----- LOCATIONS TO BE SAVED AND RESTORED, LCPYS AND LCPYR, MUST BE
C      ----- SET TO 58.
C      ----- IT IS ASSUMED THAT IN ADDITION TO THE VARIABLES IN THE ARRAY A
C      ----- SAVED BY CALLING LDASAV, THE USER ALSO SAVES THE ARRAYS SAVE,
C      ----- YLSV, YMAX, ESV, AND PW.
C      ----- TO RESTART THE USER FIRST CALLS LDARST TO RESTORE THE VALUES SAVED
C      ----- BY LDASAV, THEN RE-ENTERS LDASUB WITH JSTART < 0, AND WITH THE
C      ----- OTHER PARAMETERS THE SAME AS RETURNED FROM THE LAST ENTRY TO
C      ----- LDASUB, PARTICULARLY THOSE ARRAYS MENTIONED ABOVE.
C      -----
C      ENTRY LDASAV(SAV)
      LCPYS = 29
      CALL COPYZ (SAV,A,LCOPYS)
      CALL COPYZ (SAVE,Y,LCOPYY)
      CALL COPYZ (YLSV,YL,LCOPYL)
      RETURN
C

```

```

LDA 4820
LDA 4830
LDA 4840
LDA 4850
LDA 4860
LDA 4870
LDA 4880
LDA 4890
LDA 4900
LDA 4910
LDA 4920
LDA 4930
LDA 4940
LDA 4950
LDA 4960
LDA 4970
LDA 4980
LDA 4990
LDA 5000
LDA 5010
LDA 5020
LDA 5030
LDA 5040
LDA 5050
LDA 5060
LDA 5070
LDA 5080
LDA 5090
LDA 5100
LDA 5110
LDA 5120
LDA 5130
LDA 5140
LDA 5150
LDA 5160
LDA 5170
LDA 5180
LDA 5190
LDA 5200
LDA 5210
LDA 5220
LDA 5230
LDA 5240
LDA 5250
LDA 5260
LDA 5270
LDA 5280
LDA 5290

```

```

ENTRY LDARST(SAV)
LCOPYR = 29
CALL COPYZ (A, SAV, LCOPYR)
RETURN
-----
1 FORMAT (2I5, I2, 1P2E10.2, 7E14.6 / ((32X, 7E14.6))
2 FORMAT ((32X, 1P7E14.6))
3 FORMAT (1I, I3, ' NL =', I3, ' RMSEPS =', 1PE9.2, ' TEND =',
4 1, E9.2, ' H =', E9.2 / //)
4 1 NS NW Q H', 8X, 'T ', 8X, 'Y(1,*) AND YL(*)' //)
END
-----
SUBROUTINE COPYZ(S, Y, L)
DIMENSION S(1), Y(1)
-----
THIS SUBROUTINE COPIES THE ARRAY Y, OF LENGTH L, INTO THE ARRAY S
-----
IF(L.LE.0) RETURN
DO 100 J=1, L
S(J) = Y(J)
RETURN
END
100
-----
SUBROUTINE Derval (Y, YL, T, N, NY, W, KERET)
THIS SUBROUTINE CALCULATES THE INITIAL VALUES OF THE DERIVATIVES
IN THE GENERAL CASE. IT IS WRITTEN SO THAT IT SHOULD WORK IF THE
FIRST NY EQUATIONS ALL INVOLVE DERIVATIVES. IT ATTEMPTS TO SOLVE
THE FIRST NY EQUATIONS USING NEWTON'S METHOD, BUT SINCE IT TRIES
TO EVALUATE DF/DY, BY CALLING JACMAT IN SUCH A WAY AS TO MAKE THE
DF/DY TERM INSIGNIFICANT, IT IS POSSIBLE THAT IT MAY FAIL FOR THAT
REASON. IT MAY FAIL FOR OTHER REASONS, AS WELL. IF IT DOES FAIL
THE USER CAN SUPPLY HIS OWN VERSION OF Derval, OR MODIFY THIS
ROUTINE IN SUITABLE FASHION. THIS ROUTINE ASSUMES THAT VALUES OF
THE LINEAR VARIABLES HAVE BEEN SUPPLIED PREVIOUSLY. IF THOSE
MUST BE SOLVED FOR SIMULTANEOUSLY WITH THE DERIVATIVES, THE USER
MUST SUPPLY HIS OWN VERSION OF Derval.
-----
THE CALLING SEQUENCE FOR THIS SUBROUTINE IS
CALL Derval(Y, YL, T, N, NY, W, KERET)
WHERE THE PARAMETERS ARE DEFINED AS FOLLOWS

```



DER 690  
DER 700  
DER 710  
DER 720  
DER 730  
DER 740  
DER 750  
DER 760  
DER 770  
DER 780  
DER 790  
DER 800

IF (ER.LT.EPS2) GO TO 150  
140 CONTINUE  
C  
GO TO 170  
C  
150 DO 160 I=1,NY  
160 Y(2,I) = Y(3,I)  
C  
RETURN  
170 KERET = 1  
RETURN  
END

-----  
THIS SUBROUTINE IS REQUIRED BY THE TIME INTEGRATION PACKAGE AND  
MUST BE SUPPLIED BY THE USER. ITS PURPOSE IS TO EVALUATE THE  
FUNCTION AT CURRENT VALUES OF THE VARIABLES.  
-----

D-005  
D-010  
D-015  
D-020  
D-025  
D-035  
  
D-050  
D-055  
  
D-065  
D-075  
D-080  
D-085  
D-090  
D-100  
D-110  
D-115  
D-120  
D-125  
D-130  
D-135  
D-140

SUBROUTINE DIFFUN(Y,YL,T,HINV,DY)  
REAL\*8 C1,C2,C4,C5  
REAL\*8 BIGG,BIGG,BIGH  
INTEGER\*2 NAME,JA,J8,NNZ,JC,NUMNP,NUMEL,NELDOF,CONN  
COMMON/GTRY2/NAME(4615),JA(183),JB(184),NNZ,JC,NUMNP,NUMEL,NELDOF,  
1CONN(128,15)  
DIMENSION Y(7,1),YL(1),DY(1)  
COMMON/DELAY/SJM(183),PSI(93)  
COMMON/COEF/C1(183),C2(183),C4(183),C5(183)  
COMMON/SYSMT1/BIGG(4615)  
COMMON/SYSMT2/BIGG(4615)  
COMMON/SYSMT3/BIGH(4615)  
DATA TOLD/-1.0E-30/  
IF(T.EQ.TOLD) GO TO 97  
CALL SUMT(Y,TOLD,T-TOLD)  
TOLD=T  
96 CONTINUE  
97 CALL FEEDBK(Y,TOLD)  
DO 110 I=1,NNZ  
IF(I.GT.93) GO TO 401  
PSI(I)=Y(1,I)  
401 CONTINUE  
DY(I)=0.0  
J8=JB(I)  
JE=JB(I)+JA(I)-1  
DO 120 J=J8,JE  
LL=NAME(J)



D-145

```

IF(LL-GT-NNZ) 30 TO 120
DY(1)=DY(1)+BIGG(J)*(HINV*Y(2,LL)+C2(LL)*Y(1,LL)+C5(LL)*SUM(LL))+C
11(LL)*BIGGG(J)*Y(1,LL)+C4(LL)*BIGH(J)*Y(1,LL)
120 CONTINUE
110 RETURN
END

```

D-180  
D-185  
D-195  
D-200

-----  
 THIS SUBROUTINE IS REQUIRED BY THE TIME INTEGRATION PACKAGE AND  
 MUST BE SUPPLIED BY THE USER. ITS PURPOSE IS TO EVALUATE THE J  
 MATRIX NEEDED WHEN THE CORRECTOR EQUATION IS BEING SOLVED.  
 -----

J-005

```

SUBROUTINE JACMAT(Y, YL, T, HINV, A2, N, NY, EPS, DY, F1, PW)
REAL*8 C1, C2, C4, C5
REAL*8 BIGG, BIGGG, BIGH
INTEGER*2 NAME, JA, JB, NNZ, JC, NUMNP, NUMEL, NELDOF, CONN
COMMON/ GTRY2/ NAME(4615), JA(183), JB(184), NNZ, JC, NUMNP, NUMEL, NELDOF,
1 CONN(128, 15)
DIMENSION Y(7, 1), YL(1), F1(1), DY(1), PW(1)
COMMON/ COEF/ C1(183), C2(183), C4(183), C5(183)
COMMON/ SYSM1/ BIGG(4615)
COMMON/ SYSM2/ BIGGG(4615)
COMMON/ SYSM3/ BIGH(4615)
AH = -A2 * HINV
DO 300 I=1, NNZ
JB8=JB(I)
JE=JB(I)+JA(I)-1
DO 310 J=JB8, JE
LL=NAME(J)
PW(J)=BIGG(J)*(AH+C2(LL))+C1(LL)*BIGGG(J)+C4(LL)*BIGH(J)
310 CONTINUE
300 RETURN
END

```

J-010  
J-015  
J-020  
J-025  
J-035  
J-045  
J-050  
J-065  
J-075  
J-080  
J-085  
J-090

J-115  
J-120  
J-130  
J-135

-----  
 THIS SUBROUTINE IS REQUIRED BY THE TIME INTEGRATION PACKAGE AND  
 MUST BE SUPPLIED BY THE USER. ITS PURPOSE IS TO SOLVE A LINEAR  
 SYSTEM OF EQUATIONS FOR THE NEWTON ITERATES WHEN THE CORRECTOR  
 EQUATION IS BEING SOLVED.  
 -----

N-005  
N-010

```

SUBROUTINE NUTSL(PW, DY, F1, N, NY, EPS, YMAX, NEWPW, KRET)
INTEGER*2 K, JA, JB, NNZ, JC, NUMNP, NUMEL, NELDOF, CONN

```



N-015  
N-020  
N-025  
N-030  
N-040  
N-045  
N-050  
N-055  
N-060  
N-065  
N-070  
N-075  
N-080  
N-085  
N-090  
N-095  
N-100  
N-105  
N-110  
N-115  
N-120  
N-125  
N-130  
N-135  
N-140  
N-145  
N-150  
N-155  
N-160  
N-165  
N-170  
N-175  
N-180  
N-185  
N-190  
N-195

COMMON/GTRY2/(<(4615),JA(183),JB(184),VVZ,JC,NUMNP,NUMEL,NELDOF,CON

LN(128,15)  
DIMENSION PW(1),DY(1),FI(1),YMAX(1)  
DATA SPD,SPDMI/1.05,.05/  
KRET = 0  
EPSS = EPS\*\*2  
EPSA2 = EPSS\*.0001

NOIT = N

280 DO 281 I=1,NY

LL=JB(I)

281 FI(I)=DY(I)/PW(LL)

DO 287 IT=1,NOIT

RCH = 0.

CH = 0.

DO 285 I=1,NY

LL=JB(I)

JBB=JB(I)+1

JE=JB(I)+JA(I)-1

FN = DY(I)

DO 284 J=JBB,JE

IF(K(J).LE.0.DR.K(J).GT.NY) GO TO 284

FN=FN-PW(J)\*FI(K(J))

CONTINUE

FN=FN/PW(LL)

FN = FN\*SPD - SPDMI\*FI(I)

ACH = FI(I) - FN

CH = CH + (ACH/YMAX(I))\*\*2

282 RCH = RCH + (ACH/AMAX1(ABS(FN),EPS))\*\*2

285 FI(I) = FN

IF(RCH.LT.EPSS)GO TO 288

IF(CH.LE.EPSA2)GO TO 288

287 CONTINUE

KRET = 3

288 CONTINUE

RETURN

END

-----  
THIS SUBROUTINE CALCULATES THE GGG ELEMENT MATRIX USING 21 POINTS  
OF INTEGRATION. IT THEN PUTS THE GGG ELEMENT MATRIX INTO THE BIGH  
SYSTEM MATRIX.  
-----

SUBROUTINE FEEDBK(Y,TOLD)  
REAL\*8 GGG,BIGH  
REAL\*8 WL,WS,S,CL1,CL2,CL3,FN,DL1,DL2,DL3,DS,DETJ  
INTEGER\*2 NAME,JA,JB,NNZ,JC,NUMNP,NUMEL,NELDOF,CONN

T-005  
T-010  
T-015  
T-020

```

COMMON/GTRY2/NAME(4615),JA(183),JB(184),NNZ,JC,NUMNP,NUMEL,NELDOF,
1CONN(128,15)
COMMON/GTRY1/X(505),P(505),Z(505)
COMMON/XOCAL/XX(15),YY(15),ZZ(15),PPSI(15)
DIMENSION Y(7,1)
COMMON/TEMP/C3(183),C6(15)
COMMON/GGGMAT/GGG(15,15)
COMMON/SYSMT3/BIGH(4615)
COMMON/GAUSS/WL(7),WS(5),S(5),CL1(7),CL2(7),CL3(7),FN(15,21),DL1(1
15,21),DL2(15,21),DL3(15,21),DS(15,21),DETJ(21)
DO 300 I=1,JC
BIGH(I)=0.0
300 CONTINUE
NNA=7
NNSS=3
DO 800 L=1,NUMEL
DO 600 J=1,15
DO 610 J=1,15
GGG(I,J)=0.0
610 CONTINUE
600 CONTINUE
DO 805 JJ=1,15
NN=CONN(L,JJ)
XX(JJ)=X(NN)
YY(JJ)=P(NN)
ZZ(JJ)=Z(NN)
IF(NN.GT.NNZ) GO TO 803
C6(JJ)=C3(NN)
PPSI(JJ)=Y(1,NN)
GO TO 805
803 PPSI(JJ)=0.0
C6(JJ)=0.0
805 CONTINUE
A5=2.0/(ZZ(1)-ZZ(15))
DETJJ=0.0
DO 802 K=1,NNSS
DETJ=0.0
DO 798 M=1,NNA
IF(K.EQ.1) GO TO 111
IF(K.EQ.2) GO TO 222
IF(K.EQ.3) GO TO 333
GO TO 788
111 N=M
GO TO 788
222 N=M+7
GO TO 788
333 N=M+14
788 CONTINUE

```

T-025  
T-030  
T-035  
T-045  
T-040  
  
T-055  
  
T-065  
T-070  
  
T-085  
T-090  
T-095  
T-100  
  
T-120  
T-125  
T-130  
T-135  
T-140  
T-145  
T-155  
T-160  
T-165  
T-170  
T-175  
  
T-180  
T-185  
T-190  
  
T-195  
T-200  
T-205  
T-210  
T-215  
T-220  
T-225  
T-230  
T-235  
T-240  
T-245  
T-250  
T-255  
T-260  
T-265  
T-270

T-275  
T-280  
T-285  
T-290  
T-295  
T-300  
T-305  
T-310  
T-315  
T-320  
T-325  
T-330  
T-335  
T-340  
T-345  
T-350  
T-355  
T-360  
T-365  
T-370  
T-375  
T-380  
T-385  
T-390  
T-395  
T-400  
T-405  
T-410  
T-415  
T-420  
T-425  
T-430  
T-435  
T-440  
T-445  
T-450  
T-455  
T-480  
T-485  
T-490  
T-495  
T-500  
T-505  
T-550

```

T1=DL1(1,N)*XX(1)+DL1(2,N)*XX(2)-DL3(4,N)*XX(4)-DL3(5,N)*XX(5)
T2=DL1(7,N)*XX(7)-DL3(9,N)*XX(9)+DL1(10,N)*XX(10)+DL1(11,N)*XX(11)
T3=(DL1(6,N)-DL3(6,N))*XX(6)-DL3(13,N)*XX(13)-DL3(14,N)*XX(14)
T4=(DL1(15,N)-DL3(15,N))*XX(15)
DJ1=T1+T2+T3+T4
D1=DL1(1,N)*YY(1)+DL1(2,N)*YY(2)-DL3(4,N)*YY(4)-DL3(5,N)*YY(5)
D2=DL1(7,N)*YY(7)-DL3(9,N)*YY(9)+DL1(10,N)*YY(10)+DL1(11,N)*YY(11)
D3=(DL1(6,N)-DL3(6,N))*YY(6)-DL3(13,N)*YY(13)-DL3(14,N)*YY(14)
D4=(DL1(15,N)-DL3(15,N))*YY(15)
DJ2=D1+D2+D3+D4
T5=DL2(2,N)*XX(2)+DL2(3,N)*XX(3)-DL3(5,N)*XX(5)-DL3(6,N)*XX(6)
T6=DL2(8,N)*XX(8)-DL3(9,N)*XX(9)+(DL2(4,N)-DL3(4,N))*XX(4)
T7=DL2(11,N)*XX(11)+DL2(12,N)*XX(12)+(DL2(13,N)-DL3(13,N))*XX(13)
T8=-DL3(14,N)*XX(14)-DL3(15,N)*XX(15)
DJ21=T5+T6+T7+T8
D5=DL2(2,N)*YY(2)+DL2(3,N)*YY(3)-DL3(5,N)*YY(5)-DL3(6,N)*YY(6)
D6=DL2(8,N)*YY(8)-DL3(9,N)*YY(9)+(DL2(4,N)-DL3(4,N))*YY(4)
D7=DL2(11,N)*YY(11)+DL2(12,N)*YY(12)+(DL2(13,N)-DL3(13,N))*YY(13)
D8=-DL3(14,N)*YY(14)-DL3(15,N)*YY(15)
DJ22=D5+D6+D7+D8
DETJ(N)=DJ1+DJ22-DJ12+DJ21
DETJ1=DETJ(N)*WL(M)+DETJ1
CONTINUE
798 DETJJ=DETJJ+WS(K)*DETJ1
802 CONTINUE
DO 700 J=1,15
DO 710 I=1,15
FHH=0.0
DO 806 K=1,NNSSS
FH=0.0
DO 799 M=1,NNAAA
TT1=0.0
TT2=0.0
TT3=0.0
IF(K.EQ.1) GO TO 1111
IF(K.EQ.2) GO TO 2222
IF(K.EQ.3) GO TO 3333
GO TO 7888
1111 N=M
GO TO 7888
2222 N=M+7
GO TO 7888
3333 N=M+14
CONTINUE
7770 TT1=FN(1,N)*PPSI(1)*C6(1)+FN(2,N)*PPSI(2)*C6(2)+FN(3,N)*PPSI(3)*C6
1(3)+FN(4,N)*PPSI(4)*C6(4)+FN(5,N)*PPSI(5)*C6(5)+FN(6,N)*PPSI(6)*C6
1(6)+FN(7,N)*PPSI(7)*C6(7)+FN(8,N)*PPSI(8)*C6(8)
TT2=FN(9,N)*PPSI(9)*C6(9)+FN(10,N)*PPSI(10)*C6(10)+FN(11,N)*PPSI(11

```

```

11)*C6(11)+FN(12,N)*PPSI(12)*C6(12)+FN(13,N)*PPSI(13)*C6(13)+FN(14,
IN)*PPSI(14)*C6(14)+FN(15,N)*PPSI(15)*C6(15)
TT3=TT1+TT2+1.0
FH=FH+WL(M)*FN(J,N)*FN(I,N)*ALOG(TT3)*DETJ(N)
799 CONTINUE
FHH=WS(K)*FH+FHH
806 CONTINUE
GGG(J,I)=FHH/A5
710 CONTINUE
700 CONTINUE
C INSERT INTO SYSTEM MATRIX
DO 20 K=1,15
KK=CONN(L,K)
IF(KK.GT.NNZ) GO TO 20
KKK=JA(KK)
LLL=JB(KK)-1
DO 10 I=1,15
II=CONN(L,I)
DO 91 M=1,KKK
MM=LLL+M
KKM=NAME(MM)
IF(II.EQ.KKM)GO TO 92
91 CONTINUE
92 CONTINUE
BIGH(MM)=BIGH(MM)+GGG(K,I)
10 CONTINUE
20 CONTINUE
800 CONTINUE
RETURN
END

C-----
C THE CUMULATIVE CONTRIBUTION OF THE DELAYED NEUTRON FLUX IS
C CALCULATED BY THIS SUBROUTINE.
C-----
C
SUBROUTINE SUMT(Y,T,H)
DIMENSION Y(7,1)
COMMON/DELAY/SUM(183),PSI(93)
Q=0.4349710
TC=-Q*H
DO 100 I=1,93
SUM(I)=SUM(I)*EXP(-Q*H)+0.50*H*(PSI(I)*EXP(TC)+Y(1,I))
100 CONTINUE
RETURN
END

```

T-580  
T-585  
T-590  
T-595  
T-600  
T-605  
T-610  
T-615  
T-620  
T-625  
T-630  
T-635  
T-640  
T-645  
T-650  
T-655  
T-660  
T-665  
T-670  
T-675  
T-680  
T-685  
T-690  
T-695  
T-700  
T-705  
T-710  
T-715  
T-720

S-005  
S-010  
  
S-030  
S-040  
  
S-050  
S-055  
S-060



## LIST OF REFERENCES

1. Nguyen, D. H. and D. Salinas, "Finite Element Solution of Space-Time Nonlinear Reactor Dynamics," Nuclear Science and Engineering, v. 60, p. 120-130, June 1976.
2. Hanford Engineering Development Laboratories Report HEDL-TME74-47, Melt III-A Neutronics Thermal-Hydraulic Computer Program for Fast Reactor Safety, v. 1, by A. E. Walter and others, 1974.
3. Hetrick, D. L., Dynamics of Nuclear Reactors, p. 1-15, University of Chicago Press, 1971.
4. Lamarch, J. R., Introduction to Nuclear Reactor Theory, Addison-Wesley, 1972.
5. Nguyen, D. H., "The Time-Dependent Nuclear Reactor with Feedback," Nuclear Science and Engineering, v. 55, p. 307-319, June 1974.
6. Nguyen, D. H., "The New Equilibrium State of a Perturbed Nuclear Reactor with Negative Feedback," Nuclear Science and Engineering, v. 52, p. 292-298, June 1973.
7. Naval Postgraduate School Report NPS-53Fe76051, A Program for the Numerical Solution of Large Sparse Systems of Algebraic and Implicitly Defined Stiff Differential Equations, by R. Franke, May 1976.
8. Naval Postgraduate School Report NPS-59Zc761111, An Optimum Compact Storage Scheme for Nonlinear Reactor Problems by FEM, by D. Salinas, D. H. Nguyen, and R. Franke, 1976.
9. Norrie, D. H. and G. de Vries, The Finite Element Method; Fundamentals and Applications, Chapter 5, Academic Press, 1973.
10. Salinas, D., D. H. Nguyen and T. W. Southworth, "Finite Element Solution of a Nonlinear Nuclear Reactor Dynamics Problem," International Conference on Computational Methods in Nonlinear Mechanics, Austin, Texas, p. 541-550, 1974.
11. Zienkiewicz, O. C., The Finite Element Method in Engineering Science, McGraw-Hill, 1971.
12. Cook, R. D., Concepts and Applications of Finite Element Analysis, Wiley & Sons, 1974.



# INITIAL DISTRIBUTION LIST

	No. Copies
1. Defense Documentation Center Cameron Station Alexandria, Virginia 22314	2
2. Library, Code 0142 Naval Postgraduate School Monterey, California 93940	2
3. Department Chairman, Code 69 Department of Mechanical Engineering Naval Postgraduate School Monterey, California 93940	1
4. Dr. D. H. Nguyen (thesis advisor) 4625 Larchmont NE Albuquerque, New Mexico 87115	1
5. Assoc. Professor D. Salinas (thesis advisor) Department of Mechanical Engineering Naval Postgraduate School Monterey, California 93940	1
6. Assoc. Professor R. Franke (second reader) Department of Mathematics Naval Postgraduate School Monterey, California 93940	1
7. LT E. C. Bermudes, USN (student) 3721-D McCornack Rd. Schofield Barracks, Hawaii 96557	1
8. Professor Gilles Cantin Department of Mechanical Engineering Naval Postgraduate School Monterey, California 93940	1

--- DIM	DO W(2)	DO W(3)	HIN	KER	EPS	DO DO	DO DO	Y(2)	CAL CAL	CAL NEW	DO DO	DO W(1)	CAL CAL	IF IF	ER ER	DO DO	Y(3)	ER ER	
C		100	C			C		110	C		C		120	C				130	C